UNIVERSIDADE FEDERAL DE MINAS GERAIS
FACULDADE DE FARMÁCIA
PROGRAMA DE PÓS-GRADUAÇÃO EM CIÊNCIAS FARMACÊUTICAS

ANA LUIZA CHAVES MAIA

LIPOSSOMAS TERMOSSENSÍVEIS CONTENDO COMPLEXOS DE GADOLÍNIO COMO POTENCIAL ESTRATÉGIA PARA O TRATAMENTO SELETIVO DO CÂNCER DE MAMA

Belo Horizonte – MG
2019

ANA LUIZA CHAVES MAIA

LIPOSSOMAS TERMOSSENSÍVEIS CONTENDO COMPLEXOS DE GADOLÍNIO COMO POTENCIAL ESTRATÉGIA PARA O TRATAMENTO SELETIVO DO CÂNCER DE MAMA

Tese, apresentada ao Programa de Pós-Graduação em Ciências Farmacêuticas da Faculdade de Farmácia da Universidade Federal de Minas Gerais, como requisito parcial, para obter o grau de Doutora em Ciências Farmacêuticas.

Orientadores: Prof. Gilson Andrade Ramaldes (*In memoriam*)
Prof. André Luís Branco de Barros
Coorientadores: Prof. Daniel Crístian Ferreira Soares
Prof. Christian Fernandes

Belo Horizonte – MG
2019

Maia, Ana Luiza Chaves.
M217l Lipossomas termossensíveis contendo complexos de gadolínio como potencial estratégia para o tratamento seletivo do câncer de mama / Ana Luiza Chaves Maia. – 2019.
163 f. : il.

Orientadores: Gilson Andrade Ramaldes e André Luís Branco de Barros.
Coorientadores: Daniel Cristian Ferreira Soares e Christian Fernandes.

Tese (doutorado) – Universidade Federal de Minas Gerais, Faculdade de Farmácia, Programa de Pós-Graduação em Ciências Farmacêuticas.

1. Câncer de mama – Teses. 2. Lipossomas termossensíveis – Teses. 3. Lipossomos – Teses. 4. Gadodiamida – Teses. 5. Hipertermia – Teses. I. Ramaldes, Gilson Andrade. II. Barros, André Luís Branco de. III. Soares, Daniel Cristian Ferreira. IV. Fernandes, Christian. V. Universidade Federal de Minas Gerais. Faculdade de Farmácia. VI. Título.

CDD: 616.994

Elaborado por Darlene Teresinha Schuler – CRB-6/1759

FOLHA DE APROVAÇÃO

LIPOSSOMAS TERMOSSENSÍVEIS CONTENDO COMPLEXOS DE GADOLÍNIO COMO POTENCIAL ESTRATÉGIA PARA O TRATAMENTO SELETIVO DO CÂNCER DE MAMA

ANA LUIZA CHAVES MAIA

Tese submetida à Banca Examinadora designada pelo Colegiado do Programa de Pós-Graduação em CIÊNCIAS FARMACÊUTICAS, como requisito para obtenção do grau de Doutora em CIÊNCIAS FARMACÊUTICAS, área de concentração CIÊNCIAS FARMACÊUTICAS.

Aprovada em 31 de maio de 2019, pela banca constituída pelos membros:

Prof. Gilson Andrade Ramaldes – Orientador (In memorian)
UFMG

Prof. André Luís Branco de Barros - Orientador
UFMG

Pro. Prof. Dr. Christian Fernandes - Coorientador
UFMG

Prof. Daniel Cristian Ferreira Soares - Coorientador
UNIFEI

Profa. Jacqueline de Souza
UFOP

Prof. Eryvaldo Sócrates Tabosa do Egito
UFRN

Prof. André Augusto Gomes Faraco
UFMG

Profa. Elaine Amaral Leite
UFMG

Belo Horizonte, 31 de maio de 2019.

COLABORADORES

Prof. Adriano de Paula Sabino
Dep. de Análises Clínicas e Toxicológicas, Faculdade de Farmácia, UFMG.

Aina Liz Alves César
Dep. de Produtos Farmacêuticos, Faculdade de Farmácia, UFMG.

Aline Teixeira Maciel e Silva
Dep. de Produtos Farmacêuticos, Faculdade de Farmácia, UFMG.

Prof. Ângelo Malachias de Souza
Dep. de Física, Instituto de Ciências Exatas, UFMG.

Prof.ª Cristiane dos Santos Giuberti
Centro de Ciências da Saúde, UFES.

Fernanda Cristina Gontijo Evangelista
Dep. de Análises Clínicas e Toxicológicas, Faculdade de Farmácia, UFMG.

Mariana Silva Oliveira
Dep. de Produtos Farmacêuticos, Faculdade de Farmácia, UFMG.

Pedro Henrique Reis da Silva
Dep. de Produtos Farmacêuticos, Faculdade de Farmácia, UFMG.

LOCAIS DE REALIZAÇÃO DO DOUTORADO

- Centro de Microscopia da UFMG, Belo Horizonte, MG.

- Laboratório da Sinalização da Inflamação e Oncohematologia, Faculdade de Farmácia, UFMG, Belo Horizonte, Minas Gerais.

- Laboratório de Farmacotécnica e Tecnologia Farmacêutica, Faculdade de Farmácia, UFMG, Belo Horizonte, Minas Gerais.

- Laboratório Multiusuário de Análises Biomoleculares, Centro de Ciências da Saúde, UFES, Vitória, Espírito Santo.

- Laboratório Nacional de Luz Síncrotron, Campinas, São Paulo.

DEDICATÓRIA

À minha mãe Márcia, à minha irmã Isabela e à Nina, pelo amor, incentivo e alegrias.

Ao Prof. Gilson Andrade Ramaldes, amigo ao qual eu serei eternamente grata.

AGRADECIMENTOS

A Deus, por conduzir minhas escolhas e me abençoar em todos os momentos.

À minha mãe Marcia, pelo amor, amizade, incentivo, inspiração e conselhos. À minha irmã Isabela e à Nina, por trazerem leveza e alegria em diversos momentos e por serem minha maior fonte de motivação.

Ao Professor Gilson, por ter me recebido com tanto carinho na UFMG. Obrigada pela forma como conduziu minha orientação sempre com amizade, confiança, generosidade, dedicação, interesse, otimismo e boa vontade. Durante o meu mestrado e também durante o meu doutorado, você passou por diversos problemas de saúde e por muitas adversidades profissionais, mas em todos os momentos, fez questão de continuar me orientando. Obrigada por sempre ter estado ao meu lado e por nunca ter me deixado desamparada. Você não imagina como as oportunidades e ensinamentos que você me proporcionou modificaram a minha vida e me permitiram dar maior conforto para a minha família. Da nossa breve convivência, permanecem as boas lembranças, a admiração, a gratidão e a saudade. Agradeço também à sua família: Maria do Carmo, Fernando e Marina, que sempre me trataram com muito carinho e torceram pela realização deste estudo.

Aos Professores Daniel Cristian, André Branco e Christian pela imensa contribuição científica durante esses anos em que estive na UFMG, pelos conselhos e pela amizade construída durante a nossa convivência.

À Aline, pelo companheirismo, amizade, apoio, conselhos e pelos bons momentos compartilhados. Obrigada pelo incentivo e pela ajuda durante todo o doutorado e principalmente no momento em que eu comecei a dar aulas. Você foi uma das pessoas que mais me apoiou e ficou feliz por mim.

À Aina e à Mariana pelo companheirismo, bons momentos, amizade e por me auxiliarem nas análises estatísticas de cinética de liberação e nas etapas de depósito do pedido de patente, respectivamente.

Ao Pedro por me auxiliar nas análises estatísticas de quimiometria.

À Prof.ª Cristiane Giuberti, pela colaboração nos experimentos de microcalorimetria.

Ao Prof. Ângelo Malachias, pela colaboração nas análises de SAXS.

Ao Prof. Adriano Sabino e à Fernanda Gontijo, pela colaboração nos experimentos de citotoxicidade.

Aos alunos e ex-alunos do Laboratório de Tecnologia Farmacêutica e da Radioisótopos, pela ajuda, incentivos e bons momentos compartilhados: Aina, Aline, Bruna,

Carol Oda, Carol Henriques, Caroline, Daniel Costa, Daniel Cristian, Cibele, Dani Arruda, Dani Sóter, Délia, Diêgo, Eduardo, Eliza, Elton, Fernanda Borato, Fernanda Lapa, Fernanda Noal, Flávia de Marco, Flávia Lima, Gabriel, Guilherme, Heloísa, Isabela Pereira, Izabela Mansur, Janaína, Jaque, Jú, Laís, Larissa, Leo, Linna, Lívia, Liziane, Marcela, Marcus, Mariana, Marina, Marjorie, Mayara, Michelle, Nara, Nayara, Pedro, Raquel Araújo, Raquel Gregório, Renata, Rummenigge, Samuel, Sávia, Shirleide, Sued, Valquíria e Thaís.

Aos professores e ex-professores da Faculdade de Farmácia da UFMG: André Branco, André Faraco, Armando, Christian, Elaine, Gisele, Gilson, José Eduardo, Josianne, Lucas, Marta, Mônica, Simone, Ricardo e Valbert, pela ótima convivência ao longo desses anos, por toda ajuda, conselhos e contribuições científicas que foram muito importantes para minha formação.

Aos funcionários da UFMG: Batista, Eduardo, Hernane, Lúcia, Marton, Naialy, Mateus, Raquel, Jamil, Jane e Vinícius pela ajuda constante e boa convivência.

Aos professores: Luciano Gonçalves Fernandes (UFRRJ), Míriam Carmo Rodrigues Barbosa (UFES) e Suzana Pavlovic (UFOP), responsáveis pelo início da minha formação acadêmica, durante a iniciação científica.

Aos professores: André Augusto Gomes Faraco (UFMG), Délia Chaves Moreira (UFES), Elaine Amaral Leite (UFMG), Eryvaldo Socrátes Tabosa do Egito (UFRN), Gisele Assis Castro Goulart (UFMG) e Jacqueline de Souza (UFOP) pela disponibilidade em avaliar e contribuir nesta tese.

À FAPEMIG e ao CNPq pelo auxílio financeiro e à CAPES pela minha bolsa de doutorado.

Às amigas Erica, Juliana, Rafaela e Quartocrescentinas pela amizade, bons momentos, companheirismo, apoio e incentivo. Pela torcida por minhas realizações e pela compreensão nos momentos em que não pude estar presente.

Por fim, a todas as pessoas que torceram e colaboraram de alguma forma para a realização deste estudo.

Obrigada!

RESUMO

O câncer é apontado atualmente como uma das principais causas de morbimortalidade. Sendo assim, o desenvolvimento de opções terapêuticas mais seletivas é de fundamental importância. A gadodiamida (Gd-DTPA-BMA) é um complexo de gadolínio utilizado tradicionalmente em ressonância magnética. Nosso grupo de pesquisa tem demonstrado o potencial desse fármaco, encapsulado em lipossomas, para o tratamento do câncer. No presente estudo foi desenvolvido e validado método analítico, por cromatografia de interação hidrofílica, para determinação de Gd-DTPA-BMA em lipossomas termossensíveis. Além disso, foram desenvolvidas e caracterizadas duas formulações lipossomais termossensíveis contendo Gd-DTPA-BMA. Os lipossomas desenvolvidos apresentaram adequadas características físico-químicas em termos de diâmetro médio (114 a 118 nm), potencial zeta (–2,1 a –2,8 mV) e encapsulação de Gd-DTPA-BMA (23,8 a 25,7 μmol/mL). Estas formulações mantiveram-se estáveis, durante o período de 4 meses de armazenamento. Fotomicrografias obtidas destes lipossomas mostraram vesículas esféricas, unilamelares e evidenciaram, por contraste, a encapsulação do fármaco. A termossensibilidade das formulações foi demonstrada por espalhamento dinâmico da luz, microcalorimetria e espalhamento de raios-X a baixo ângulo. Os resultados obtidos pelas três técnicas foram consistentes e evidenciaram termossensibilidade em temperaturas compatíveis com as temperaturas utilizadas no tratamento do câncer por hipertermia moderada (41 °C a 45 °C). Os resultados dos estudos de liberação, realizado em soro fetal bovino, sugerem que as formulações apresentam cinética de liberação conforme modelo de Higuchi, por difusão baseada na Lei de Fick. Estas análises também evidenciaram que a composição da formulação influencia diretamente no perfil de liberação obtido. Foram realizados estudos de citotoxicidade em células de fibroblastos sadios e em células de adenocarcinoma mamário murino e humano. Nas células tumorais, os lipossomas brancos e Gd-DTPA-BMA na forma livre não apresentaram citotoxicidade significativa. Por outro lado, os lipossomas contendo Gd-DTPA-BMA apresentaram uma citotoxicidade 100 vezes maior em comparação com o fármaco livre. As análises na linhagem de células sadias revelaram a seletividade do tratamento proposto. Portanto, os resultados apresentados, sugerem que lipossomas termossensíveis contendo Gd-DTPA-BMA constituem uma alternativa promissora para o tratamento seletivo do câncer de mama.

Palavras-chave: Gadodiamida; Lipossomas termossensíveis; Hipertermia; Câncer de mama.

ABSTRACT

Currently, cancer is identified as one of the main causes of morbidity and mortality. Therefore, the development of more selective therapeutic options is of fundamental importance. Gadodiamide (Gd-DTPA-BMA) is a gadolinium complex traditionally used in magnetic resonance imaging. Our research group has demonstrated the potential of this drug, encapsulated in liposomes, for cancer treatment. In the present study, analytical method, by hydrophilic interaction chromatography, was developed and validated for determining Gd-DTPA-BMA in thermosensitive liposomes. In addition, two thermosensitive liposomal formulations containing Gd-DTPA-BMA were developed and characterized. The developed liposomes presented adequate physicochemical characteristics in terms of mean diameter (114 to 118 nm), zeta potential (−2.1 to −2.8 mV), and Gd-DTPA-BMA entrapment (23.8 to 25.7 μmol/mL). These formulations remained stable during the 4-month storage period. Photomicrographs obtained from these liposomes showed spherical, unilamellar vesicles and evidenced, by contrast, the encapsulation of the drug. The thermosensitivity of the formulations was demonstrated by dynamic light scattering, microcalorimetry, and small-angle X-ray scattering. The results obtained by the three techniques were consistent and showed thermosensitivity at temperatures compatible with the cancer treatment by moderate hyperthermia (41 °C to 45 °C). The results of release studies, performed in fetal bovine serum, suggest that the formulations present release kinetics according to the Higuchi model, by diffusion based on Fick's Law. These analyses also showed that the composition of the formulation directly influences the release profile obtained. Cytotoxicity studies were performed on healthy fibroblast cells and murine and human breast adenocarcinoma cells. In tumor cells, blank liposomes and Gd-DTPA-BMA in free form did not show significant cytotoxicity. On the other hand, Gd-DTPA-BMA-containing liposomes showed 100-fold higher cytotoxicity compared to the free drug. Analyses in the healthy cell line revealed the selectivity of the proposed treatment. Therefore, the results presented suggest that thermosensitive liposomes containing Gd-DTPA-BMA are a promising alternative for the selective treatment of breast cancer.

Keywords: Gadodiamide; Thermosensitive liposomes; Hyperthermia; Breast cancer**.**

LISTA DE ABREVIATURAS, SIGLAS E SÍMBOLOS

λ	Comprimento de onda
4T1	Adenocarcinoma mamário murino
A/O	Água em óleo
ACN	Acetonitrila
ANOVA	Análise de variância (do inglês, *Analysis Of Variance*)
A_s	Assimetria
ATCC	*American Type Culture Collection*
BANGHAM	Método de hidratação do filme lipídico (em referência a Alec Douglas Bangham, autor principal do método)
BMA	Bismetilamida
CC_{50}	Concentração citotóxica de 50% celular
CMC	Concentração micelar crítica
Cp	Capacidade calorífica
DAD	Detector de arranjo de diodos (do inglês, *Diode Array Detector*)
DLS	Espalhamento dinâmico da luz (do inglês, *Dynamic light scattering*)
DMSO	Dimetilsulfóxido
DPPC	Dipalmitoilfosfatidilcolina
DSC	Calorimetria exploratória diferencial (do inglês, *Differential Scanning Calorimetry*)
DSPC	Diestearoilfosfatidilcolina
DSPE-PEG_{2000}	Diestearoilfosfatidiletanolamina acoplada ao polietilenoglicol de massa molar 2000
DTPA	Ácido dietilenotriaminopentaacético
EDTA	Ácido etilenodiaminotetraacético
EPR	Permeabilidade e retenção aumentadas (do inglês, *Enhanced Permeability and Retention*)
FBS	Soro fetal bovino (do inglês, *Fetal bovine serum*)
Gd	Gadolínio
Gd-BOPTA	Gadobenato de dimeglumina
Gd-BT-DO3A	Gadobutrol
Gd-DOTA	Gadoterato de meglumina
Gd-DTPA	Gadopentetato de dimeglumina

Gd-DTPA-BMA	Gadodiamida
Gd-HP-DO3A	Gadoteriol
H	Altura equivalente a um prato teórico
HEPES	4-(2-hidroxietil)-ácido1-piperazina-etano-sulfônico
HILIC	Cromatografia líquida de interação hidrofílica (do inglês *Hydrophilic Interaction Liquid Chromatography*)
HPLC	Cromatografia líquida de alta eficiência (do inglês, *High Performance Liquid Chromatography*)
IC_{50}	Concentração inibitória de 50% do crescimento celular
k	Fator de retenção
Kcps	Contagem de kilo por segundo (do inglês *Kilo counts per second*)
Lβ	Fase lamelar gel ordenado
LC	Cromatografia líquida (do inglês *Liquid Chromatography*)
LC-MS	Cromatografia líquida acoplada à espectrometria de massas (do inglês *Liquid Chromatography coupled to Mass Spectrometry*)
LOD	Limite de detecção (do inglês *Limit Of Detection*)
LOQ	Limite de quantificação (do inglês *Limit Of Quantification*)
log *k*	Logaritmo decimal da constante de estabilidade termodinâmica metal-ligante
log *P*	Logaritmo decimal do coeficiente de partição octanol/água
LTSL	Lipossoma termossensível contendo lisofosfolípide branco (do inglês, *Lysolipid-containing Temperature-Sensitive Liposome*)
LTSL-Gd	Lipossoma termossensível contendo lisofosfolípide e Gd-DTPA-BMA (do inglês *Lysolipid-containing Temperature-Sensitive Liposome containing Gd-DTPA-BMA*)
LUV	Vesícula unilamelar grande (do inglês, *Large Unilamellar Vesicle*)
Lα	Fase lamelar fluída
MDA-MB 231	Adenocarcinoma mamário humano
MLV	Vesícula multilamelar (do inglês *Multilamellar Vesicle*)
MPPC	Monopalmitoilfosfatidilcolina
MRI	Resonância magnética nuclear (do inglês *Magnetic Resonance Imaging*)
MS	Espectrometria de massas (MS, do inglês *Mass Spectrometry*)

MSPC	Monoestearoilfosfatidilcolina
MTT	Brometo de 3-[4,5-dimetiltiazol-2-il]-2,5-difenil tetrazólio
N	Número de pratos teóricos
NaCa-DTPA-BMA	Caldiamida sódica
NH_4FA	Formiato de amônio
Pβ’	Fase gel inclinado
R	Coeficiente de correlação
r^2	Coeficiente de determinação
REV	Evaporação em fase reversa (do inglês, *Reverse-phase Evaporation*)
RP-LC	Cromatografia líquida de fase reversa (do inglês, *Reverse Phase Liquid Chromatography*)
RPMI	Meio de cultura *Roswell Park Memorial Institute Medium*
R_s	Resolução
RSD	Desvio padrão relativo (do inglês, *Relative Standard Deviation*)
RT2	Glioblastoma murino
SAXS	Difração de raios-X em baixo ângulo (do inglês, *Small-angle X-ray scattering*)
SD	Desvio padrão (do inglês, *Standard Deviation*)
SFM	Sistema fagocitário mononuclear
SI	Índice de seletividade (do inglês, *Selective Index*)
SUV	Vesícula unilamelar pequena (do inglês, *Small Unilamellar Vesicle*)
T_c	Temperatura de transição de fase Lβ → Lα (do inglês, *Chain melting Temperature*)
TEM	Microscopia eletrônica de transmissão (do inglês, *Transmission Electron Microscopy*)
t_r	Tempo de retenção
TTSL	Lipossoma termossensível tradicional branco (do inglês, *Traditional Temperature-Sensitive Liposome*)
TTSL-Gd	Lipossoma termossensível tradicional contendo Gd-DTPA-BMA (do inglês, *Traditional Temperature-Sensitive Liposome containing Gd-DTPA-BMA*)
u_0	Velocidade linear da fase móvel
X_1	pH do componente aquoso da fase móvel

X_2	Proporção de acetonitrila (%)
X_3	Concentração do tampão (mmol/L)
WI-26 VA4	Fibroblasto pulmonar humano
W/O	Água em óleo (do inglês *Water in Oil*)

LISTA DE FIGURAS

PARTE 1 – REVISÃO DA LITERATURA

PARTE 2 – TRABALHO EXPERIMENTAL

CHAPTER 1 – Chemometric-assisted hydrophilic interaction chromatographic method for the determination of gadolinium-based magnetic resonance imaging contrast agent in liposomes

SUPPLEMENTARY INFORMATION

CHAPTER 2 – Thermosensitive liposomes containing gadolinium-based complexes: a potential strategy for the selective breast cancer treatment

LISTA DE TABELAS

SUMÁRIO

INTRODUÇÃO GERAL

INTRODUÇÃO GERAL

O câncer é apontado atualmente como uma das principais causas de morbimortalidade mundial, e, por consequência, tornou-se uma preocupação de saúde pública (INCA, 2018; WHO, 2018). Sendo assim, o desenvolvimento de opções terapêuticas mais seletivas é de fundamental importância, visto que a farmacoterapia, disponível atualmente, apresenta diversas limitações (LOPES et al., 2013b; MROSS; KRATZ, 2011; SHI et al., 2017; ZUGAZAGOITIA et al., 2016).

A gadodiamida (Gd-DTPA-BMA) é um complexo de gadolínio, utilizado como agente de contraste em exames de ressonância magnética (LIU; ZHANG, 2012). Existem evidências científicas que Gd-DTPA-BMA também possui a capacidade de induzir apoptose, em células neoplásicas, por meio da ativação de *caspase-3* (SOARES et al., 2010). Diversos estudos relatam a encapsulação de Gd-DTPA-BMA em lipossomas explorando sua ação como contraste (GRANH et al., 2009; HOSSANN et al., 2010; HOSSANN et al., 2013). Por outro lado, nosso grupo de pesquisa tem demonstrado o potencial de Gd-DTPA-BMA, em lipossomas convencionais e lipossomas pH-sensíveis, para o tratamento do câncer (MAIA, 2015; MAIA et al., 2016; SOARES, 2010; SOARES et al., 2011a; SOARES et al., 2011b; SOARES et al., 2012; SOARES et al., 2013). Neste contexto, lipossomas termossensíveis constituem nanocarreadores promissores, ainda não investigados. Este tipo de nanossistema, requer a administração associada à alguma técnica de hipertermia. O aquecimento da região tumoral é necessário para permitir a liberação do fármaco encapsulado, mas também pode contribuir para aumentar a eficácia do tratamento. A aplicação de calor resulta em aumento da permeabilidade do ambiente tumoral e desnaturação de proteínas importantes para a progressão do tumor. Além disso, a hipertermia pode induzir a apoptose de células neoplásicas, que são mais sensíveis ao aquecimento do que as células sadias (HILDEBRANDT et al., 2002; KUMAR; MOHAMMAD, 2011).

A determinação de Gd-DTPA-BMA em amostras ambientais e biológicas tem sido realizada por técnicas que requerem instrumentação complexa, análises dispendiosas e em alguns casos, apresentam baixos limites de detecção (TELGMANN et al., 2013). Nosso grupo de pesquisa, demonstrou a determinação de Gd-DTPA-BMA, em lipossomas, por cromatografia líquida de fase reversa e espectrofotometria derivada. Em ambas as técnicas, a detecção foi realizada na região ultravioleta (MAIA et al., 2015). Embora os métodos desenvolvidos por nosso grupo, sejam mais simples, rápidos, e menos dispendiosos que os métodos descritos na literatura, eles não permitem a determinação de Gd-DTPA-BMA em

amostras complexas, como por exemplo, soro fetal bovino. Um método analítico que permita este tipo de análise é importante no desenvolvimento de lipossomas, para aplicação em estudos de liberação, nos quais se pretenda simular condições biológicas.

Diante do exposto, os objetivos dessa tese foram: (*i*) desenvolver e validar método analítico simples, rápido e que permita a determinação de Gd-DTPA-BMA em lipossomas e amostras complexas, empregando cromatografia líquida de interação hidrofílica e detecção por espectrofotometria de absorção na região do ultravioleta; (*ii*) desenvolver, caracterizar e avaliar a potencial atividade citotóxica de lipossomas termossensíveis contendo Gd-DTPA-BMA, frente às células tumorais 4T1 (adenocarcinoma mamário murino) e MDA-MB-231 (adenocarcinoma mamário humano); (*iii*) investigar o índice de seletividade em células sadias de fibroblastos pulmonares humanos (WI -26 VA 4).

A tese foi dividida em duas partes: a primeira parte contém a *"Revisão da literatura"* e a segunda parte contém o *"Trabalho experimental"*, apresentado em dois capítulos:

No capítulo 1 foram descritos o desenvolvimento e a validação do método analítico.

No capítulo 2 foram apresentados o desenvolvimento, a caracterização e os estudos de citotoxicidade dos lipossomas termossensíveis.

OBJETIVOS

OBJETIVOS

1 Objetivo geral

Desenvolver, caracterizar e otimizar lipossomas termossensíveis contendo Gd-DTPA-BMA e avaliar sua potencial atividade citotóxica, em diferentes linhagens de câncer de mama.

2 Objetivos específicos

- Identificar por meio de técnicas analíticas (espectrometria nas regiões do infravermelho e ultravioleta e cromatografia líquida) se Gd-DTPA-BMA permanece estável nas condições de aquecimento requeridas para o preparo de lipossomas termossensíveis;
- Desenvolver duas formulações de lipossomas termossensíveis com diferentes composições, contendo Gd-DTPA-BMA, para avaliar a influência da composição lipídica no perfil de liberação e na potencial atividade citotóxica;
- Desenvolver, otimizar e validar um método analítico para determinação de Gd-DTPA-BMA em lipossomas termossensíveis e em amostras complexas, como por exemplo: soro fetal bovino;
- Preparar as formulações desenvolvidas, empregando diferentes métodos de preparo, afim de identificar a influência do método utilizado, nas características físico-químicas dos lipossomas;
- Preparar as formulações desenvolvidas, empregando diferentes concentrações de Gd-DTPA-BMA, afim de identificar a influência da concentração de fármaco adicionado, no teor de encapsulação obtido;
- Caracterizar as formulações termossensíveis dos pontos de vista físico-químico e morfológico, quanto ao diâmetro médio das vesículas, lamelaridade, índice de polidispersão, potencial zeta, mobilidade eletroforética e teor de encapsulação;
- Avaliar o diâmetro médio, o índice de polidispersão, o potencial zeta e o teor de encapsulação das formulações termossensíveis armazenadas a 4 ºC durante o período de 180 dias;
- Caracterizar as formulações termossensíveis do ponto de vista térmico;

- Avaliar a cinética de liberação, *in vitro*, de Gd-DTPA-BMA a partir das formulações termossensíveis;
- Avaliar a citotoxicidade *in vitro* do tratamento empregando lipossomas termossensíveis, contendo Gd-DTPA-BMA, associado ou não à hipertermia, nas linhagens de células tumorais 4T1 (adenocarcinoma mamário murino) e MCF-7 (adenocarcinoma mamário humano);
- Avaliar o índice de seletividade do tratamento empregando lipossomas termossensíveis, contendo Gd-DTPA-BMA, associado ou não à hipertermia, na linhagem de células sadias WI-26 VA 4 (fibroblastos pulmonares humanos).

PARTE 1 – REVISÃO DA LITERATURA

REVISÃO DA LITERATURA

1 Câncer e a necessidade de terapias inovadoras

Câncer é um termo genérico empregado para denominar diversos distúrbios celulares, que apresentam em comum, a proliferação e a disseminação desordenada de células, que se tornaram indiferenciadas, em virtude de algum tipo de modificação genética (INCA, 2018). O câncer é apontado, atualmente, como uma das principais causas de morbimortalidade mundial (WHO, 2018). No Brasil, o Instituto Nacional de Câncer José Alencar Gomes da Silva, estima que, no período entre 2018-2019, possam surgir 600 mil novos casos, sendo que, os cânceres de próstata (68 mil) em homens, e mama (60 mil) em mulheres, serão os mais frequentes (INCA, 2018). Os dados apresentados evidenciam a alta prevalência desta doença e justificam a necessidade de pesquisas que objetivam reverter essa realidade.

A quimioterapia é, atualmente, a modalidade clínica de tratamento do câncer mais utilizada (ALMEIDA et al., 2005; INCA, 2018). Diversos fármacos são empregados como agentes antineoplásicos, dentre eles os complexos de platina (cisplatina, carboplatina e oxaplatina), as antraciclinas (doxorrubicina e daunorrubicina), os taxanos (paclitaxel e docetaxel), os antimetabólitos (metotrexato e citarabina), as campotecinas (irinotecano e topotecano) e os alcalóides da vinca (vincristina, vimblastina e vindesina). Entretanto, quando comparados a outras classes de fármacos, os agentes quimioterápicos apresentam reduzida especificidade, susceptibilidade à resistência, elevada toxicidade e direcionamento ineficiente aos tecidos e órgãos alvos. Além disso, grande parte destes fármacos apresenta baixo índice terapêutico, podendo dessa forma, dependendo da concentração utilizada, ocasionar danos às células normais (ISMAEL et al., 2008; KAELIN JR, 2005).

Os efeitos colaterais relacionados à quimioterapia tradicional incluem complicações neurológicas (cefaleia, confusão mental e convulsão), cardiovasculares (miocardiopatia e hipotensão), respiratórias (fibrose pulmonar e dispneia), gástricas (faringite e mucosite) e hematológicas (danos à medula óssea). Dentre os efeitos adversos mais prevalentes e incômodos destacam-se a xerostomia e a êmese. A severidade das complicações citadas depende da dose e do agente quimioterápico empregado no tratamento (ARISAWA et al., 2005).

Diante do exposto, o desenvolvimento de novos fármacos e sistemas carreadores aplicados à terapia antineoplásica tem se tornado cada vez mais relevante, visto que a farmacoterapia disponível atualmente apresenta diversas limitações (LOPES et al., 2013b;

MROSS; KRATZ, 2011; SHI et al., 2017; ZUGAZAGOITIA et al., 2016). Neste contexto, várias formulações nanotecnológicas têm sido desenvolvidas, principalmente formulações lipossomais, que têm apresentado relevantes resultados pré-clínicos e clínicos (LOPES et al., 2013b; SEMPKOWSKI et al., 2014).

2 Lipossomas

Lipossomas (**Figura 1**) são vesículas esféricas compostas por uma ou mais bicamadas lipídicas concêntricas, que circundam um núcleo aquoso interno. Eles são formados geralmente por fosfolípides, os quais se organizam espontaneamente nessa conformação, quando dispersos em meio aquoso (BATISTA et al., 2007; LASIC, 1998). Sua estrutura anfifílica permite encapsular fármacos que apresentem qualquer tipo de polaridade. Além disso, suas propriedades (diâmetro médio, lamelaridade, carga, fluidez e superfície) podem ser modificadas em função dos requisitos farmacológicos, por meio da escolha da composição lipídica e do método de preparo (FRÉZARD et al., 2005).

Figura 1 – Representação esquemática das características estruturais dos lipossomas.

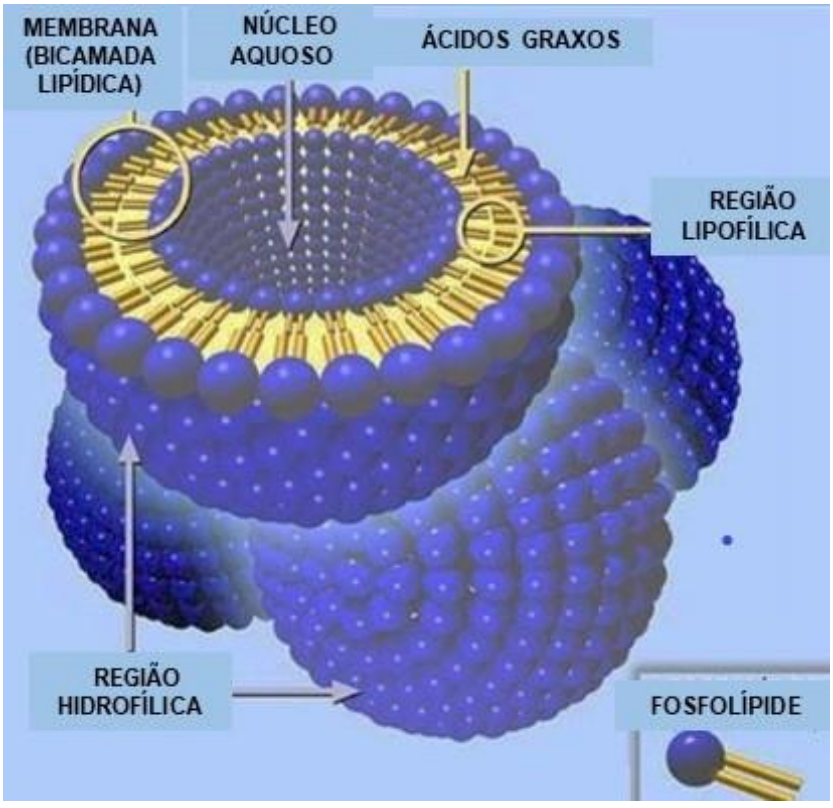

Adaptado de SR Brasil - Disponível em: <http://www.srbrasil.com/lipossomas.html>. Acesso em 9 de abril de 2019.

Os lipossomas podem ser classificados de acordo com o diâmetro médio e o número de bicamadas (LOPES et al., 2013a). Vesículas unilamelares pequenas (SUV, do inglês *Small Unilamellar Vesicle*) apresentam uma única bicamada lipídica com diâmetro médio entre 25 e 100 nm. Vesículas unilamelares grandes (LUV, do inglês *Large Unilamellar Vesicle*) são compostas por apenas uma bicamada e possuem diâmetro médio superior a 100 nm. Vesículas multilamelares (MLV, do inglês *Multilamellar Vesicle*) apresentam várias bicamadas concêntricas, cujo diâmetro médio total, encontra-se na faixa entre 1.000 e 5.000 nm (LASIC, 1998; LOPES et al., 2013a; VEMURI; RHODES, 1995) (**Figura 2**).

Figura 2 – Lipossomas classificados em termos de diâmetro médio e lamelaridade.

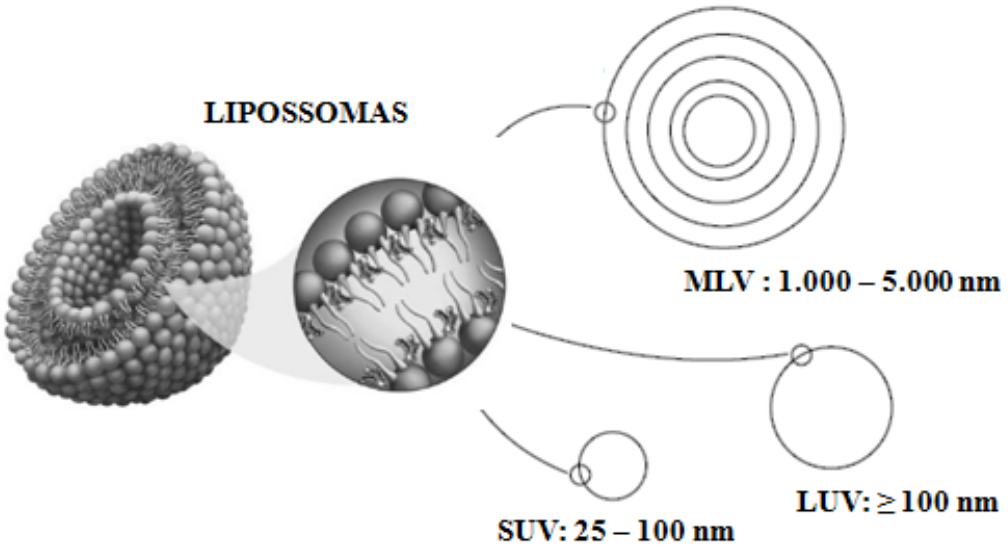

Adaptado de LASIC, 1998.
Abreviaturas: MLV, vesículas multilamelares; LUV, vesículas unilamelares grandes; SUV, vesículas unilamelares pequenas.

Durante o avanço da utilização de lipossomas como carreadores de fármacos, modificações estruturais têm sido realizadas, com o objetivo de assegurar a eficácia terapêutica. Os lipossomas passaram a ser classificados, também, com base na sua composição, mecanismo de liberação de fármacos e interação com sistemas biológicos (FERREIRA et al., 2013; LOPES et al., 2013a). Nesse contexto, destacam-se os lipossomas convencionais, de circulação prolongada e polimórficos.

2.1 Lipossomas convencionais

Os lipossomas convencionais podem apresentar diferentes composições; entretanto, os lípides mais utilizados nessas formulações são as fosfatidilcolinas e o colesterol. Fosfolípides carregados, negativamente ou positivamente, também podem ser adicionados nesse tipo de preparação, para favorecer a estabilidade, impedindo a coalescência das vesículas, por meio de repulsões eletrostáticas (BATISTA et al., 2007; FRÉZARD et al., 2005). A principal limitação dos lipossomas convencionais está relacionada ao seu curto tempo de circulação (HUWYLER et al., 2008). Quando administrados por via intravenosa, esses lipossomas sofrem adsorção de proteínas séricas denominadas opsoninas (imunoglobulinas, proteínas do sistema complemento, fibrinogênio), resultando em reconhecimento pelo sistema fagocitário mononuclear (SFM). O SFM é uma parte do sistema imune composta por monócitos e macrófagos, localizados no tecido conjuntivo reticular que envolve fígado, baço e medula óssea. Sendo assim, os lipossomas convencionais são rapidamente removidos da corrente sanguínea, devido à captação por células do SFM. Portanto, se acumulam preferencialmente em órgãos que compõem esse sistema (SHARMA, A.; SHARMA, U.S., 1997; TORCHILIN et al., 1994; ULRICH, 2002).

2.2 Lipossomas de circulação prolongada

Os lipossomas de circulação prolongada foram propostos após um estudo ter demonstrado que eritrócitos recobertos por uma camada hidrofílica, composta por um denso glicocálice, contendo alta concentração de ácido siálico, eram menos captados por macrófagos do SFM, quando comparados, com eritrócitos sem essas características de superfície (DUROCHER et al., 1975). Esse mesmo conceito foi aplicado ao desenvolvimento de lipossomas, objetivando aumentar o tempo de circulação, por meio da incorporação de componentes hidrofílicos naturais, como monossialogangliosídeo GM1, esfingomielina e fosfatidilinositol, à superfície lipossomal (BATISTA et al., 2007). Dentre os materiais sintéticos utilizados para aumentar o tempo de circulação de lipossomas, destaca-se o polietilenoglicol (PEG). Sabe-se que a adição de 5 a 10% de derivados lipídicos de PEG, às formulações lipossomais, reduz a opsonização, minimizando o reconhecimento pelas células do sistema imune, devido ao impedimento estérico, causado por esse polímero (KLIBANOV et al., 1990) (**Figura 3**). A utilização dessa proporção de PEG em lipossomas, também pode ser benéfica para a estabilidade das formulações, impedindo a coalescência das vesículas, por meio de repulsões estéricas (ULRICH, 2002). O uso de PEG na composição de lipossomas significou um grande avanço para o desenvolvimento desses nanosistemas, uma vez que esse polímero pode ser facilmente

produzido em escala industrial e não necessita dos processos de extração e purificação complexos, que os componentes hidrofílicos naturais requerem (LOPES et al., 2013a).

Figura 3 – Lipossoma de circulação prolongada contendo DSPE-PEG$_{2000}$ na superfície.

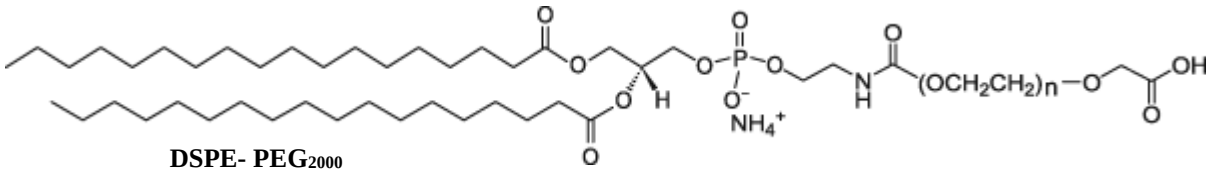

DSPE- PEG$_{2000}$

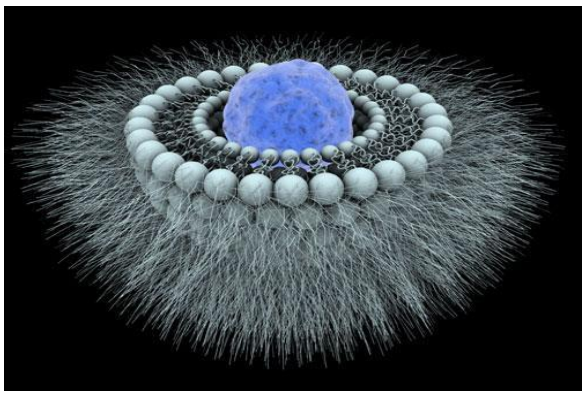

Adaptado de CNRS Photothèque Sagascience/ François Caillaud/Institut Galien Paris-Sud.
Disponível em: <http://phototheque.cnrs.fr>. Acesso em 9 de abril de 2019.
Abreviatura: DSPE-PEG$_{2000}$, diestearoilfosfatidiletanolamina acoplada ao polietilenoglicol de massa molar 2000.

2.3 Lipossomas polimórficos

Lipossomas convencionais e de circulação prolongada podem apresentar lenta liberação do fármaco encapsulado ou não serem capazes de fundir-se com o endossoma após a internalização celular (FERREIRA et al., 2013). Os lipossomas polimórficos, reativos a estímulos endógenos (pH, concentração plasmática de enzimas e agentes redutores) e exógenos (temperatura, campo magnético, ultrassom, luz, pulsos elétricos) podem ser utilizados para contornar esses problemas. Os nanocarreadores reativos a estímulos endógenos apresentam algumas limitações, uma vez que dependem de características impossíveis de controlar e que apresentam alta variabilidade entre diferentes pacientes (ex.: pH da região tumoral e níveis séricos de enzimas). Provavelmente por esse motivo, os nanosistemas responsivos a estímulos externos são considerados mais promissores e são os únicos nanocarreadores dessa classe que conseguiram chegar à fase de estudos clínicos, até o momento (**Tabela 1**) (MURA; COUVREUR, 2012; US NATIONAL LIBRARY OF MEDICINE, 2019).

Tabela 1 – Nanocarreadores responsivos a estímulos exógenos, em estudos clínicos.

Nanocarreador	Fármaco/Medicamento/Fabricante	Alvo	*Status* clínico	Referência *
Lipossomas termossensíveis	Doxorrubicina/ ThermoDox®/ Celsion Corporation (EUA) Composição: DPPC/MSPC/DSPE-PEG_{2000} (86,5:9,7:3,8) Doxorrubicina: 2 mg/mL	Carcinoma hepatocelular	Fase III	NCT00617981
		Carcinoma hepatocelular	Fase III	NCT02112656
		Câncer de mama recorrente	Fase I e II	NCT008226085
		Câncer de mama	Fase II	NCT02850419
		Metástases hepáticas de câncer coloretal	Fase II	NCT01464593
		Metástases ósseas, câncer de mama, câncer de pulmão de não pequenas células, câncer de pulmão de pequenas células, adenocarcinoma	Fase II	NCT01640847
		Carcinoma hepatocelular, neoplasia hepática	Fase I	NCT00441376
		Tumor hepático	Fase I	NCT02181075
		Câncer de mama	Fase I	NCT00346229
		Tumor sólido, câncer pediátrico (rabdomiossarcoma, Sarcoma de Ewing, sarcoma de partes moles, osteossarcoma, neuroblastoma, tumor de Wilms, tumor hepático, tumor de células germinativas)	Fase I	NCT02536183
Nanopartículas termossensíveis de sílica e ouro	Aurolase®/Nanospectra Biosciences (EUA)	Tumores pulmonares primários e metastáticos	Fase I	NCT01679470
		Câncer de cabeça e pescoço	Fase I	NCT00848042
		Neoplasia de próstata	Fase I	NCT02680535
Nanopartículas magnéticas de ferro e carbono	Doxorrubicina/MTC-DOX®/ FeRX (EUA)	Carcinoma hepatocelular	Fase II e III	NCT00034333
		Carcinoma hepatocelular	Fase I e II	NCT00054951
		Câncer de fígado metastático	Fase I e II	NCT00041808
Nanopartículas magnéticas de ferro	NanoTherm AS1®/MagForce Nanotechnologies (Alemanha)	Glioblastoma	Fase I	http://www.magforce.de/en/studien.html
		Carcinoma de próstata e pâncreas	Fase I e II	

Adaptado de MURA; COUVREUR, 2012. *Disponível em: <http://www.clinicaltrials.gov>. Acesso em 9 de abril de 2019. Abreviaturas: DPPC, dipalmitoilfosfatidilcolina; MSPC, monoesteroilfosfatidilcolina; DSPE-PEG_{2000}, diestearoilfosfatidiletanolamina acoplada ao polietilenoglicol de massa molar 2000.

2.3.1 Lipossomas polimórficos termossensíveis

Lipossomas termossensíveis são compostos por fosfolípides sintéticos, como por exemplo: a dipalmitoilfosfatidilcolina (DPPC) e a diestearoilfosfatidilcolina (DSPC). Geralmente, o fosfolípide DPPC (*Tc* = 41,4 °C) é empregado em maior proporção nas formulações, pois apresenta uma temperatura de transição de fase (*Tc*, do inglês *Chain melting Temperature*) pouco acima da temperatura corporal (37 °C) (DEMEL; DE KRUYFF, 1976).

Os fosfolípides possuem diversas formas de organização supramolecular, com temperaturas de transições características. A *Tc* corresponde à transição do estado em fase lamelar gel ordenado (Lβ), para fase lamelar fluída (Lα). Quando um lipossoma é composto por vários fosfolípides miscíveis, que apresentam diferentes valores de *Tc*, a transição Lβ → Lα, ocorre em uma temperatura intermediária entre a temperatura de todos os componentes (FRÉZARD et al., 1999). A liberação de um fármaco encapsulado em um lipossoma termossensível ocorre por transferência passiva, mediada por gradiente de concentração, e é máxima quando a temperatura é próxima à *Tc* (**Figura 4**) (GRÜLL; LANGEREIS, 2012; KNEIDL et al., 2014).

Figura 4 – Mecanismo de liberação de fármacos encapsulados em lipossomas termossensíveis.

Adaptado de KNEIDL et al., 2014.
Legenda: 1, à temperatura corporal, os fosfolípides estão organizados em Lβ e por isso a membrana apresenta baixa permeabilidade; **2**, ao elevar a temperatura acima da *Tc*, os fosfolípides assumem uma organização Lα, aumentando dessa forma, a permeabilidade da bicamada lipossomal; **3**, em uma temperatura próxima à *Tc*, a permeabilidade é máxima devido à coexistência de domínios Lβ e Lα.

Nas formulações termossensíveis, o fosfolípide DSPC (*Tc* = 54,9 °C) geralmente é empregado em menor proporção que DPPC. O objetivo deste componente no lipossoma é aumentar a estabilidade e evitar que ocorra liberação, do fármaco encapsulado, à temperatura corporal (GRÜLL; LANGEREIS, 2012).

A primeira formulação termossensível foi descrita no final da década de 1970. A composição original de DPPC: DSPC em razão molar de 3:1, foi modificada ao longo dos anos com o objetivo de contornar limitações, como por exemplo: rápida eliminação da circulação sanguínea e liberação lenta mesmo sob aquecimento (YATVIN et al., 1978).

Fosfolípides acoplados ao PEG passaram a ser incorporados na composição de lipossomas termossensíveis com o objetivo de criar uma barreira estérica que dificulta a ligação com opsoninas sanguíneas e reduz dessa forma, o reconhecimento pelo sistema imune. Estes lipossomas podem possuir um tempo de circulação prolongado e permitir uma distribuição do fármaco para outros órgãos além do SFM (PAPAHADJOPOULOS; GABIZON, 1990).

Tensoativos da classe dos lisofosfolípides, como por exemplo: monopalmitoilfosfatidilcolina (MPPC) e monoestearoilfosfatidilcolina (MSPC), também passaram a serem adicionados às formulações termossensíveis com o objetivo de permitir uma liberação mais rápida do conteúdo encapsulado. Isso ocorre porque na temperatura correspondente à *Tc*, o tensoativo desestabiliza a bicamada por meio da formação de poros na membrana lipossomal (KNEIDL et al., 2014). Em um estudo recente, empregando lipossomas termossensíveis compostos por MPPC e contendo doxorrubicina, foi demostrado a liberação de 80% do fármaco encapsulado, em apenas 20 segundos, quando os lipossomas foram incubados à temperatura de 41,3 °C (TA; PORTER, 2013). Por outro lado, para que uma formulação semelhante não contendo MPPC em sua composição, liberasse apenas 40% da doxorrubicina encapsulada, foi necessário um tempo superior (30 minutos) e uma temperatura mais elevada (42 °C) (GABER et al., 1995; NEEDHAM et al., 2000).

Um estudo *in vivo* recente investigou o efeito do tratamento quimioterápico com doxorrubicina nas formas livre, encapsulada em Doxil® (lipossoma de circulação prolongada) e encapsulada em lipossoma termossensível. Os resultados demonstraram que o tratamento com a formulação termossensível ocasionou um aumento significativo de fármaco disponível na região tumoral quando comparado aos outros grupos. Os pesquisadores atribuíram o sucesso da terapia termossensível à associação com a técnica de hipertermia local. Utilizando esta abordagem, regiões tumorais com escassa perfusão, conhecidas pela dificuldade de tratamento, devido ao mecanismo de resistência mediado por hipóxia, também podem ser alcançadas (**Figura 5**) (MANZOOR et al., 2012).

Figura 5 – Estimulação da liberação do conteúdo encapsulado em lipossomas termossensíveis.

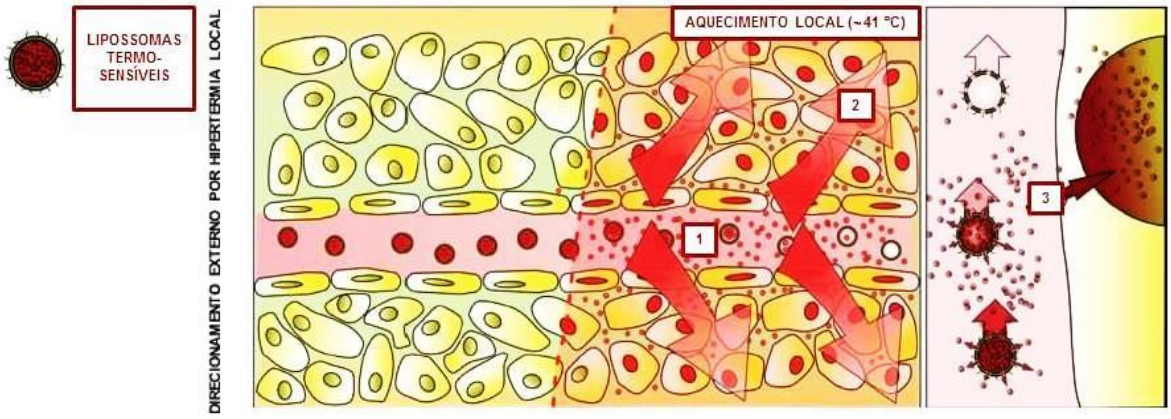

Adaptado de KNEIDL et al., 2014
Legenda: 1, A estimulação da liberação de conteúdo encapsulado em lipossomas termossensíveis ocorre de forma externa e mediada por hipertermia. Além disso, o controle do foco de aquecimento permite uma liberação intravascular (caso o aquecimento seja realizado imediatamente após a administração da formulação) ou intracelular (caso o aquecimento seja realizado após a internalização celular do nanossistema), gerando uma alta concentração de fármaco na região; **2**, o gradiente de concentração aumenta a profundidade de penetração do fármaco dentro do tumor; **3**, a liberação do fármaco na área alvo desencadeada por aquecimento permite que o fármaco esteja totalmente biodisponível para ser internalizado nas células tumorais (liberação intravascular) ou dentro das células tumorais (liberação intracelular).

A hipertermia é uma modalidade clínica em que o tecido tumoral é aquecido por um período de tempo pré-determinado (HILDEBRANDT et al., 2002). Esse tipo de tratamento é classificado conforme a faixa de aquecimento utilizada: (*i*) termoablação, (*ii*) hipertermia moderada e (*iii*) diatermia. Na termoablação, os tumores são submetidos às temperaturas entre 46 °C e 56 °C, resultando em morte celular por necrose. A hipertermia moderada é o procedimento mais empregado na terapia antitumoral. Neste caso, o tumor é exposto às temperaturas entre 41 °C e 45 °C. Esta faixa de aquecimento promove a desnaturação de proteínas importantes para a progressão do tumor e favorece a apoptose de células neoplásicas. A diatermia emprega temperaturas mais brandas, inferiores a 41 °C e é muito utilizada em fisioterapia (ISSELS et al., 2016; KUMAR; MOHAMMAD, 2011).

A hipertermia também pode ser classificada de acordo com a localização do aquecimento utilizado. A hipertermia total é aplicada aos cânceres metastáticos e seu maior desafio, até o momento, diz respeito à especificidade do tratamento. Maiores investigações ainda são necessárias para garantir que danos não sejam causados aos tecidos saudáveis (MURA; COUVREUR, 2012). A hipertermia regional envolve o aquecimento completo de tecidos e órgãos. A hipertermia local é empregada em um alvo limitado, como por exemplo, um tumor primário (FALK; ISSELS, 2001; HABASH et al., 2006). Em comparação com os outros tipos de hipertermia, a local tem sido a mais utilizada devido à sua maior especificidade e à maior

penetração na região de interesse, podendo inclusive realizar aquecimento intracelular (KUMAR; MOHAMMAD, 2011).

Várias técnicas são capazes de gerar aquecimento, e, portanto, podem ser utilizadas para induzir hipertermia. Dentre as mais empregadas destacam-se: aplicação de radiação infravermelha, ultrassom, micro-ondas e indução magnética (MURA; COUVREUR, 2012; NCI, 2011; THERMOSOME, 2016).

3 Métodos de preparo de lipossomas

A escolha adequada da composição lipídica e do método de preparo de lipossomas pode modular as características físico-químicas das vesículas obtidas, e dessa forma, influenciar o sucesso terapêutico da formulação (FRÉZARD et al., 2005). Embora os lipossomas sejam formados espontaneamente a partir da hidratação de fosfolípides, diferentes métodos de obtenção de vesículas são descritos, e etapas adicionais de calibração de tamanho e separação do conteúdo não encapsulado, são necessárias, para obtenção de formulações adequadas para aplicação clínica. Sendo assim, o preparo completo de lipossomas envolve três principais etapas: (*i*) formação; (*ii*) calibração e (*iii*) purificação das vesículas (LOPES et al., 2013a).

O método de hidratação do filme lipídico (BANGHAM) é um dos mais utilizados na etapa de formação das vesículas (BANGHAM et al., 1965). Ele consiste inicialmente, na preparação de soluções estoque de fosfolípides, e de outros constituintes lipídicos da formulação, por meio da dissolução desses compostos, em um solvente orgânico volátil, como por exemplo clorofórmio, éter ou álcoois. O preparo de soluções estoques concentradas de fosfolípides ajuda a garantir a reprodutibilidade dos lipossomas, pois evita o erro experimental associado às pesagens sucessivas de quantidades muito reduzidas desses componentes. Alíquotas das soluções preparadas, são adicionadas em um balão de fundo redondo e a evaporação do solvente é realizada sob pressão reduzida em um evaporador rotativo. A capacidade volumétrica do balão de fundo redondo e suas condições de inclinação e rotação no evaporador rotativo, devem ser adequadas, para permitir a obtenção de um filme lipídico de menor espessura possível, para aumentar a superfície de contato disponível para hidratação na etapa seguinte, podendo assim, favorecer o aumento da taxa de encapsulação (NEW, 1990; SZOKA; PAPAHADJOPOULOS, 1980). O filme lipídico obtido é então, hidratado com uma solução aquosa, geralmente tamponada, em temperatura superior à T_c do componente lipídico mais rígido da formulação. Após dispersão dos lípides por meio de agitação em vórtex, com auxílio de pérolas de vidro, são obtidas as vesículas MLV (**Figura 6**). Fármacos lipofílicos

devem ser adicionados junto aos fosfolípides da formulação, enquanto fármacos hidrofílicos devem ser adicionados na etapa de hidratação do filme lipídico, dissolvidos ou dispersos na solução aquosa. As vesículas obtidas por esse método são heterogêneas, apresentando diâmetro médio elevado, variando entre 1.000 e 5.000 nm (LAOUINI et al., 2012). Embora o método de BANGHAM seja o procedimento mais simples e rápido, e que apresenta o menor custo para obtenção de lipossomas, seu uso é limitado, devido às baixas porcentagens de encapsulação obtidas para substâncias hidrofílicas, correspondendo entre 5 e 15% da quantidade inicial de fármaco adicionado durante o preparo (NEW, 1990; MAIA et al., 2015; SHARMA, A.; SHARMA, U., 1997). Sabe-se que a associação entre um longo tempo de hidratação e agitação suave em vórtex, podem garantir que taxas mais altas de encapsulação sejam obtidas (SZOKA; PAPAHADJOPOULOS, 1980).

Figura 6 – Mecanismo de formação de lipossomas MLV pelo método de BANGHAM.

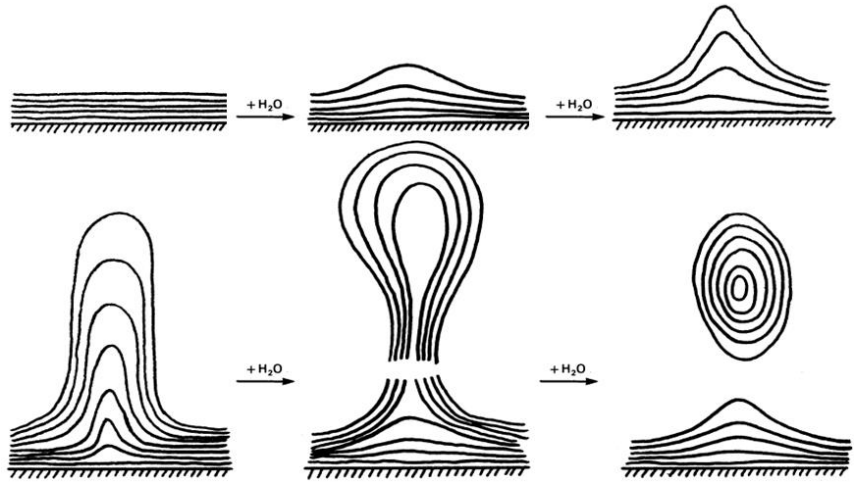

Adaptado de DELATTRE et al., 1993; LASIC, 1988.

A evaporação em fase reversa (REV) constitui outro método, amplamente utilizado na etapa de formação das vesículas (SZOKA; PAPAHADJOPOULOS, 1978). Este procedimento, é o mais indicado para encapsulação de substâncias hidrofílicas, devido à produção de lipossomas LUV, que apresentam uma grande cavidade aquosa interna (MAIA et al., 2015). Nesse método, não é necessário a formação prévia de um filme lípidico, entretanto, muitas vezes essa etapa é realizada a fim de favorecer a reprodutibilidade da formulação, uma vez que o filme lipídico é obtido a partir das soluções estoque de lípides.

No procedimento por REV, inicialmente, os fosfolípides e outros constituintes lípidicos da formulação, são dissolvidos em éter dietílico ou em uma mistura de éter e clorofórmio em

proporção igual a 1:1, dependendo da solubilidade dos componentes (**Figura 7 A**) (NEW, 1990). O éter adicionado na preparação, deve ser previamente tratado com uma solução aquosa de bissulfito de sódio ou tampão HEPES, afim de eliminar peróxidos que podem degradar os lípides e/ou o fármaco encapsulado (SZOKA; PAPAHADJOPOULOS, 1980).

Figura 7 – Mecanismo de formação de lipossomas LUV pelo método REV.

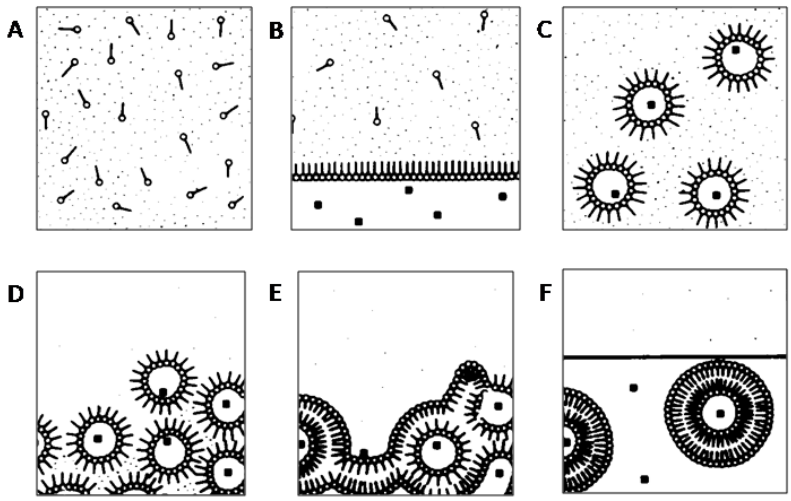

Adaptado de SZOKA; PAPAHADJOPOULOS, 1978.

Em seguida, o material aquoso é adicionado diretamente à mistura de fosfolípides e solventes. A proporção utilizada de fase aquosa/éter, é igual a 1:3, respectivamente, e fase aquosa/mistura de éter e clorofórmio, igual a 1:6, respectivamente (NEW, 1990). Nesse momento, os fosfolípides se posicionam na interface entre as duas fases imiscíveis (**Figura 7B**). Após agitação em vórtex durante cinco minutos, os lípides que compõem a preparação se organizam em micelas inversas, resultando na formação de uma emulsão do tipo água em óleo (A/O) (**Figura 7C**). A formação adequada dessa emulsão é uma condição essencial para se obter lipossomas LUV com altas taxas de encapsulação. O próximo passo, consiste em remover o solvente orgânico, por evaporação sob pressão reduzida. Novamente, a escolha adequada da capacidade do balão de fundo redondo, é importante, pois caso a razão entre área superficial e volume de preparação, for muito elevada, o solvente poderá ser removido rapidamente, podendo inclusive, ocasionar a formação de lipossomas MLV (SZOKA; PAPAHADJOPOULOS, 1980). A evaporação do solvente, resulta na aproximação das micelas inversas (**Figura 7D**) e na formação de um gel viscoso (**Figura 7E**). Na etapa seguinte, a pressão é reduzida à um valor ainda menor, para favorecer à evaporação completa do éter. Quando todo o solvente residual é removido, a fase de gel é rompida, e as

monocamadas das micelas inversas se unem para formar as bicamadas lipossomais (**Figura 7F**). É importante remover todos os vestígios de solventes após a preparação, para garantir a estabilidade de armazenamento dos lipossomas preparados por esse método (SZOKA; PAPAHADJOPOULOS, 1980). As vesículas LUV obtidas, apresentam diâmetro médio entre 100 e 1.000 nm (LOPES et al., 2013a). A porcentagem de encapsulação varia entre 20 e 65%, dependendo da força iônica da solução aquosa utilizada (MAIA et al., 2015). Quanto maior a força iônica, menor será a porcentagem de encapsulação, podendo inclusive, ser inferior aos 20% definidos como a porcentagem mínima de encapsulação obtida por esse método (SZOKA; PAPAHADJOPOULOS, 1980). Embora REV proporcione altas taxas de encapsulação para substâncias hidrofílicas, trata-se de um procedimento longo e complexo. Além disso, os fosfolípides que compõem a formulação devem ser solúveis em éter dietílico ou éter e clorofórmio (NEW, 1990; SZOKA; PAPAHADJOPOULOS, 1978).

Os métodos de calibração das vesículas são utilizados para obter formulações homogêneas, com diâmetro médio adequado para administração intravenosa. Dentre os métodos mais utilizados destacam-se a sonicação, utilizando sondas de ultrassom de alta energia, e a extrusão em membranas de policarbonato, sob alta pressão. A sonicação consiste em um procedimento simples e rápido, entretanto, a alta energia utilizada pode ser prejudicial às vesículas, causando defeitos na membrana lipossomal, podendo resultar em liberação indesejável do material encapsulado. Durante a sonição é produzido um aerossol que pode conter substâncias da preparação (citostáticos, material radioativo). Sendo assim, medidas de segurança devem ser adotadas, para evitar contaminação ao manipulador (DELATTRE et al., 1993). Além disso, outra desvantagem dessa técnica é que o material presente na sonda (geralmente titânio) pode contaminar os componentes da formulação (VEMURI; RHODES, 1995). A extrusão em membranas de policarbonato é o método mais reprodutível para calibração das vesículas. Por esse procedimento, é possível obter formulações homogêneas, cujo diâmetro médio pode ser modulado com base no tamanho do poro das membranas de policarbonato utilizadas. Trata-se de um método não agressivo, uma vez que as vesículas são flexíveis e se reorganizam após passar pelo extrusor. Em comparação com a sonicação, a extrusão é um procedimento mais demorado, entretanto, produz melhores resultados em termos de diâmetro e índice de polidispersão reduzidos (DELATTRE et al., 1993).

Dentre os métodos de purificação de vesículas os mais empregados, para fármacos hidrofílicos são: cromatografia de exclusão de tamanho, diálise e ultracentrifugação (LAOUINI, et al. 2012). Os géis de dextrano reticulado (Sephadex®) são os mais utilizados para separação de substâncias não encapsuladas, em lipossomas, por cromatografia por

exclusão de tamanho. Para esse tipo de separação, o diâmetro das esferas de gel devem ser selecionados de acordo com o tamanho das vesículas obtidas. Também é recomendado que a coluna seja previamente eluída com lipossomas brancos, a fim de saturar os sítios de adsorção de lípides e prevenir perdas durante o processo. Essa técnica apresenta como principal limitação, a diluição das formulações. A separação do conteúdo não encapsulado em lipossomas por diálise, embora seja um procedimento demorado, não requer a utilização de nenhum tipo de equipamento especial. Nesse caso, o cuidado necessário diz respeito à escolha adequada das condições de separação, para garantir que não ocorra a indução de liberação do material encapsulado. Em razão das diferenças de densidade entre os componentes dos lipossomas, é possível utilizar a ultracentrifugação como um método de separação (DELATTRE et al., 1993). Nessa técnica, os lipossomas contendo material encapsulado sedimentam-se formando *pellets* no fundo do tubo de ultracentrifugação, enquanto o material não encapsulado encontra-se solubilizado no sobrenadante. A definição do tempo e da velocidade de rotação irá depender do tamanho dos lipossomas obtidos. Sabe-se que partículas maiores sedimentam-se mais rapidamente do que partículas menores com forma e densidades similares (KARP, 2005).

4 Gd-DTPA-BMA: potencial agente quimioterápico

Gd-DTPA-BMA (591,67 g/mol) é um complexo de gadolínio (Gd), cuja estrutura é composta por dois grupos carboxilatos do ácido dietilenotriaminopentaacético (DTPA) substituídos por dois grupos metilamida (BMA) (**Figura 8**). Sua utilização clínica teve início em 1993, com a aprovação da solução injetável Omniscan®, nos Estados Unidos. Gd-DTPA-BMA é um agente de contraste paramagnético, linear, não iônico, cuja atividade é extracelular e inespecífica. Sua ampla utilização em diagnóstico por imagem empregando a técnica de ressonância magnética ocorre devido a sua baixa quimiotoxicidade e alta estabilidade em pH fisiológico (RUNGE, 2000; LIU; ZHANG, 2012).

O gadolínio presente em Gd-DTPA-BMA é uma mistura de sete isótopos: ^{152}Gd (0,20%), ^{154}Gd (2,18%), ^{155}Gd (14.80%), ^{156}Gd (20,47%), ^{157}Gd (15, 65%), ^{158}Gd (24,84%) e ^{160}Gd (21,86%). O isótopo mais abundante (^{158}Gd), quando submetido à irradiação neutrônica, captura um nêutron, e se torna ^{159}Gd (GOORLEY; NIKJOO, 2000; MAIA et al., 2016; SOARES et al., 2010). Até recentemente, o radioisótopo ^{159}Gd era citado na literatura como um potencial radiofármaco para o tratamento antitumoral baseado apenas em suas características físicas: meia vida física de 18,59 horas, modo de decaimento beta negativo

com energia média de 1,01 MeV e energia gama associada de 0,36 MeV, assim como, alta atividade específica (NEVES et al., 2005; OLIVEIRA et al., 2006; SAHA, 2010).

Figura 8 – Estrutura química de Gd-DTPA-BMA.

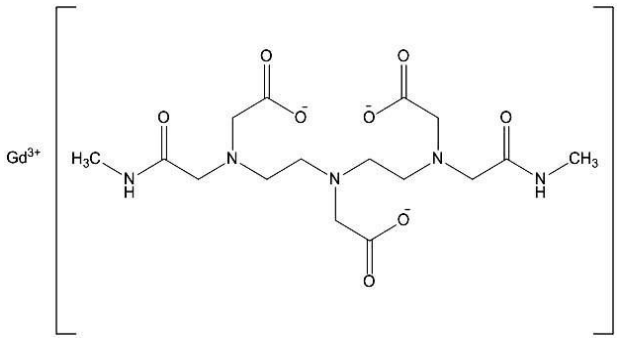

Em 2009, nosso grupo de pesquisa iniciou estudos para avaliar a atividade citotóxica de Gd-DTPA-BMA irradiada e não irradiada, livre ou encapsulada em lipossomas, empregando os modelos tumorais Ehrlich (adenocarcinoma mamário murino) e RT2 (glioblastoma murino). Os resultados mostraram que o fator que mais influenciou na atividade citotóxica *in vitro* foi a forma de apresentação do fármaco em lipossomas, pois permitiu a internalização celular desse complexo, que é extremamente hidrofílico. Também foi observado que a atividade citotóxica pode ser potencializada utilizando o complexo na forma radioativa (SOARES et al., 2011a; SOARES et al., 2011b).

Um estudo *in vivo*, realizado por nosso grupo, mostrou que camundongos portadores do tumor de Ehrlich, submetidos ao tratamento com Gd-DTPA-BMA lipossomal apresentaram redução significativa no volume tumoral. Estudos de biodistribuição, utilizando o mesmo modelo animal e empregando o complexo radioativo, mostraram que a encapsulação em lipossomas permitiu um acúmulo do fármaco lipossomal na região tumoral 82 vezes superior que os valores encontrados para o fármaco na forma livre (SOARES et al., 2012).

A atividade citotóxica de Gd-DTPA-BMA não radioativo, também foi demonstrada por nosso grupo, frente ao modelo tumoral 4T1 (adenocarcinoma mamário murino), cujo comportamento é altamente invasivo e mais agressivo, que os modelos anteriormente investigados. Para esta avaliação foram empregadas três formulações: lipossoma pH-sensível, lipossoma pH-sensível de circulação prolongada e lipossoma convencional. A citotoxicidade de Gd-DTPA-BMA nos três lipossomas foi superior à citotoxicidade de Gd-DTPA-BMA na forma livre. O aumento na atividade citotóxica foi de cerca de 5 vezes para a formulação

convencional e entre 25 e 37 vezes para as formulações pH-sensível de circulação prolongada e pH-sensível, respectivamente (MAIA, 2015; MAIA et al., 2016).

Resultados obtidos por nosso grupo de pesquisa sugerem que o provável mecanismo de ação antitumoral de Gd-DTPA-BMA, na forma radioativa, ocorre por apoptose, envolvendo a ativação de caspases-3. Além disso, esse processo parece ser dependente da ação da proteína *p53* (SOARES et al., 2013).

Em relação à atividade antitumoral da forma não radioativa, ainda não há nenhum estudo que tenha investigado seu mecanismo. Uma hipótese provável é que ele ocorra de maneira semelhante à forma radioativa. Em ambos os casos, o processo de apoptose seria iniciado por estresse oxidativo, como ocorre com o quimioterápico Motexafin-Gadolinium, um complexo de Gd não radioativo semelhante à Gd-DTPA-BMA (SINGH et al., 2010).

Diversos estudos são reportados na literatura utilizando Gd-DTPA-BMA encapsulada em lipossomas termossensíveis, com finalidade de diagnóstico. Um estudo atual comparou lipossomas contendo os seguintes complexos de Gd: Gd-DTPA-BMA, gadopentetato de dimeglumina (Gd-DTPA), gadobenato de dimeglumina (Gd-BOPTA), gadoterato de meglumina (Gd-DOTA), gadobutrol (Gd-BT-DO3A) e gadoteriol (Gd-HP-DO3A). Os resultados revelaram que a estrutura (linear ou macrocíclica) e a carga (iônica ou não iônica) desses complexos não influenciaram as características físico-químicas dos lipossomas. Independente do complexo utilizado, não houve diferença significativa entre os valores de diâmetro médio, potencial zeta e índice de polidispersão de todas as formulações. Os lipossomas com maior teor de encapsulação foram os que continham Gd-DTPA-BMA e Gd-HP-DO3A, devido à menor osmolaridade desses complexos em comparação com os demais. Ao final do estudo, considerou-se a formulação de Gd-DTPA-BMA mais promissora, devido à quantidade de fármaco encapsulado e à sua estabilidade. Foi comprovado que os outros complexos induziram a hidrólise lipídica das formulações. O lipossoma contendo Gd-DTPA-BMA foi o único que pôde ser armazenado por várias semanas, mantendo-se estável (HOSSANN et al., 2013).

Não há relatos de estudos na literatura, até a presente data, que tenham investigado o potencial de lipossomas termossensíveis contendo Gd-DTPA-BMA para o tratamento do câncer. Desta forma, a proposta principal do presente trabalho consistiu em desenvolver, e caracterizar lipossomas termossensíveis contendo Gd-DTPA-BMA. Além disso, objetivou-se avaliar sua potencial atividade citotóxica frente às diferentes linhagens de câncer de mama.

PARTE 2 – TRABALHO EXPERIMENTAL

CHAPTER 1

Chemometric-assisted hydrophilic interaction chromatographic method for the determination of gadolinium-based magnetic resonance imaging contrast agent in liposomes. *J. Braz. Chem. Soc.*, v. 29, n. 11, p. 2426-2440, 2018.

CHEMOMETRIC-ASSISTED HYDROPHILIC INTERACTION CHROMATOGRAPHIC METHOD FOR THE DETERMINATION OF GADOLINIUM-BASED MAGNETIC RESONANCE IMAGING CONTRAST AGENT IN LIPOSOMES

Ana Luiza C. Maia[a], Pedro Henrique R. da Silva[a], Christian Fernandes[a], Aline T. M. e Silva[a], André Luís B. de Barros[b], Daniel Crístian F. Soares[c]*, and Gilson A. Ramaldes[a]

[a] Departamento de Produtos Farmacêuticos, Faculdade de Farmácia, Universidade Federal de Minas Gerais, Belo Horizonte, Minas Gerais, Brazil.

[b] Departamento de Análises Clínicas e Toxicológicas, Faculdade de Farmácia, Universidade Federal de Minas Gerais, Belo Horizonte, Minas Gerais, Brazil.

[c] Departamento de Química e Matemática, Instituto de Ciências, Universidade Federal de Itajubá, Itabira, Minas Gerais, Brazil.

* soares@unifei.edu.br

ABSTRACT

Gadodiamide (Gd-DTPA-BMA) is a gadolinium (Gd) chelate composed of two carboxylate groups of diethylenetriaminepentaacetic acid (DTPA) and of two amide groups (BMA). Gd complexes are the most widely used contrast agents in nuclear magnetic resonance. Furthermore, our research group has demonstrated the potential of liposomes containing Gd-DTPA-BMA for cancer therapy. The aim of this study was to develop and validate a chemometric-assisted method by hydrophilic interaction liquid chromatography (HILIC) for determination of Gd-DTPA-BMA in liposomes. The chromatographic conditions obtained were: Sequant® ZIC®-HILIC Merck (150 x 4.6 mm, 3.5 μm, 100 Å) column, mobile phase composed of ACN/NH_4FA 5 mmol L^{-1}, pH 4.5 (60:40 v/v) at 0.6 mL min^{-1}, injection volume of 20 μL, temperature of 30 °C, and detection at 210 nm. The linear range was of 40 to 120 nmol mL^{-1}. The use of chemometrics allowed obtaining optimal chromatographic parameters, in terms of signal-to-noise ratio, resolution, and asymmetry.

KEYWORDS: gadodiamide, liposomes, hydrophilic interaction chromatography, chemometrics, Box-Behnken.

1 INTRODUCTION

Gadodiamide (Gd-DTPA-BMA, **Figure 1**), a gadolinium (Gd) complex, is one of the most commonly used contrast agent in diagnosis by imaging, due to its low chemotoxicity. In addition, several studies have reported that there is no evidence of endogenous transmetalation or *in vivo* metabolism of this complex. Despite this, its administration is contraindicated in patients which presenting chronic renal failure due to the risk of developing Nephrogenic Systemic Fibrosis.[1-3] Recently, the European Medicines Agency (EMA) reported that Gd deposition can occurs in brain tissues following use contrast agents containing Gd. Until the present date, there is no evidence that Gd deposition in the brain has caused any harm to patients. In order to prevent any risks that could potentially be occurs, EMA has recommended restrictions and suspensions for use of some intravenous linear agents containing Gd.[4] Several studies have reported the encapsulation of Gd-DTPA-BMA and other Gd complexes in liposomes for diagnostic purposes.[5-7] The antitumor activity of this complex in the liposomal form is also being investigated, since Gd-DTPA-BMA induces the apoptosis of neoplastic cells through the activation of *caspase-3*.[3,8-12] In this context, thermosensitive liposomes constitute promising nanocarriers since they may contribute to increased treatment efficacy due to the association with hyperthermia techniques.[13]

Figure 1 – Structure and spectrum in the ultraviolet region of Gd-DTPA-BMA at 57 mg mL^{-1} in purified water.

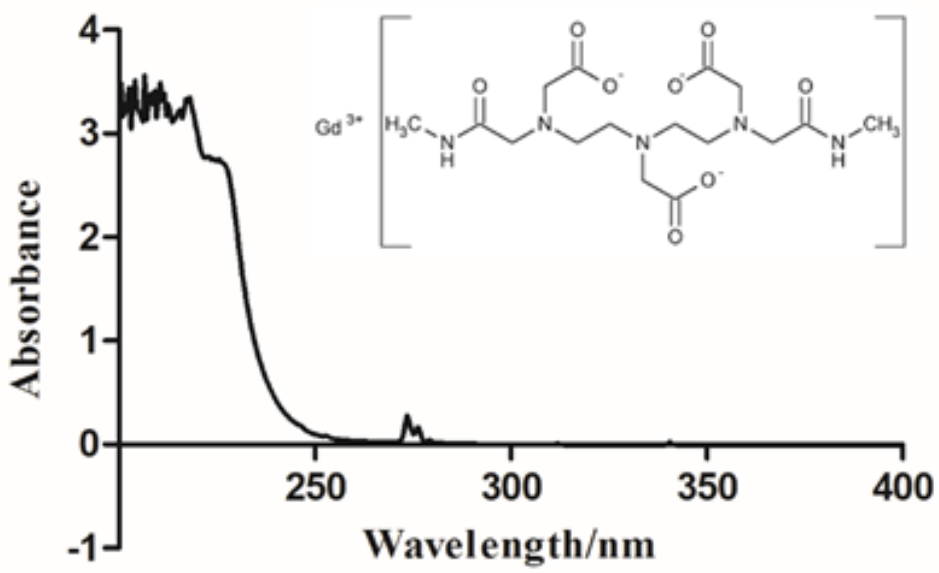

The determination of Gd-DTPA-BMA in environmental and biological samples has been performed most often by expensive techniques requiring complex instrumentation, such as inductively coupled plasma optical emission spectrometry and high performance liquid chromatography coupled to mass spectrometry (LC-MS).[14-17] The Gd-DTPA-BMA quantification method described in the United States Pharmacopeia employs LC with post-column derivatization to enable the detection of the complex in the region of the visible spectrum.[18] However, derivatization generally requires special instrumentation and high reagent consumption. In addition, this additional step makes the analysis more time consuming.[2] The determination of Gd-DTPA-BMA by LC using radioactivity detectors has also been described.[17,19] In this case, the main disadvantage is related to the requirement of prior radiolabelling of the complex. In this context, the development of simpler, faster and low cost methods for determination of Gd-DTPA-BMA is extremely useful, mainly for determination of this complex in liposomal formulations. The development of liposomes can be laborious and consists of several stages. Thus, rapid information about the influence of changes in the formulation or in the preparation method on the amount of drug entrapment is required. Our group recently developed methods for quantification of Gd-DTPA-BMA by reverse phase liquid chromatography (RP-LC) and derivative spectrophotometry. In both methods, detection was performed in the ultraviolet region.[2] The spectrophotometric method presented low detectability, while retention of Gd-DTPA-BMA in RP-LC was challenging due to its high polarity. Moreover, RP-LC method is not appropriate for determination of this drug in more complex matrices, such as serum, plasma, culture medium or buffers fortified with blood proteins. In these cases, RP-LC does not present adequate resolution. In addition, due to the impossibility to use any organic solvent in the mobile phase, optimization is limited.

Hydrophilic interaction liquid chromatography (HILIC) has been the technique of choice for the determination of polar compounds, especially metallic complexes.[20] The increased use of HILIC may be related to its ability to resolve limitations of conventional chromatography. An example is the analysis of polar substances that present low retention in RP-LC.[21] In HILIC, several chromatographic parameters can interfere in the retention and separation of the compounds. For this reason, the use of chemometric tools during the development of analytical methods is a useful approach.[21,22] Recently, chemometrics have gained importance in the development of chromatographic methods, as can be observed in the scientific literature.[23,24]

Some methods for Gd-DTPA-BMA determination in biological and environmental samples by HILIC are described in the literature.[20,25-29] However, none of these studies reported the determination of Gd-DTPA-BMA in liposomes, making necessary further investigations. Moreover, few data are presented in these studies concerning method optimization. In addition, to our knowledge, no studies have been reported on the development of method for determination of Gd-DTPA-BMA by HILIC, in which a rational approach has been used.

In this context, the aim of this study was to develop and validate an analytical method for the determination of Gd-DTPA-BMA in liposomes by HILIC. For this, Box-Behnken factorial planning and response surface methodology were used during method development. The method was validated according to the Brazilian legislation and the Validation Guidelines for Analytical Procedures ICH QR2 and applied for determination of Gd-DTPA-BMA entrapment in liposomes.[30,31]

2 EXPERIMENTAL

2.1 Materials

Gd-DTPA-BMA (Omniscan®, General Electric Healthcare Company, Ireland) was purchased from HDL Logística Hospitalar (Uberlândia, Brazil), batch 12.747.449, content of 99.7%. Dipalmitoylphosphatidylcholine (DPPC), distearoylphosphatidylcholine (DSPC), and distearoylphosphatidylethanolamine-polyethyleneglycol$_{2000}$ (DSPE-PEG$_{2000}$) were purchased from Lipoid GmbH (Ludwigshafen, Germany). Monostearoylphosphatidylcholine (MSPC) was purchased from Avanti Lipids (Alabama, USA). HEPES (4-(2-hydroxyethyl)-1-piperazine-ethanesulfonic acid) was purchased from Sigma Chemical Company (St. Louis, USA). Acetonitrile (ACN) HPLC grade was purchased from Tedia Brazil (Rio de Janeiro, Brazil) and from J. T. Baker (Pennsylvania, USA). Hydrochloric acid and chloroform were purchased from LabSynth (São Paulo, Brazil). Diethyl ether, and isopropyl alcohol HPLC grade were purchased from Vetec (Rio de Janeiro, Brazil). The water used to prepare all the solutions and samples was purified on a Milli-Q® Direct-Q3 Millipore system (Billerica, USA). Ammonium acetate (NH_4Ac) was purchased from Neon (São Paulo, Brazil). Ammonium formate (NH_4FA) was purchased from Spectrum (São Paulo, Brazil) and from Vetec (Rio de Janeiro, Brazil).

2.2 Chromatographic conditions

HILIC was performed using a 1260 series chromatograph (Agilent Technologies, California, USA), equipped with a degasser, a quaternary pump (G1311B), a column oven (G1316A), an autosampler (G1329B), and a diode array detector (DAD) (G4212B), coupled to the EzChrom integration program. The chromatographic conditions of the developed method were: Sequant® ZIC®-HILIC Merck (150 x 4.6 mm, 3.5 μm, 100 Å) column (Darmstadt, Germany), mobile phase composed of ACN/NH_4FA 5 mmol L^{-1}, pH 4.5 (60:40 v/v) isocratically eluted at a flow-rate of 0.6 mL min^{-1}, injection volume of 20 μL, temperature of 30 °C, and detection at 210 nm.

2.3 Preparation of liposomes

Thermosensitive formulations containing Gd-DTPA-BMA were prepared by reverse-phase evaporation method using the procedure described in a previous study by our research group.[3,32] The total lipid concentration for the two liposomes was 40 mmol L^{-1}. The composition of each formulation was chosen based on the studies of Li *et al.*[33] For the preparation of the traditional thermosensitive liposome (TTSL-Gd), chloroform aliquots of DPPC, DSPC, and DSPE-PEG_{2000}, in a lipid molar ratio of 80:15:5 were transferred to a round-bottomed flask and subjected to solvent evaporation under reduced pressure. The thermosensitive liposome containing lysophospholipid (LTSL-Gd) was prepared from chloroform aliquots of DPPC, MSPC, and DSPE-PEG_{2000}, in lipid molar ratio of 85:10:5. The lipid film obtained in both cases was dissolved in diethyl ether, previously treated with a solution of 10 mmol L^{-1} HEPES buffer. After complete dissolution of the lipids, an aqueous solution of Gd-DTPA-BMA (250 μmol mL^{-1}) was added, maintaining the aqueous phase: organic phase ratio at 1:3. Then, the dispersion obtained was subjected to vigorous vortexing at 3000 rpm for 5 minutes, producing a water in oil (W/O) emulsion. Subsequently, the W/O emulsion was subjected to evaporation under reduced pressure to remove the organic solvent, enabling the formation of lipid vesicles. Then, the obtained liposomes were calibrated employing 10 cycles of extrusion on polycarbonate membranes of 0.4, 0.2, and 0.1 μm pore sizes, under nitrogen pressure, at 55 °C. Nonentrapped Gd-DTPA-BMA was separated from liposomes by ultracentrifugation at 350,000 x *g*, at 4 °C for 2 hours. After ultracentrifugation, the pellet was reconstituted in HEPES buffer to obtain the same initial volume. To obtain the

traditional thermosensitive liposomes (TTSL) and thermosensitive liposome containing lysophospholipid (LTSL) without Gd-DTPA-BMA, the same experimental protocol was performed, except for the step of addition of the drug, which was replaced by the addition of HEPES buffer.

2.4 HILIC method development

Initially, a review of the literature was carried out to determine the critical independent variables for the development of methods for determination of Gd-DTPA-BMA by HILIC. To determine the detection wavelength, the UV spectrum in the range of 200 to 400 nm of a Gd-DTPA-BMA sample at 57 mg mL^{-1} was obtained. The analyses were performed using a Shimadzu 1800 series UV-Vis spectrophotometer (Tokyo, Japan). Then, 11 experiments were performed as described in **Table 1** to investigate the range of variation and levels at which independent variables should be evaluated in a factorial design. In each experiment, nine determinations were performed, being three determinations on a sample of Gd-DTPA-BMA at 0.5 μmol mL^{-1}, three determinations on a sample of TTSL spiked with Gd-DTPA-BMA at 0.5 μmol mL^{-1} and three determinations on a sample of LTSL spiked with Gd-DTPA-BMA at 0.5 μmol mL^{-1}.

Table 1 – **Variables screening for development of method for determination of Gd-DTPA-BMA in liposomes by HILIC.**

Experiment	Parameter evaluated	Independent variable	Mobile phase composition
1	Type of buffer	NH_4Ac	ACN/NH_4Ac 10 mmol L^{-1}, pH 5.8, (70:30 v/v)
2		NH_4FA	ACN/NH_4FA 10 mmol L^{-1}, pH 4.7, (70:30 v/v)
3	ACN ratio	60%	ACN/NH_4FA 10 mmol L^{-1}, pH 4.7, (60:40 v/v)
4		70%	ACN/NH_4FA 10 mmol L^{-1}, pH 4.7, (70:30 v/v)
5		75%	ACN/NH_4FA 10 mmol L^{-1}, pH 4.7, (75:25 v/v)
6	Buffer concentration	5 mmol L^{-1}	ACN/NH_4FA 5 mmol L^{-1}, pH 4.7, (70:30 v/v)
7		10 mmol L^{-1}	ACN/NH_4FA 10 mmol L^{-1}, pH 4.7, (70:30 v/v)
8		15 mmol L^{-1}	ACN/NH_4FA 15 mmol L^{-1}, pH 4.7, (70:30 v/v)
9	The aqueous phase pH of the mobile phase	2.7	ACN/NH_4FA 10 mmol L^{-1}, pH 2.7,(70:30 v/v)
10		3.7	ACN/NH_4FA 10 mmol L^{-1}, pH 3.7, (70:30 v/v)
11		4.7	ACN/NH_4FA 10 mmol L^{-1}, pH 4.7, (70:30 v/v)

The optimization of the chromatographic parameters was performed using Box-Behnken factorial design and response surface methodology.[34] Three independent variables at three levels (−1, 0 and 1) were evaluated: X_1 = buffer pH, level −1 = 3.7, level 0 = 4.2 and level +1 = 4.7; X_2 = ACN ratio in the mobile phase (%), level −1 = 60, level 0 = 65, level +1 = 70; X_3 = buffer concentration (mmol L^{-1}), level −1 = 5, level 0 = 15, level +1 = 25. The dependent variables evaluated as responses were: signal-to-noise ratio, resolution (R_s), and asymmetry (A_s). Fifteen experiments were performed in random order, including three replicates of the central point. Six determinations were performed in each experiment, being three determinations on a sample of Gd-DTPA-BMA at 0.3 μmol mL^{-1} and three determinations on a sample of TTSL and LTSL spiked with Gd-DTPA-BMA at 0.3 μmol mL^{-1}. The coefficients of determination (r^2) and correlation (r) were obtained using the least squares method. The model was evaluated using analysis of variance (ANOVA) and the estimation of the errors was calculated by means of experiments at the central point. The results were evaluated using the software Statistica 7.0 (StatSoft®, Tulsa, USA).

In order to determine the linear velocity in which the height equivalent to a theoretical plate (H) is minimal, a Van Deemter curve was constructed.[36] For this, mobile phase flow-rate was varied as follows: 0.04; 0.06; 0.08; 0.1; 0.2; 0.3; 0.4; 0.5; 0.6; 0.7; 0.8; 0.9; 1.0; 1.5 and 2.0 mL min^{-1}. For each flow-rate its correspondent number of theoretical plates (N) and retention time (t_r) were obtained. The curve was obtained by plotting the H as a function of the linear velocity of the mobile phase (u_0).

2.5 Method validation

Selectivity was demonstrated by the separation of Gd-DTPA-BMA from all potentially interfering compounds, with adequate resolution. Gd-DTPA-BMA chromatograms in the lower concentration of analytical curve (40 nmol mL^{-1}) and those from mobile phase, isopropyl alcohol, TTSL/LTSL, and fetal bovine serum were overlapped to demonstrate the absence of interfering peaks in the same t_r of Gd-DTPA-BMA. The fetal bovine serum was previously ultrafiltered in a centrifugal filter device (Amicon® Ultra-4 10kDa MWCO, Millipore, Billerica, USA) by centrifugation at 14,000 x g for 20 min. All samples were prepared using mobile phase as solvent. The liposomes were previously solubilized in isopropyl alcohol at the ratio of 1:10 for complete disruption of the vesicles. Peak purity was also evaluated.[30, 31]

Five concentration levels were used, in triplicate, to determine linearity. The linear range evaluated was 50 to 150% of the working concentration (80 nmol mL^{-1}), which corresponds to the concentrations of 40, 60, 80, 100, and 120 nmol mL^{-1}. The peak areas were used to construct the analytical curve. Linear regression was verified by the least squares method using GraphPad Prism 5.0 software program (GraphPad Software Inc., San Diego, USA).[37] The coefficients r and r^2 were evaluated.

The limits of detection (LOD) and quantification (LOQ) were initially determined by evaluating the signal-to-noise ratio. For this, Gd-DTPA-BMA solutions were prepared, using mobile phase as solvent, in decreasing concentrations in the range of 50 nmol mL^{-1} to 0.05 nmol mL^{-1}. LOD and LOQ were defined as the concentrations for which signal-to-noise ratios of 3:1 and 10:1, respectively, were obtained. After determination of linearity, LOD and LOQ were also calculated based on the standard deviation (SD) of the *y*-intercept when $x = 0$ and the slope of the calibration curve of Gd-DTPA-BMA.[38]

Intra-day precision was evaluated by means of nine determinations, being three concentrations (50%, 100% and 150% of the working concentration) in triplicate, corresponding to the concentrations of 40, 80 and 120 nmol mL^{-1}. To determine inter-days precision, the same procedure was performed on alternate days. The relative standard deviation (RSD) of the determinations was calculated.

The accuracy was determined by quantification of Gd-DTPA-BMA in the presence of the components of the formulations. TTSL and LTSL, without the drug, were spiked with Gd-DTPA-BMA at 40, 80 and 120 nmol mL^{-1}. Samples were prepared in triplicate and the results were expressed as percentage recovery of the drug added to the placebo.

The robustness was evaluated by means of the Youden test by deliberately modifying seven conditions of the chromatographic method: ACN ratio in the mobile phase, mobile phase aqueous component pH, buffer concentration, column temperature, flow-rate, ACN brand, and buffer brand.[39] The levels of the modified variables as well as the factorial combination of the experimental planning are described in **Table 2**. The seven parameters and their respective modifications were combined in eight experiments that were performed in random order. Six determinations were performed in each condition, being three determinations on a sample of Gd-DTPA-BMA at 80 nmol mL^{-1}, and three determinations on a sample of TTSL and LTSL spiked with Gd-DTPA-BMA at 80 nmol mL^{-1}.

Table 2 – **Experimental planning for robustness assessment by means of Youden test.**

Analytical parameter	Condition		Factorial combination							
	Nominal	Varied	1	2	3	4	5	6	7	8
ACN ratio in the mobile phase (%)	60 (A)	63 (a)	A	A	A	A	a	a	a	a
The aqueous phase pH of the mobile phase	4.5 (B)	4.7 (b)	B	B	b	b	B	B	b	b
Buffer concentration (mmol L^{-1})	5 (C)	5.5 (c)	C	c	C	c	C	c	C	c
Column temperature (°C)	30 (D)	33 (d)	D	D	d	d	d	d	D	D
Flow rate (mL min^{-1})	0.6 (E)	0.7 (e)	E	e	E	e	e	E	e	E
ACN brand	Tedia (F)	J.T. Baker (f)	F	f	f	F	F	f	f	F
Buffer brand	Vetec (G)	Spectrum (g)	G	g	g	G	g	G	G	g

3 RESULTS AND DISCUSSION

3.1 HILIC method development

In general, the stationary phase and the mobile phase are the most important factors for the development of analytical methods by HILIC.[21,22] In the present study, a SeQuant® ZIC®-HILIC (150 x 4.6 mm, 3.5 μm, 100 Å) column was used. This column was chosen based on the chemical structure and some physical-chemical properties of Gd-DTPA-BMA. ZIC®-HILIC, which contains a sulfobetaine binder, is indicated for the analysis of ionic and non-ionic polar compounds.[21,40] Gd-DTPA-BMA is a non-ionic complex, relatively stable due to its log *ks* (logarithm of the complex stability constant) value equal to 16.85.[1] The absence of charges in the complex suggests that the hydrophilic partition is probably the main retention mechanism. The sulfobetaine binder adsorbs a large amount of water on the surface of the stationary phase through hydrogen bonding.[22,40] Thus, Gd-DTPA-BMA will possibly exhibit higher affinity for the stationary phase compared to affinity for the solvent-rich mobile phase. Gd-DTPA-BMA is freely soluble in water and has a log *P* of –2.13.[41,42] These characteristics support the hypothesis of the hydrophilic partition retention mechanism.

A typical mobile phase employed in HILIC is composed of an organic portion (water miscible polar solvent) in a ratio equal to or higher than 60% and an aqueous portion containing or not some type of buffer in a ratio equal to or higher than 2%.[21,43] ACN and methanol are the most commonly used organic solvents in HILIC. In the present study, ACN was selected since the use of a protic solvent, such as methanol, could drastically reduce the retention of Gd-DTPA-BMA. In this case, the use of a higher amount of solvent would be necessary to obtain the same retention provided by an aprotic solvent.[22,44] Buffers are employed in HILIC if the control of the mobile phase pH is required and when peak asymmetry can be a problem.[22] Commonly, the determination of Gd-DTPA-BMA by RP-LC reveals tailing peaks and high value of A_s.[17,45,46] Therefore, pH control of the mobile phase using buffers was used in the proposed method. The buffers usually used in HILIC are NH_4Ac and NH_4FA, due to the high solubility in organic solvents, even in high concentrations, and due to the volatility they present, being compatible with MS detectors.[21] Although they exhibit similar characteristics, the use of NH_4Ac or NH_4FA may result in different elution profiles.[47,48] For this reason, both buffers were investigated at this initial screening.

To determine the detection wavelength, the UV spectrum in the range of 200 to 400 nm of a Gd-DTPA-BMA sample at 57 mg mL^{-1} was obtained. Due to the lack of extended chromophores in its structure, Gd-DTPA-BMA showed maximum absorption at 210 nm (**Figure 1**).

After choosing the stationary phase type (ZIC®-HILIC), the organic solvent (ACN), the possible buffers (NH_4Ac and NH_4FA), the detection wavelength (210 nm), the temperature (30 °C), and the injection volume (20 μL), 11 experiments were carried out, in order to define the variables and range of variation to be evaluated in a later factorial design. The results of this step are showed in **Table S1** (Supplementary Information (SI) section).

The use of NH_4FA (pH = 4.7) resulted in a signal-to-noise ratio about three times higher than that obtained with NH_4Ac (pH = 5.8), leading to higher detectability. A higher value of N is another advantage observed with the use of NH_4FA. The R_s between Gd-DTPA-BMA and liposomes peaks, obtained with NH_4FA (R_s = 6.9), under the conditions evaluated, was lower than that obtained with NH_4Ac (R_s = 11.8); however it was adequate ($R_s \geq 2$) according to the validation guides.[49-51] For these reasons, NH_4FA buffer was selected to compose the mobile phase and to be used in the following experiments.

The range selected for evaluation of the percentage of ACN, based on the results of **Table S1** (SI section), was between 60% and 70%. The minimum level of 60% was selected because in this condition t_r was appropriate (t_r = 4.3 min) and the value of retention factor (k) obtained

(k = 1.7) is within the recommended range 0.5 < k < 20.[51] The maximum level of 70% was also chosen based on t_r and k values obtained (t_r = 8.6 min, k = 4.4). Ratios of ACN above 70% were not considered, since the t_r of Gd-DTPA-BMA becomes very long.

The concentration of NH_4FA buffer was evaluated in the experiments 6, 7, and 8 (**Table 1**). The range of variation chosen for evaluation in a factorial design was between 5 and 25 mmol L^{-1}. The minimum level of 5 mmol L^{-1} was selected because it is the minimum concentration necessary to obtain symmetrical peaks.[21] The maximum level of 25 mmol L^{-1}, although not tested experimentally, was selected because it is described in the literature as the limit concentration in which there is no probability of precipitation in contact with ACN.[52]

Experiments 9, 10, and 11 were performed to evaluate the mobile phase aqueous component pH (**Table 1**). The entire NH_4FA buffering range was investigated. Based on the results (**Table S1**, SI section), pH values between 3.7 and 4.7 were chosen for evaluation in a factorial design. The minimum level of 3.7 was selected, since it corresponded to the lowest pH value in which Gd-DTPA-BMA remained stable. When using pH 2.7, it was not possible to calculate most of the dependent variables expressed in **Table S1** (SI section), due to the deformation of the chromatographic peak corresponding to the drug. The maximum level of 4.7 was selected, because in this condition satisfactory results were obtained. In addition, this value corresponds to the maximum pH of the NH_4FA buffering range.

The variables chosen to compose the factorial planning, based on the initial screening, were: mobile phase aqueous component pH (X_1), ACN ratio (X_2), and buffer concentration (X_3). The other chromatographic conditions were fixed: SeQuant® ZIC®-HILIC (150 x 4.6 mm, 3.5 μm, 100 Å) column, isocratic elution at 1.0 mL min^{-1}, injection volume of 20 μL, temperature of 30 °C, and detection at 210 nm. The responses chosen to evaluate the efficiency of the method were: signal-to-noise ratio, R_s, and A_s. These dependent variables were selected based on the application of the proposed method. The experimental conditions evaluated, and the responses obtained are presented in **Table 3**.

The obtained signal-to-noise ratios showed high variation between the experiments (minimum 1645031 and maximum 9622069). With respect to R_s, experiments 3, 4, and 7 (**Table 3**) generated results lower than the recommended value, which should be ≥ 2.[49-51] These data suggest that the combination of low pH (3.7) and intermediate (15 mmol L^{-1}) or high (25 mmol L^{-1}) buffer concentration in the mobile phase composition should be avoided, as they may result in inadequate R_s between the Gd-DTPA-BMA peak and the liposome peak.

In terms of A_s, the observed results presented low variation (minimum 1.18 and maximum 1.33).

Table 3 – **Results from Box-Behnken experimental design used for optimization of the HILIC method.**

Independent variables		Levels		
		−1	0	1
X_1	pH	3.7	4.2	4.7
X_2	ACN ratio (%)	60	65	70
X_3	Buffer concentration (mmol L^{-1})	5	15	25

Experiment	Contrasts			Experimental conditions			Dependent variables [a]		
	X_1	X_2	X_3	X_1	X_2	X_3	Signal-to-noise ratio	R_s	A_s
1	1	1	0	4.7	70	15	7164899	7.7	1.32
2	1	−1	0	4.7	60	15	7846412	3.7	1.18
3	−1	1	0	3.7	70	15	4029493	1.3	1.31
4	−1	−1	0	3.7	60	15	6040335	0.0	1.21
5	1	0	1	4.7	65	25	1675031	5.1	1.31
6	1	0	−1	4.7	65	5	9622069	5.5	1.25
7	−1	0	1	3.7	65	25	6731611	0.0	1.27
8	−1	0	−1	3.7	65	5	7473207	4.0	1.25
9	0	1	1	4.2	70	25	2324785	7.2	1.30
10	0	1	−1	4.2	70	5	5124660	7.2	1.33
11	0	−1	1	4.2	60	25	3487648	2.7	1.23
12	0	−1	−1	4.2	60	5	6514122	3.5	1.19
13 [b,c]	0	0	0	4.2	65	15	2293381	3.7	1.27

Note: [a] Values are expressed as mean of 3 injections; [b] Values are expressed as mean (n= 3 samples, being 3 injections for each sample); [c] Central point; R_s: resolution; A_s: asymmetry.

In order to extrapolate the data obtained by the Box-Behnken matrix and calculate the optimal point for the variables X_1, X_2 and X_3, the data presented in **Table 3** were used to construct mathematical models. By combining the values of the variables and the responses obtained, the coefficients of the equations which describe the studied system were calculated (**Table S2**, SI section). These equations were elaborated from the effects of the primary linear and quadratic interactions. Secondary interactions were excluded because they generated experimentally incoherent optimal points. The ANOVA, r, r^2 and pure error data calculated from the central point replicates are described in **Table S2** (SI section). The value of r^2 obtained (close to 1) was satisfactory.[53] In addition, the residuals showed random behavior,

without tendencies, confirming the fit of the calculated model (**Figure S1**, SI section**)**. The response surfaces obtained are shown in **Figures 2**, **3**, and **4**. The independent variables were grouped two by two to evaluate the influence of the interaction between them, in the responses signal-to-noise ratio, R_s, and A_s. In the **Figures 2**, **3**, and **4**, the graphs **a-c** were obtained employing constant buffer concentration. In the graphs **d-f** the fixed parameter was the ACN ratio. The **g-i** graphs were prepared by maintaining the values of the mobile phase aqueous component pH constant. The fixed value of each of these variables is indicated in parentheses above the respective graph.

For signal-to-noise ratio evaluation, shown in **Figure 2**, it can be seen from the scale of the graphs **2a-2c** that the lower the concentration of the buffer, the higher the response. According to graph **2a**, higher values of signal-to-noise ratio are obtained when using pH ≥ 4.4, regardless of the ACN ratio used. The results showed in the graphs **2d-2f** are in agreement with these observations. The values of the scales of the graphs **2g-i**, demonstrate that the highest responses are obtained when the highest pH of the buffering range of NH_4FA was used (graph **2i**). According to graph **2i**, regardless of the ACN ratio, the highest signal-to-noise ratio was observed when the buffer concentration was 10 mmol L^{-1} or less. From the analysis of the nine response surfaces presented in **Figure 2**, mobile phase aqueous component pH (values ranging from 4.4 to 4.7) and the buffer concentration (≤ 10 mmol L^{-1}) are the factors that most influence the signal-to-noise ratio.

The results of R_s are presented in **Figure 3**. According to graphs **3a-3c**, when the lowest concentration of buffer was employed (graph **3a**), any combination of pH and ACN ratio results in $R_s \geq 2$. The results showed in the graphs **3d-3f** confirm these observations, and show that high pH values produced higher values of $\boldsymbol{R_s}$. Analyzing the scales of the graphs **3g-3i**, the benefit of using high pH was confirmed, since the highest responses were found when pH was fixed at 4.7 (graph **3i**). In general, the analysis of the nine response surfaces of **Figure 3** shows that higher R_s values were obtained when the following conditions were combined: low buffer concentration, high pH, and high ACN ratio.

Figure 2 – Response surfaces for evaluation of the dependent variable signal-to-noise ratio.

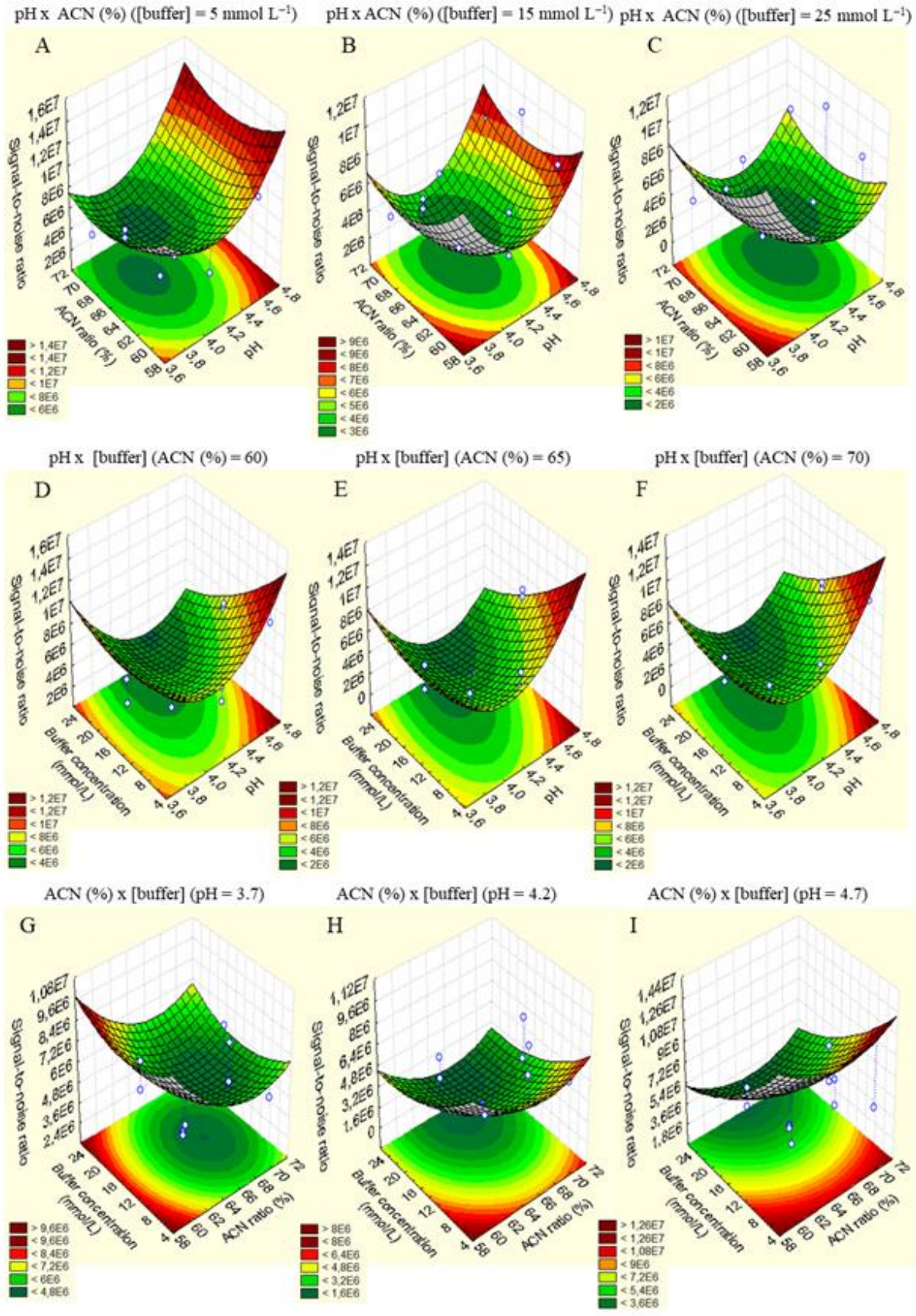

Figure 3 – Response surfaces for evaluation of the dependent variable R_s.

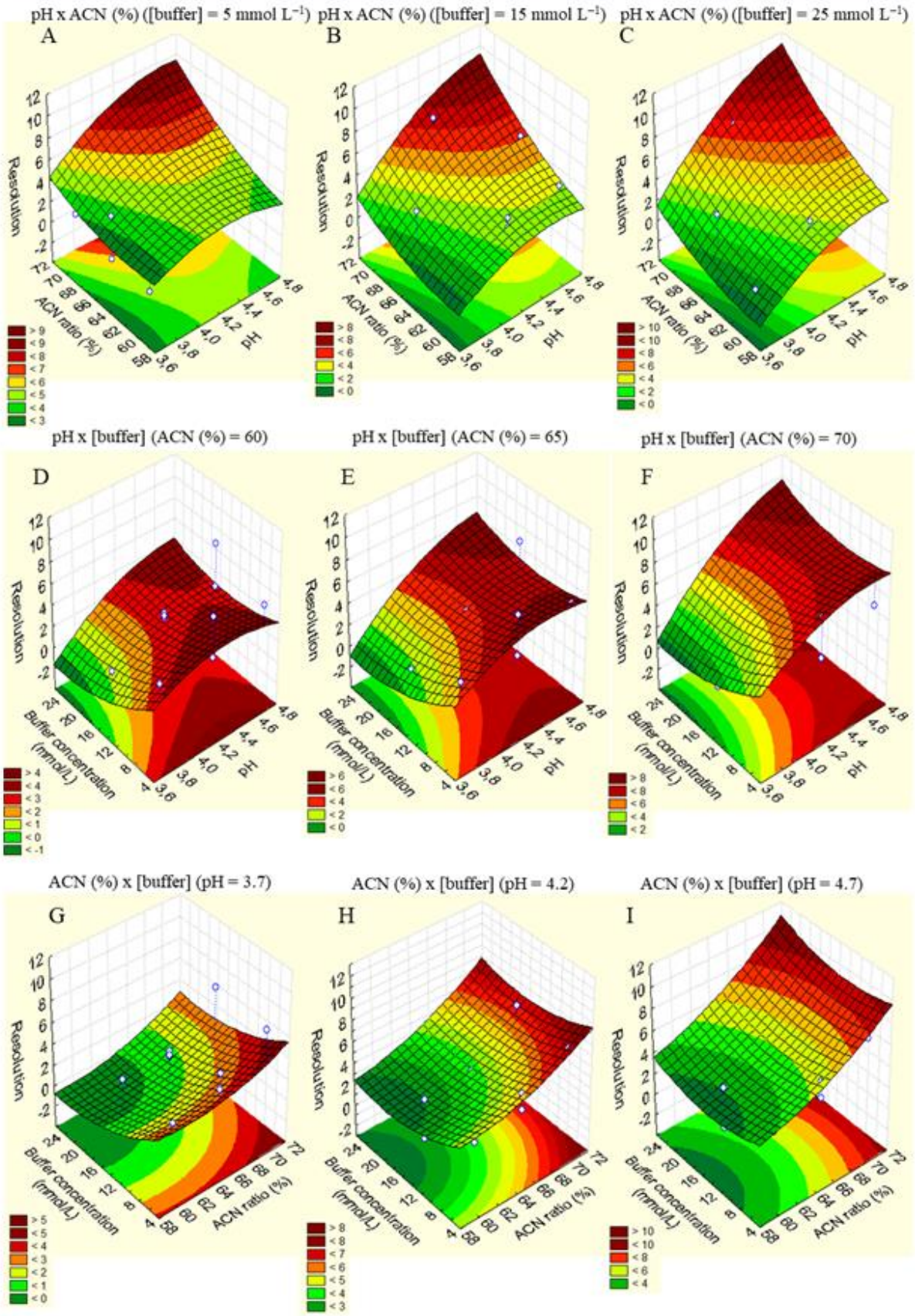

Figure 4 – Response surfaces for evaluation of the dependent variable *As*.

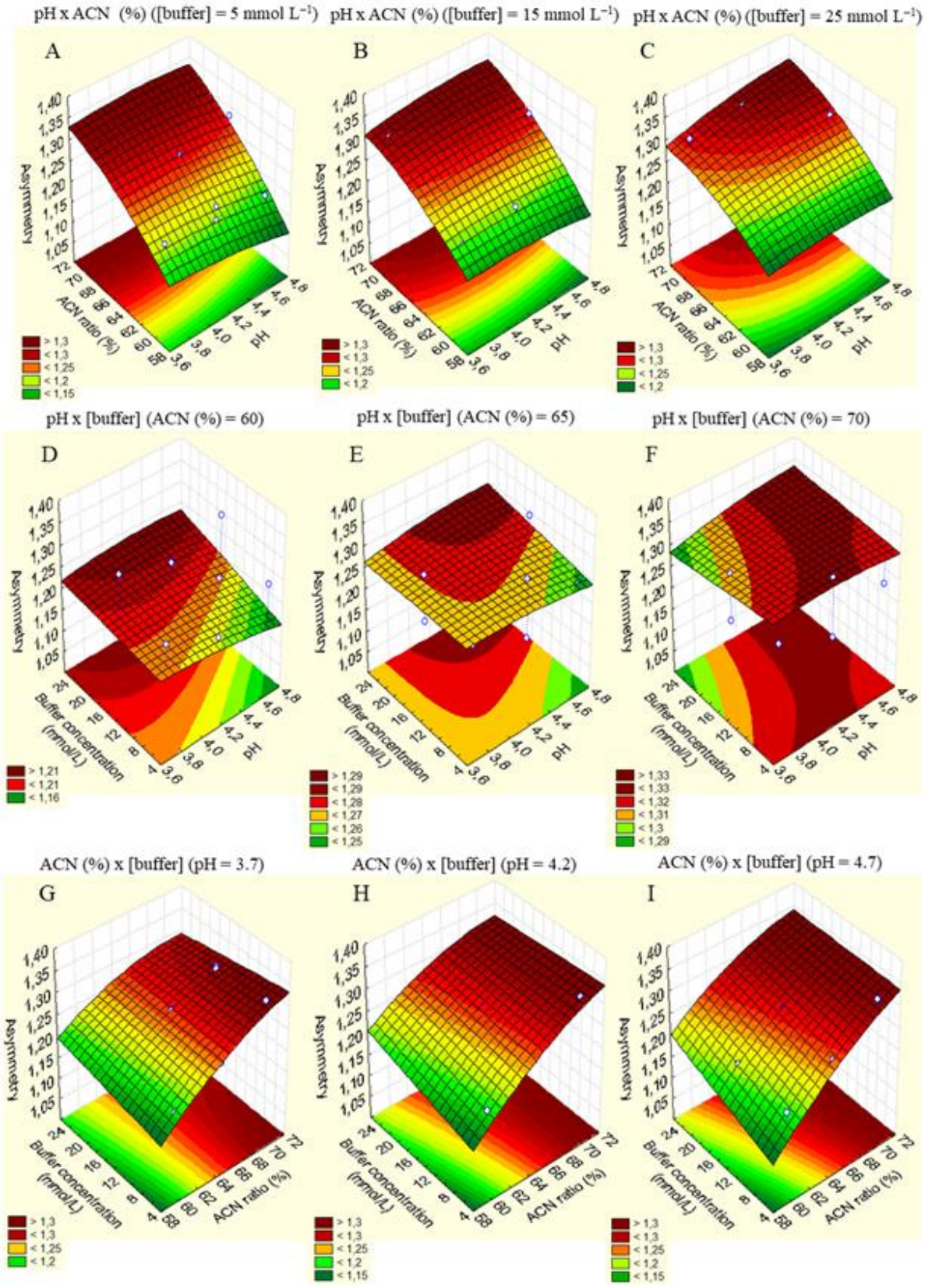

The response surfaces presented in **Figure 4** were used to evaluate A_s. Analysis of graphs **4a-4c** reveals that lower A_s values were obtained when lower buffer concentrations were employed. According to graph **4a**, the combination of low ACN ratio and high pH value results in lower A_s values. The analysis of graphs **4d-f** confirms this observation. According to graph **4d**, there was a tendency to obtain lower values of A_s when the buffer concentration is ≤ 6 mmol L^{-1} and the pH is ≥ 4.4. In the graphs **4g-4i**, regardless of the pH employed, the combination between low ACN ratio and low buffer concentration results in low A_s values.

The results of the response surface methodology are in agreement with the data obtained in the Pareto charts (data not shown). Peak height, baseline noise, *N*, peak width measured at 5% of the peak height, peak area, t_r and *k* were also evaluated as responses. From the results of these analyses, showed in **Table S3** (SI section), and from their respective response surface (data not shown), it was possible to identify the optimized conditions, considering the individual desirability of each parameter and the global desirability for the proposed method.

In order to verify if the defined optimal conditions result in optimum response values for the Gd-DTPA-BMA chromatographic peak, a new experiment was performed using mobile phase composed of 60% ACN, NH_4FA at 5 mmol L^{-1} and mobile phase aqueous component pH of 4.5. Six determinations were performed in each experiment, being three determinations on a sample of Gd-DTPA-BMA at 0.3 μmol mL^{-1} and three determinations on a sample of TTSL and LTSL spiked with Gd-DTPA-BMA at 0.3 μmol mL^{-1}. Under these conditions, the signal-to-noise ratio obtained was 9594265. This result is in agreement with the highest signal-to-noise ratio found in the Box-Behnken planning experiments (experiment 6, **Table 3**). The value of R_s obtained using the optimized conditions, was equal to 3.2. This result was considered adequate, since it is higher than the recommended value (Rs ≥ 2) to obtain a satisfactory separation between the drug and the possible interferences.[49-51] The A_s obtained after optimization of the chromatographic parameters was 1.11. This value corresponds to the best response obtained for this parameter, considering all the experiments performed. In addition, it complies with the limits established by the FDA.[54]

The Van Deemter curve obtained for optimize the mobile phase flow-rate is shown in **Figure 5**. The maximum efficiency observed *(H* around 18 μm), using the optimized chromatographic conditions, was observed in U_0 close to 0.16 mm s^{-1}, corresponding to a flow of 0.1 mL min^{-1}. This flow-rate is not feasible to be used in the routine analyses, since it results in a very long t_r for Gd-DTPA-BMA (t_r = 44.15 minutes). Thus, the optimization of the mobile phase flow-rate was performed evaluating the parameters t_r, *N*, peak height and R_s

(**Table S4**, SI section**)**. Based on the results obtained, the flow-rate of 0.6 mL min^{-1} was selected for use in the developed method. When compared to the flow-rate of 1.0 mL min^{-1}, it resulted in a higher Gd-DTPA-BMA t_r (t_r = 7.1 min). However, this flow-rate allowed increasing 29% of efficiency (N) and 12% of detectability and R_s of the proposed method.

Figure 5 – Van Deemter curve using the optimized chromatographic conditions of the developed method.

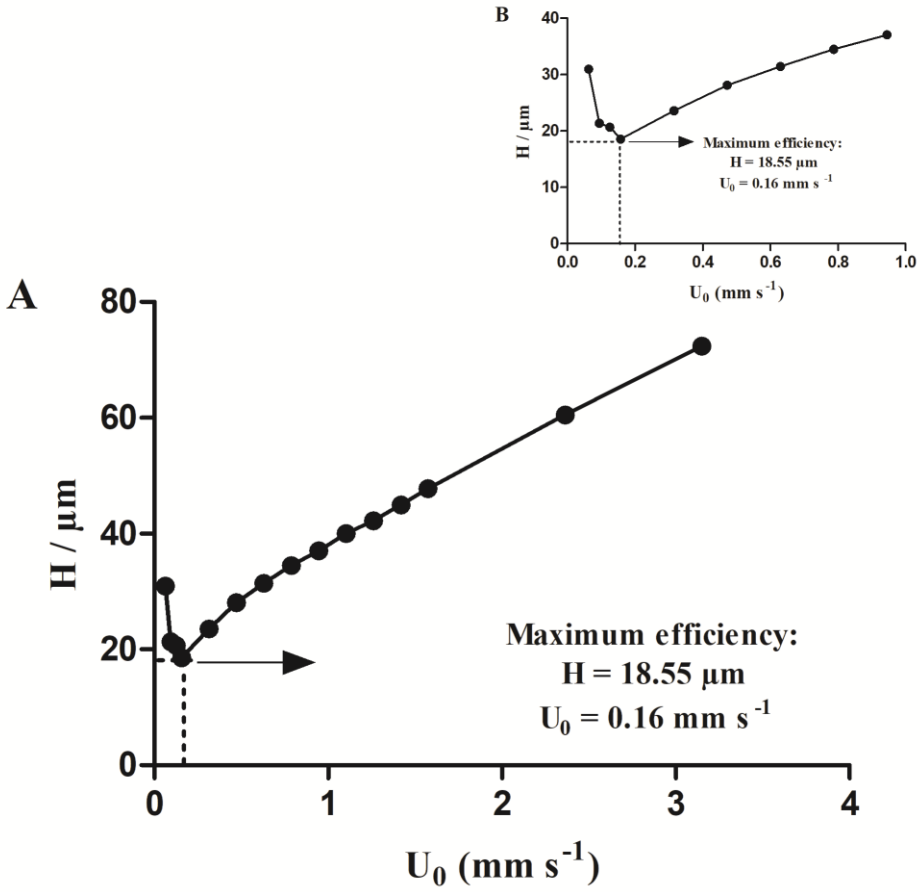

3.2 Method validation

Chromatograms of the formulations, without Gd-DTPA-BMA (TTSL/LTSL), isopropyl alcohol, fetal bovine serum, and mobile phase (**Figure 6**), showed no interfering peaks at the retention time of Gd-DTPA-BMA (t_r = 7.1 min), demonstrating the selectivity of the method. The resolution obtained between Gd-DTPA-BMA and TTSL/LTSL was adequate (R_s = 3.6). In addition, the purity of the Gd-DTPA-BMA peak, calculated by DAD, was equal to 100% in all determinations. Although the aim of this study is to determine Gd-DTPA-BMA in

liposomes, the selectivity in a biological sample (fetal bovine serum) was evaluated to demonstrate that, if necessary, the developed method can be applied in more complex matrices.

Figure 6 – Representative chromatograms from the selectivity study: fetal bovine serum, TTSL/LTSL, isopropyl alcohol, mobile phase, and Gd-DTPA-BMA (40 nmol mL^{-1}).

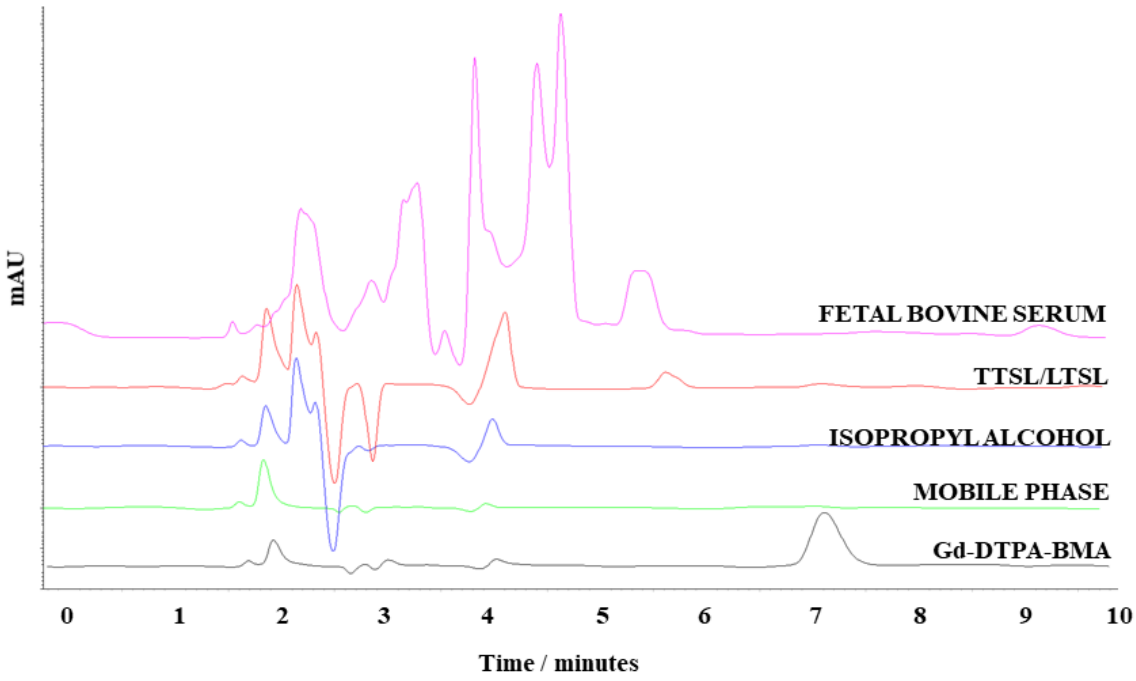

The method showed to be linear in the range between 40 and 120 nmol L^{-1}. The equation of the calibration curve obtained was y = 803100 x + 964900. The r and r^2 obtained were satisfactory (> 0.999).[30] There was no significant difference between the slopes of the three calibration curves obtained ($p < 0.05$).

The determination of LOD and LOQ of Gd-DTPA-BMA was performed initially by means of the evaluation of the signal-to-noise ratio in order to include LOQ as the lowest concentration level of the linear range of the analytical curve. After linearity evaluation, the theoretical values of LOD and LOQ, calculated based on the parameters of linear regression, were 4.56 nmol mL^{-1} and 6.78 nmol mL^{-1}, respectively.

From our knowledge, no studies dealing with Gd-DTPA-BMA determination by HILIC in liposomes have been reported in the literature until the present date. Moreover, no studies of determination of Gd-DTPA-BMA by HILIC with DAD detection were found. In contrast, some studies of determination of Gd-DTPA-BMA by HILIC using MS detection have already

been described.[20,25-29] Despite the indisputable detectability provided by MS, the high cost of analysis and instrumentation justifies the development of simpler and less costly method. In a previous study by our research group, an analytical method for the determination of Gd-DTPA-BMA by RP-LC/DAD was developed and validated.[2] It showed to be linear in the range between 100 and 500 nmol mL^{-1}. At the present HILIC method, lower concentrations can be included in the analytical curve (40 to 120 nmol mL^{-1}). In addition, comparing the LOD and LOQ obtained in the two studies, one can conclude that the HILIC method showed detectability five-fold higher using the same type of detector (DAD).

The developed method demonstrated adequate precision (**Table 4**). The obtained RSD values for intra-day and inter-day precisions were satisfactory and in agreement with the specification established by RE 899, which recommends RSD ≤ 5%.[30]

The accuracy of the developed method was demonstrated (**Table 4**). The result for mean recovery was 98.61% for TTSL/LTSL formulations. In addition, the value of RSD between measurements did not exceed 5%.

The results of robustness were present in **Table 5**. According to the obtained data, the method showed to be robust for all the evaluated parameters, since the effects of each variable were lower than the respective largest effect calculated.

3.3 Determination of Gd-DTPA-BMA entrapment and drug encapsulation percentage

The developed method was used to evaluate the Gd-DTPA-BMA content in TTSL-Gd and LTSL-Gd formulations. Three batches of each formulation were prepared for this analysis. The chromatograms were obtained by using the mobile phase as sample diluent. The values obtained were 26.41 ± 4.04 μmol mL^{-1} (10.56 ± 1.62%) and 22.95 ± 3.07 μmol mL^{-1} (9.18 ± 1.23%) for TTSL-Gd and LTSL-Gd, respectively. The amount of Gd-DTPA-BMA entrapment found, in terms of μmol/mL, was similar to the concentration determined for pH-sensitive and stealth pH-sensitive liposomes developed in a previously study from our research group.[3] The encapsulation percentages found are in agreement with values obtained in thermosensitive formulations containing Gd-DTPA-BMA, developed for use in magnetic resonance.[7] The drug entrapment is an essential physicochemical parameter in the development of a new drug delivery system. The results of this analysis confirms the applicability of the HILIC method to the development and characterization of liposomal formulations containing Gd-DTPA-BMA.

Table 4 – Intra-day precision, inter-day precision, and values of Gd-DTPA-BMA recovery obtained with HILIC method.

Linear range (%)	Gd-DTPA-BMA mean concentration ± SD (nmol mL^{-1})			RSD (%)			Accuracy result		
	Intra-day [a]		Inter-day [b]	Intra-day [a]		Inter-day [b]	Gd-DTPA-BMA amount added (nmol mL^{-1})	Gd-DTPA-BMA mean concentration (nmol mL^{-1}) [a] ± SD	Mean recovery (%) [a] ± SD
	Day 1	Day 2		Day 1	Day 2				
50	39.59 ± 0.41	38.82 ± 0.52	39.20 ± 0.59	1.05	1.33	1.51	40	38.93 ± 0.37	97.32 ± 0.93
100	79.80 ± 0.86	79.13 ± 0.23	79.47 ± 0.67	1.08	0.29	0.85	80	79.41 ± 0.31	99.26 ± 0.38
150	119.50 ± 0.60	119.49 ± 0.94	119.50 ± 0.71	0.50	0.79	0.59	120	119.10 ± 1.97	99.25 ± 1.65
Mean [c]									98.61 ± 1.37
RSD (%) [c]									1.38

Note: [a] Mean of three determinations; [b] Mean of six determinations; [c] Mean of nine determinations. Gd-DTPA-BMA: gadodiamide; SD: standard deviation; RSD: relative standard deviation.

Table 5 – Evaluation of the effect of the variables, in terms of content, R_s and A_s in the determination of Gd-DTPA-BMA using the developed method.

Variables	Content (%) [a]	R_s [a]	A_s [a]
ACN ratio in the mobile phase (A = 60%; a = 63%)	101.37 – 100.87 = 0.50	3.21 – 4.57 = − 1.36	1.32 – 1.28 = 0.04
The aqueous phase pH of the mobile phase (B = 4.5; b = 4.7)	100.61 – 101.64 = − 1.03	4.06 – 3.72 = 0.34	1.26 – 1.34 = − 0.08
Buffer concentration (C = 5 mmol L^{-1}; c = 5,5 mmol L^{-1})	101.46 – 100.78 = 0.68	3.56 – 4.22 = − 0.66	1.29 – 1.30 = − 0.01
Column temperature (D = 30 °C; d = 33 °C)	101.35 – 100.90 = 0.45	3.80 – 3.98 = − 0.18	1.29 – 1.31 = − 0.02
Flow (E = 0.6 mL min^{-1}; e = 0.7 mL min^{-1})	101.16 – 101.09 = 0.07	4.37 – 3.41 = 0.96	1.28 – 1.31 = − 0.03
ACN brand (F = Tedia; f = J.T.Baker)	101.54 – 100.70 = 0.84	3.83 – 3.95 = − 0.12	1.25 – 1.35 = − 0.10
Buffer brand (G = Vetec; g = Spectrum)	101.26 – 100.98 = 0.28	4.05 – 3.73 = 0.32	1.26 – 1.34 = − 0.08
Largest effect [b]	1.24	36.06	8.97

Note: [a] Mean values obtained at nominal conditions subtracted from the mean values obtained under the varied conditions; [b] RSD (relative standard deviation) between the values obtained in the 8 experiments multiplied by root of 2. R_s: resolution; A_s: asymmetry.

CONCLUSIONS

In the present study, an analytical method for the determination of Gd-DTPA-BMA in liposomes by HILIC was developed, using chemometric tools, validated and applied for determination of Gd-DTPA-BMA entrapment and drug encapsulation percentage in liposomes. The developed method showed to be simple, fast and selective. In addition, it presented adequate detectability, proving to be suitable to determine Gd-DTPA-BMA in the development of liposomal formulations. Although this method has been used to determine a single analyte, it presented selectivity to be used in more complex samples, as demonstrated for fetal bovine serum sample. In this context, the use of Box-Behnken factorial design and response surface methodology was effective for method development. This approach allowed evaluating the interaction between the parameters and obtaining results that probable would

not be observed in a univariate analysis. Although some methods for determining Gd-DTPA-BMA in different matrices by HILIC have been described, none has been applied for analysis of liposomes. In addition, from our knowledge, until the present date, no quantification study of Gd-DTPA-BMA by a rational chemometric-assisted HILIC has been found in the literature.

ACKNOWLEDGEMENTS

The authors would like to thank CNPq (Conselho Nacional de Desenvolvimento Científico e Tecnológico), FAPEMIG (Fundação de Amparo à Pesquisa do Estado de Minas Gerais) and CAPES (Coordenação de Aperfeiçoamento de Pessoal de Nível Superior) for their financial support.

REFERENCES

1. Telgmann, L.; Sperling, M.; Karst, U; *Anal Chim Acta* **2013**, *764*, 1.

2. Maia, A. L. C.; Silva, T. D.; Oliveira, C. N. P.; Silveira, J. N.; Ramaldes, G. A.; *Anal. Methods* **2015**, *7*, 8315.

3. Maia, A. L. C.; Fernandes, C.; Oliveira, C. N. P.; Teixeira, C. S.; Oliveira, M. S.; Soares, D. C. F.; Ramaldes, G.A.; *Curr. Drug. Deliv.* **2017**, *14*, 566.

4. EMA/625317/2017: *EMA's Final Opinion Confirms Restrictions on Use of Linear Gadolinium Agents in Body Scans*, European Medicines Agency (EMA): London, UK, 2017.

5. Ghaghada, K.; Hawley, C.; Kawaji, K.; Annapragada, A.; Mukundan, S. JR.; *Acad. Radiol.* **2008**, *15*, 1259.

6. Grahn, A. Y.; Bankiewicz, K. S.; Dugich-djordjevic, M.; Bringas, J. R.; Hadaczek, P.; Johnson, G. A.; Eastman, S.; Luz, M.; *J. Neurooncol.* **2009**, *95*, 185.

7. Hossann, M.; Wang, T.; Wiggenhorn, M.; Schmidt, R.; Zengerle, A.; Winter, G.; Eibl, H.; Peller, M.; Reiser, M.; Issels, R. D.; Lindner, L. H.; *J. Control. Release*, **2010**, *147*, 436.

8. Soares, D. C. F.; Oliveira, M. C.; Barros, A. L. B.; Cardoso, V. N.; Ramaldes, G. A.; *Eur. J. Pharm. Sci.* **2011a**, *43*, 290.

9. Soares, D. C. F.; Oliveira, M. C.; Santos, R. G.; Andrade, M. S.; Vilela, J. M. C.; Cardoso, V. N.; Ramaldes, G. A. *Eur. J. Pharm. Sci.* **2011b**, *42*, 462.

10. Soares, D. C. F.; Cardoso, V. N.; Barros, A. L. B.; Souza, C. M.; Cassali, G. D.; Oliveira, M. C.; Ramaldes, G. A.; *Eur. J. Pharm. Sci*. **2012**, *45*, 58.

11. Dewi N.; Yanagie, H.; Zhu, H.; Demachi, K.; Shinohara, A.; Yokoyama, K.; Sekino, M.; Sakurai, Y.; Morishita, Y.; Iyomoto, N.; Nagasaki, T.; Horiguchi, Y.; Nagasaki, Y.; Nakajima, J.; Ono, M.; Kakimi, K.; Takahashi, H.; *Biomed. Pharmacother.* **2013**, *67*, 451.

12.Soares, D. C. F.; Barros, A. L. B.; Santos, R. G. S.; Sousa, E. M. B.; Ramaldes, G. A.; *J. Radioanal. Nucl. Chem.* **2013**, *295*, 63.

13.Issels, R.; Kampmann, E.; Kanaar, R.; Lindner, L. H.; *Int. J. Hyperthermia* **2016**, *32*, 89.

14.Behra-miellet, J.; Briand, G.; Kouach, M.; Gressier, B.; Cazin, M.; Cazin, J. C.; *Biomed. Chromatogr.* **1998**, *12*, 21.

15. Frenzel, T.; Lensfeld, P.; Schirmer, H.; Hütter, J.; Weinmann, H. J.; *Invest. Radiol.* **2008**, *43*, 817.

16. Kahakachchi, C. L.; Moore, D. A.; *J. Anal. At. Spectrom.* **2009**, *24*, 1389.

17. Kindberg, G. M.; Uran, S.; Friisk, G.; Martinsen, I.; Skotland, T.; *Eur. Radiol.* **2010**, *20*, 1636.

18. United States Pharmacopeia (USP); USP 34-NF 29; The United States Pharmacopeial Convention: Rockville, 2011, p. 2934-2937.

19. Normann, P. T.; Hals, P. A.; *Eur. J. Drug. Metabol. Pharmacokinet.* **1995**, *20*, 307.

20. Raju, C. S. K.; Cossmer, A.; Scharf, H.; Panne, U.; Lück, D.; *J. Anal. At. Spectrom.* **2010**, *25*, 55.

21. Greco, G.; Letzel, T.; *J. Chromatogr. Sci.* **2013**, *51*, 684.

22. Buszewski, B.; Noga, S.; *Anal. Bioanal. Chem.* **2012**, *402*, 231.

23. Acevska, J.; Stefkov, G.; Petkovska, R.; Kulevanova, S.; Dimitrovska, A.; *Anal. Bioanal. Chem.* **2012**, *403*, 1117.

24. Sahu, P. K.; Patro, C. S.; *J. Liq. Chromatogr. Relat. Technol.* **2014**, *37*, 2444.

25. Künnemeyer, J.; Terborg, L.; Nowak, S.; Scheffer, A.; Telgmann, L.; Tokmak, F.; Günsel, A.; Wiesmüller, G.; Reichelt, S.; Karst, U.; *Anal. Chem.* **2008**, *80*, 8163.

26. Künnemeyer, J.; Terborg, L.; Meermann, B.; Brauckmann, C.; Möller, I.; Scheffer, A.; Karst, U.; *Environ. Sci. Technol.* **2009**, *43*, 2884.

27. Telgmann, L.; Wehe, C. A.; Birka, M.; Künnemeyer, J.; Nowak, S.; Sperling, M.; Karst, U.; *Environ. Sci. Technol.* **2012**, *46*, 11929.

28. Lindner, U.; Lingott, J.; Richter, S.; Jakubowski, N.; Panne, U.; *Anal. Bioanal. Chem.* **2013**, *405*, 1865.

29. Lindner, U.; Lingott, J.; Richter, S.; Jiang, W.; Jakubowski, N.; Panne, U; *Anal. Bioanal. Chem.* **2015**, *407*, 2415.

30. Ministério da Saúde, Agência Nacional de Vigilância Sanitária; Resolução RE nº 899, de 29 de maio de 2003, *Guia de Validação de Métodos Analíticos e Bioanalíticos*, Diário Oficial da União, Brasília, 2003.

31. International Conference on Harmonisation of Technical Requirements for Registration of Pharmaceuticals for Human Use (ICH); *Guideline Q2 (R1) – Validation of Analytical Procedures: Text and Methodology*; ICH: Geneva, 2005.

32. Szoka, JR. F.; Papahadjopoulos, D.; *Proc. Natl. Acad. Sci*. **1978**, *75*, 4194.

33. Li, L.; Hagen, T. L. M. T.; Hossann, M.; Süss, R.; Rhoon, G. C. V.; Eggermont, A. M. M.; Haemmerich, D.; Koning, G.A.; *J. Control. Release*, **2013**, *168*, 142.

34. Bezerra, M. A.; Santelli, R. E.; Oliveira, E. P.; Villar, L. S.; Escaleira, L. A.; *Talanta* **2008**, *76*, 965.

35. *Statistica 7.0*, StatSoft®, Tulsa, USA, 2004.

36. Van Deemter, J. J.; Zuiderweg, F. J.; Klinkenberg, A.; *Chem. Eng. Sci.* **1956**, *5*, 271.

37. *GraphPad Prism 5.0*, GraphPad Software Inc., San Diego, USA, 2007.

38. Ribeiro, F. A. L.; Ferreira, M. M. C.; Morano, S. C.; Silva, L. R.; Schneider, R. P.; *Quím. Nova* **2008**, *31*, 164.

39. Youden, W. J.; Steiner, E. H.; *Statistical Manual of AOAC*; Association of Official Analytical Chemistry (AOAC); Washington, USA, 1975.

40. Cass, Q. B.; Cassiano, N.; *Cromatografia Líquida: Novas Tendências e Aplicações*, 1ª ed.; Elsevier: Rio de Janeiro, 2015.

41. Control No. 169935: *Product monograph: Omniscan™* (Gadodiamide Injection USP), GE Healthcare: Ontario, Canada, 2013.

42. Merbach A.; Helm, L.; Tóth, E.; *The Chemistry of Contrast Agents in Medical Magnetic Resonance Imaging*, 2nd ed.; John Wiley & Sons: United Kingdom, 2013.

43. Chirita, R. I.; West, C.; Finaru, A. L.; Elfakir, C.; *J Chromatogr A* **2010**, *1217*, 3091.

44. Hemström, P.; Irgum, K.; *J. Sep. Sci.* 2006, 29, 1784.

45. Vora, M. M.; Wukovnig, S.; Finn, R. D.; Emran, A. M.; Boothe, T. E.; Kothari, P. J.; *J. Chromatogr.* **1986**, *369*, 187.

46. Hvattum, E., Normann, P. T.; Jamieson, G. C.; Lai, J. J.; Skotland, T.; *J. Pharm. Biomed. Anal.* **1995**, *13*, 927.

47. Guo, Y.; Gaiki, S.; *J. Chromatogr. A* **2011**, *1218*, 5920.

48. Karatapanis, A. E.; Fiamegos, Y. C.; Stalikas, C. D.; *J. Chromatogr. A* **2011**, **1218**, 2871.

49. United States Food and Drug Administration; *Guidance for Industry, Analytical Procedures and Methods Validation*, Rockville, USA, 2000.

50. Ribani, M.; Bottoli, C. B. G.; Collins, C. H.; Jardim, I. C. S. F.; Melo, L. F. C.; *Quím. Nova* **2004**, *27*, 771.

51. Snyder, L. R.; Kirkland, J. J.; Geajch, J. L.; *Practical HPLC Method Development*, 2nd ed.; John Wiley & Sons: New York, 2007.

52. Thermo Scientific; *HILIC Separations Technical Guide. A Practical Guide to HILIC Mechanisms, Method Development and Troubleshooting, Thermo Scientific*, 2014.

53. Teófilo, R. F.; Ferreira, M. M. C.; *Quim. Nova* **2006**, *29*, 338.

54. United States Food and Drug Administration; *Reviewer Guidance Validation of Chromatographic Methods*, Center for Drug Evaluation and Research: Rockville, USA, 1994.

SUPPLEMENTARY INFORMATION

Supplementary information is available free of charge at http://jbcs.sbq.org.br as PDF file.

Table S1 – Results of variables screening for the development of method for determination of Gd-DTPA-BMA in liposomes by HILIC.

Experiment	Independent variables	Dependent variables [a]									
		Signal-to-noise ratio	R_s	A_s	Peak height (mAU)	Noise (mAU)	N	Peak Width	Peak area	t_r (min)	k
1	NH_4Ac	2586043	11.8	1.44	9852825	3.81	3687	0.76	218788085	8.9	4.6
2	NH_4FA	8389613	6.9	1.44	10990393	1.31	4106	0.72	233993993	8.6	4.4
3	ACN 60%	10730254	7.5	1.25	16095381	1.50	3018	0.39	189478831	4.3	1.7
4	ACN 70%	8389613	6.9	1.44	10990393	1.31	4106	0.72	233993993	8.6	4.4
5	ACN 75%	9169528	15.6	1.71	6326974	0.69	4610	1.37	235782267	16.2	9.2
6	NH_4FA 5 mmol L^{-1}	16385674	8.1	1.42	10650688	0.65	3912	0.76	234068457	8.9	4.6
7	NH_4FA 10 mmol L^{-1}	8389613	6.9	1.44	10990393	1.31	4106	0.72	233993993	8.6	4.4
8	NH_4FA 15 mmol L^{-1}	3766828	7.8	1.45	10170436	2.70	4255	0.73	212774504	8.9	4.6
9 [b]	pH 2.7 [b]	–	–	–	–	1.60	–	–	–	–	–
10	pH 3.7	7788154	7.0	1.44	10436127	1.34	3377	0.72	239358814	8.8	4.6
11	pH 4.7	8389613	6.9	1.44	10990393	1.31	4106	0.72	233993993	8.6	4.4

Note: [a] Values are expressed as mean (n= 3 samples, being 3 injections for each sample). [b] In this condition it was not possible to calculate the majority of the dependent variables evaluated, due to the degradation of Gd-DTPA-BMA. **Mobile phase used in each experiment: 1.** ACN/NH_4Ac 10 mmol L^{-1}, pH 5.8, (70:30 v/v); **2.** ACN/NH_4FA 10 mmol L^{-1}, pH 4.7, (70:30 v/v); **3.** ACN/NH_4FA 10 mmol L^{-1}, pH 4.7, (60:40 v/v); **4.** ACN/NH_4FA 10 mmol L^{-1}, pH 4.7, (70:30 v/v); **5.** ACN/NH_4FA 10 mmol L^{-1}, pH 4.7, (75:25 v/v); **6.** ACN/NH_4FA 5 mmol L^{-1}, pH 4.7, (70:30 v/v); **7.** ACN/NH_4FA 10 mmol L^{-1}, pH 4.7, (70:30 v/v); **8.** ACN/NH_4FA 15 mmol L^{-1}, pH 4.7, (70:30 v/v); **9.** ACN/NH_4FA 10 mmol L^{-1}, pH 2.7, (70:30 v/v); **10.** ACN/NH_4FA 10 mmol L^{-1}, pH 3.7, (70:30 v/v); **11.** ACN/NH_4FA 10 mmol L^{-1}, pH 4.7, (70:30 v/v).

Table S2 – Coefficients of the mathematical model obtained by Box-Behnken and summary of ANOVA.

	Dependent variables					
	Signal-to-noise ratio		R_s		A_s	
Independent variables	Coefficient	p-value	Coefficients	p-value	Coefficients	p-value
X_1	229221	0.03514	2.09589	0.00166	0.00169	0.10157
X_1^2	− 1521253	0.00046	0.49960	0.01551	0.00319	0.01758
X_2	− 680585	0.00418	1.69384	0.00254	0.05653	0.00011
X_2^2	− 514916	0.00396	− 0.23383	0.06546	0.00610	0.00492
X_3	− 1814373	0.00059	− 0.66067	0.01636	0.01092	0.00284
X_3^2	− 542513	0.00357	− 0.48766	0.01626	0.00026	0.59944
X_1 X_2	382332	0.02564	0.68013	0.03022	0.00784	0.01088
X_1 X_3	− 1801360	0.00120	0.90450	0.01742	0.01104	0.00553
X_2 X_3	56650	0.45995	0.21786	0.21355	− 0.01400	0.00345
Intercept	5686189	0.00004	4.00106	0.00030	1.26278	0.00000
Pure error	155887 x 10^5		0.0585495		0.0000027	
R	0.9530		0.9729		0.9794	
r^2	0.9082		0.9465		0.9592	

Note: X_1, pH; X_2, ACN ratio (%); X_3, buffer concentration (mmol L^{-1}); $p < 0.05$ (ANOVA).

Table S3 – Results from Box-Behnken experimental design of development and optimization of the method for determination of Gd-DTPA-BMA in liposomes by HILIC.

Independent variables		Levels		
		−1	0	1
X_1	pH	3.7	4.2	4.7
X_2	ACN ratio (%)	60	65	70
X_3	Buffer concentration (mmol L^{-1})	5	15	25

Experiment	Experimental conditions			Dependent variables [a]						
	X_1	X_2	X_3	Peak height (mAU)	Baseline noise (mAU)	*N*	Peak width	Peak area	t_r (min)	*k*
1	4.7	70	15	6541768	0.91	4086	0.76	139983991	8.9	4.6
2	4.7	60	15	13132828	1.67	4132	0.34	131824176	4.3	1.7
3	3.7	70	15	5955899	1.48	3359	0.76	135430549	8.7	4.5
4	3.7	60	15	12616128	2.02	3438	0.38	139555792	4.2	1.7
5	4.7	65	25	9659601	5.77	4012	0.49	134050337	5.8	2.6
6	4.7	65	5	9906433	1.03	3774	0.50	143104879	5.8	2.6
7	3.7	65	25	9715330	1.44	3339	0.52	145532548	5.7	2.6
8	3.7	65	5	9160782	1.22	3058	0.53	144444010	5.7	2.6
9	4.2	70	25	6350614	2.73	3872	0.73	132688574	8.5	4.3
10	4.2	70	5	6178102	1.20	3467	0.78	137785630	8.5	4.3
11	4.2	60	25	14248215	4.08	4067	0.34	142228701	4.2	1.6
12	4.2	60	5	13050675	2.00	3504	0.37	142678121	4.2	1.7
13 [b,c]	4.2	65	15	10461231	4.66	3749	0.50	151422350	5.7	2.6

Note: [a] Values are expressed as mean of 3 injections; [b] Values are expressed as mean (n= 3 samples, being 3 injections for each sample); [c] Central point.

Table S4 – Effect of the flow-rate in the parameters t_r, peak height, N and R_s, using the chromatographic conditions of the developed method.

Flow (mL min^{-1})	Dependent variables [a]				Increase compared to flow of 1.0 mL min^{-1} (%)			
	t_r (min)	Peak height (mAU)	N	R_s	t_r (min)	Peak height (mAU)	N	R_s
0.6	7.1	13939706	4047	3.56	68	12	29	12
0.7	6.1	13506172	3745	3.44	44	7	19	9
0.8	5.3	13405633	3552	3.36	26	8	13	6
0.9	4.7	12687237	3337	3.23	11	2	6	2
1.0	4.2	12472545	3140	3.17	–	–	–	–

Note: [a] Values are expressed as mean of 3 injections.

Figure S1 – Graphs of distributions residuals from the analysis of dependent variables: signal-to-noise ratio (A), R_s (B) and A_s (C).

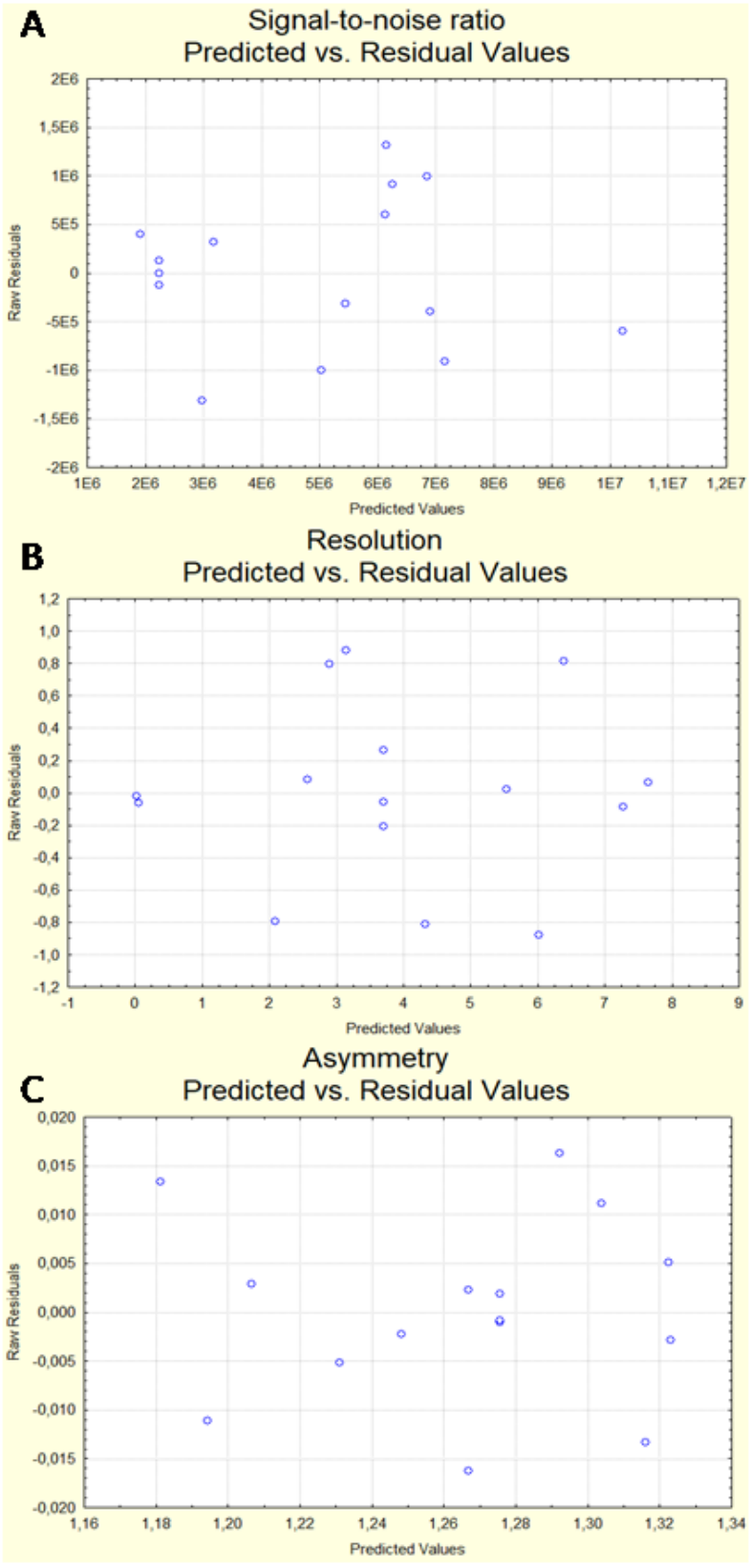

CAPÍTULO 2

Thermosensitive liposomes containing gadolinium-based complexes: a potential strategy for the selective breast cancer treatment.

THERMOSENSITIVE LIPOSOMES CONTAINING GADOLINIUM-BASED COMPLEXES: A POTENTIAL STRATEGY FOR SELECTIVE BREAST CANCER TREATMENT

Ana Luiza C. Maia[a], Aline T. M. e Silva[a], Aina L. A. César [a], Cristiane S. Giuberti [b], Fernanda C. G. Evangelista [c], Adriano P. Sabino [c], Ângelo M. Souza [d], Christian Fernandes[a], André L. B. de Barros[c], Daniel C. F. Soares[e], and Gilson A. Ramaldes[a]

[a] Departamento de Produtos Farmacêuticos, Faculdade de Farmácia, Universidade Federal de Minas Gerais, Belo Horizonte, Minas Gerais, Brazil.

[b] Centro de Ciências da Saúde, Faculdade de Farmácia, Universidade Federal do Espírito Santo, Vitória, Espírito Santo, Brazil.

[c] Departamento de Análises Clínicas e Toxicológicas, Faculdade de Farmácia, Universidade Federal de Minas Gerais, Belo Horizonte, Minas Gerais, Brazil.

[d] Departamento de Física, Instituto de Ciências Exatas, Universidade Federal de Minas Gerais, Belo Horizonte, Minas Gerais, Brazil.

[e] Departamento de Química e Matemática, Instituto de Ciências, Universidade Federal de Itajubá, Itabira, Minas Gerais, Brazil.

ABSTRACT

Gadodiamide (Gd-DTPA-BMA) is a gadolinium-based complex, used as a contrast in magnetic resonance imaging (MRI). This complex also can induce the apoptosis in neoplastic cells through activation of caspase-3. In this context, the aim of this study was to develop, characterize, and assess the cytotoxic activity and selective index of two thermosensitive liposomes containing Gd-DTPA-BMA. Formulations were prepared by two different methods and their physicochemical, morphological, and thermal properties were evaluated. These liposomes maintained storage stability at 4 °C for 120 days. The cytotoxic studies on the breast cancer cell lines demonstrated that the Gd-DTPA-BMA-loaded liposomes showed higher cytotoxicity than free Gd-DTPA-BMA. Moreover, these liposomes presented minimal toxicity in normal cell line when compared to the free Gd-DTPA-BMA. Therefore, the results of this study suggest that thermosensitive liposomes containing Gd-DTPA-BMA might be a new promising nanocarrier system for breast cancer treatment.

KEYWORDS: gadodiamide, thermosensitive liposomes, breast cancer.

1 INTRODUCTION

Currently, malignant neoplasms are identified as one of the main causes of worldwide morbidity and mortality, corresponding to the second highest cause of death due to illness in Brazil (INCA, 2018; WHO, 2018). Therefore, the search for new alternatives for antitumor pharmacological treatment is of extreme relevance, since many types of cancers do not respond to the available treatments (KAELIN JR, 2005; LOPES et al., 2013b; MROSS; KRATZ, 2011; ZUGAZAGOITIA et al., 2016).

To reduce toxic effects, bypass resistance, increase therapeutic index, and selectively target drugs to the tumor region, various nanotechnological formulations have been developed, mainly, liposomal formulations containing promising anticancer agents (BARBOSA et al., 2015; LIU; ZHANG, 2012; MAIA, 2015; MAIA et al., 2016; YINGCHONCHAROEN et al., 2016). As previously reported, studies conducted by our research group have demonstrated important *in vitro* and *in vivo* activity of Gd complexes (Gd-DTPA-BMA and Gd-DTPA-BMA radioactive) against different tumor models (SOARES et al., 2011a; SOARES et al., 2011b; SOARES et al., 2012; SOARES et al., 2013; MAIA et al., 2016). Gd-DTPA-BMA is an extracellular contrast agent, extremely hydrophilic, which present low cellular internalization (LIU; ZHANG, 2012; MAIA et al., 2016). The administration of this drug encapsulated in liposomes may favor its internalization, and consequently, potentiate its antitumor action. The clinical use of Gd is exclusively performed in the complexed form, in order to avoid the toxicity induced by the Gd^{3+} ion. In the free form, this ion presents prolonged half-life and can compete with endogenous metals (LIU; ZHANG, 2012). The Gd-DTPA-BMA injection (Omniscan®, GE Healthcare), commercially available, contains caldiamide sodium (NaCa-DTPA-BMA) in the composition to ensure the stability of the complex and the safety of the solution, preventing the presence of Gd^{3+} ions (GE HEALTHCARE, 2013). The clinical use of Gd-DTPA-BMA is considered safe, due to its high stability at physiological pH, although its use is not recommended in patients with advanced renal disease, due to the risk of developing Systemic Nephrogenic Fibrosis, a rare side effect associated with the use of Gd contrasts (FDA, 2018; SHELLOCK; KANAL, 1999). In this context, the encapsulation of Gd-DTPA-BMA in liposomes may also be useful, since the administration of this contrast in the liposomal form in Ehrlich tumor-bearing Swiss mice did not result in alterations in the tubular or the glomerular renal functions of the treated animals (SOARES et al., 2012).

During the advancement of the use of liposomes as drug carriers, different structural modifications have been made in order to ensure the effectiveness of treatment. The current trend is to develop systems that allow an image-guided drug delivery. This procedure offers the possibility to trigger and monitor in real time the drug release (GARELLO; TERRENO, 2018). For this, thermosensitive liposomes have been developed employing the coencapsulation of antitumor drugs and contrast agents that can be visualized by means of MRI (HAEMMERICH; MOTAMARRY, 2018; HIJNEN et al., 2017; LAMICHHANE et al., 2018). The thermosensitive liposomal formulations proposed in this study cover these aspects. Several studies have been reporting the use of Gd-DTPA-BMA in liposomes for MRI applications (GRAHN et al., 2009; HOSSAN et al., 2010; HOSSAN et al., 2013). However, thermosensitive liposomes are an advantageous, promising tool, yet not investigated for the treatment of cancer employing Gd-DTPA-BMA. The success of therapy with thermosensitive liposomes has been attributed to the association with hyperthermia techniques, being the moderate hyperthermia the most used procedure in antitumor therapy (KUMAR; MOHAMMAD, 2011; MANZOOR et al., 2012). The beneficial effects of hyperthermia go beyond the modulation of the local conditions of the neoplastic region (increased blood flow and vascular permeability modification), since the heat interferes directly in the cellular environment, promoting the denaturation of important proteins for tumor progression, and induces death by apoptosis, which may contribute to a greater efficacy of the chemotherapeutic treatment (HILDEBRANDT et al., 2002; ISSELS, 2008; ISSELS et al., 2016). In view of the theoretical basis presented, the aim of the study was to develop, characterize, and assess the potential cytotoxic activity of different thermosensitive liposomal formulations containing Gd-DTPA-BMA (TTSL-Gd and LTSL-Gd) against breast tumor models. The formulations were designed aiming to the possibility of image-guided drug delivery, in future *in vivo* studies (**Figure 1**).

Gd-DTPA-BMA was used in the non-radioactive form to avoid toxic effects associated with radiation and the complexity of preparation of liposomes containing radioisotopes (handling of radioactive material and license granted by government agencies) (MAIA et al., 2016). The formulations were prepared by REV and BANGHAM methods, in order to compare the encapsulation percentages obtained by each of these procedures (BANGHAM et al., 1965; SZOKA; PAPAHADJOPOULOS, 1978). The percentage of encapsulated drug is a relevant parameter, since the liposomes efficacy *in vitro* and *vivo*, as well as their physicochemical properties, may depend on the total drug loaded into these nanosystems (LOPES et al., 2013a). The preparation of two liposomes with different compositions aims to

evaluate the influence of the composition on the release profile and on the potential cytotoxic activity of Gd-DTPA-BMA. Two breast cancer cell lines were selected for performing cytotoxicity studies. This type of cancer, among the non-melanoma types, is the most frequent in women in Brazil and the responsible for the majority of deaths in women worldwide (INCA, 2018; SAADEH et al., 2014; WHO, 2018). For this, 4T1 (murine breast adenocarcinoma) and MDA-MB-231 (human breast adenocarcinoma) lines were selected. 4T1 cells, when injected into mice, spontaneously metastasize to the lungs, liver, lymph nodes, and brain, similar to the dissemination of human breast tumor cells (PULASKY; OSTRAND-ROSENBERG, 2011). The MDA-MB-231 cells also are derived from metastatic sites (LIU et al., 2018). These models were chosen because of the high prevalence of breast cancer and more than 90% of deaths associated with cancer are caused by metastases (CHAFFER; WEINBERG, 2011). Finally, a normal human lung fibroblast cell line (WI-26 VA4) was used to confirm selectivity (KIM et al., 2018).

Figure 1 – Representation of the approach proposed for this study and for future studies from our research group.

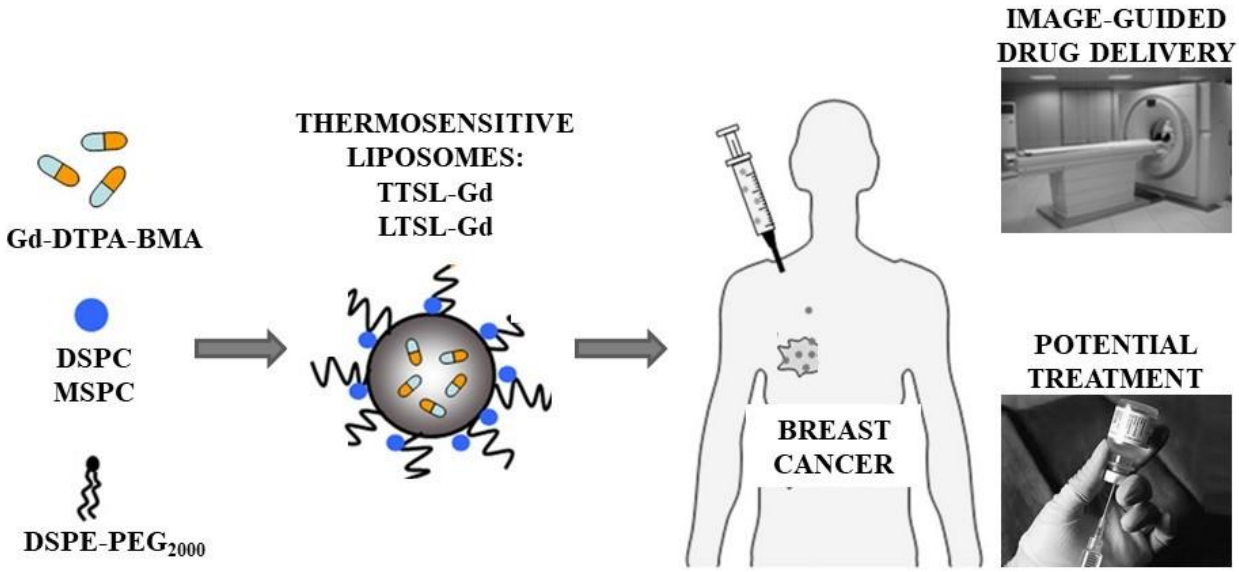

Adapted from PRADHAN et al., 2010; LIU; ZHANG, 2012.

2 MATERIALS AND METHODS

2.1 Materials

In the experiments, of this chapter, the same items described in section *"2.1 Materials"* from the *"Chapter 1"* were used.

For *in vitro* studies, the Roswell Park Memorial Institute Medium (RPMI) 1640 was purchased from American Type Culture Collection (ATCC) (Manassas, USA). Fetal bovine serum (FBS), 3-(4,5-dimethylthiazolyl-2)-2,5-diphenyltetrazolium bromide (MTT), trypsin-EDTA solution, and dimethylsulfoxide (DMSO) were purchased from Sigma Chemical Company (St. Louis, USA). The cancer cell lines 4T1 and MDA-MB-231 were purchased from ATTC (Manassas, USA). Cell line WI-26 VA4 was kindly supplied by Professor Adriano de Paula Sabino (Universidade Federal de Minas Gerais, Belo Horizonte, Brazil).

2.2 Methods

2.2.1 Thermal stability of Gd-DTPA-BMA

The thermal stability of Gd-DTPA-BMA was determined to verify if the drug suffers degradation when is heated under the same conditions that should be employed during the preparation of the liposomes. The analyses were performed by means of infrared spectrometry, ultraviolet spectrometry, and HILIC chromatography. The determinations were performed, in triplicate, on the samples: (*i*) Gd-DTPA-BMA without heating, (*ii*) Gd-DTPA-BMA after 30 min of heating at 55 °C, and (*iii*) Gd-DTPA-BMA after 60 min of heating at 55 °C.

Absorption spectra in the infrared region were recorded in the range of 4,000 to 400 cm^{-1} using a spectrophotometer Spectrum One Perkin-Elmer (Massachusetts, USA) with attenuated total reflectance system. These analyses were performed using aliquots of Gd-DTPA-BMA at 0.5 mmol/mL. During sample preparation, the aliquots were frozen and lyophilized on a 48 h cycle using the Modulyod 115, a Thermo Fisher Scientific freeze dryer (Massachusetts, USA).

Absorption spectra in the ultraviolet region, between 200 and 400 nm, were obtained on a UV-Vis Shimadzu 1800 series spectrometer (Tokyo, Japan), connected to the UV Probe 2.33

program. The analyses were performed on samples of Gd-DTPA-BMA diluted in purified water at a concentration of 57 mg/mL.

HILIC analyses were performed using the chromatographic conditions described in section *"2.2 Chromatographic conditions"* from the *"Chapter 1"*. Chromatograms of Gd-DTPA-BMA at 0.5 μmol/mL were obtained using mobile phase as solvent (MAIA et al., 2018).

2.2.2 Preparation of liposomes

The TTSL (traditional temperature-sensitive liposomes), TTSL-Gd (traditional temperature-sensitive liposome containing Gd-DTPA-BMA), LTSL (lysolipid-containing temperature-sensitive liposome), and LTSL-Gd (lysolipid-containing temperature-sensitive liposomes containing Gd-DTPA-BMA) formulations were prepared by REV and BANGHAM methods. The total lipid concentration defined for all liposomes was 40 mmol/L. The composition of each formulation was chosen based on the studies of Li and collaborators (2013).

The liposomes were prepared by the REV method, as described in section *"2.3 Preparation of liposomes"* from the *"Chapter 1"* (MAIA et al., 2018; SZOKA; PAPAHADJOPOULOS, 1978).

The liposomes were also prepared by lipid hydration method (BANGHAM et al., 1965). To prepare TTSL-Gd, aliquots of chloroform solutions of DPPC, DSPC, and DSPE-PEG_{2000}, in the lipid molar ratio of 80:15:5 respectively, were transferred to a round bottom flask and subjected to evaporation of the solvent under reduced pressure, in a rotary evaporator R-210 Büchi Labortechnik (Flawil, Switzerland) employing the conditions: 103 mbar, 120 rpm, for 2 h. Similarly, for the preparation of LTSL-Gd, aliquots of chloroform solutions of DPPC, MSPC, and DSPE-PEG_{2000}, in lipid molar ratio of 85:10:5, respectively, were transferred to a round bottom flask and chloroform was evaporated using the same conditions above mentioned. The lipid film obtained, in both cases, was hydrated with a solution of Gd-DTPA-BMA (250 μmol/mL) diluted in HEPES buffer, preheated at 55 °C for 60 min. The obtained dispersion was then subjected to shaking in a Mini-shaker Ika, model MS1 (Wilmington, USA), with the aid of glass beads, at 300 rpm, until MLV vesicles were obtained. To obtain TTSL and LTSL liposomes without Gd-DTPA-BMA, the same experimental protocol was performed, except for the step of addition of the drug, which was replaced by the addition of HEPES buffer at 10 mmol/L.

The calibration of the obtained liposomes was performed using 10 extrusion cycles (Extruder T001, Lipex Biomembranes, Burnaby, Canada), in polycarbonate membranes of 0.4, 0.2, and 0.1 μm pore size, respectively, under nitrogen flow and at 55 °C. Each cycle corresponds to the passage of the complete formulation volume by the extruder.

Non-entrapped Gd-DTPA-BMA and HEPES buffer were separated from liposomes by ultracentrifugation at 350,000 x *g*, 4 °C, for 2 h (Optima Ultracentrifuge L-XP series, Beckman Coulter, California, USA). Before the purification, the liposomes were diluted 3-times in purified water. After ultracentrifugation, the pellet was reconstituted in HEPES buffer to obtain the same initial volume (before dilution).

2.2.3 Determination of mean vesicle diameter, polydispersity index, and zeta potential

The mean diameter and the polydispersity index of the vesicles were determined by dynamic light scattering (DLS), at 25 °C, at an angle of 90°. The zeta potential was determined by DLS associated with electrophoretic mobility, at pH 7.4, at an angle of 90°. The measurements were performed, in triplicate, in a Nano ZS 90 Zetasizer (Malvern Instruments, England). The samples were diluted using HEPES buffer as a solvent, at a ratio of 1:20. The results were expressed as the mean ± SD of three different batches of each formulation.

2.2.4 Determination of Gd-DTPA-BMA entrapment and drug encapsulation percentage

The determination of Gd-DTPA-BMA entrapment (concentration of Gd-DTPA-BMA encapsulated into liposomes in terms of μmol/mL) was performed after liposomes purification by ultracentrifugation. The drug encapsulation percentage was defined as the ratio between the amount of Gd-DTPA-BMA encapsulated into the liposomes and the total of Gd-DTPA-BMA added in the preparation. The total amount of drug added in the preparation of the liposomes was evaluated before purification procedures. The drug encapsulation percentage was calculated from Equation 1:

$$\textit{Drug encapsulation percentage (\%)} = [Gd_E] / [Gd_T] \times 100 \quad (1)$$

Where: Gd_E is the concentration of Gd-DTPA-BMA entrapped (μmol/mL) in the liposome purified (determined after ultracentrifugation) and Gd_T is the concentration of total Gd-DTPA-BMA (μmol/mL) added in the preparation of the liposomes (determined before ultracentrifugation) (MAIA et al., 2016).

The determination of Gd-DTPA-BMA in the samples was performed by HILIC employing the chromatographic conditions described in section *"2.2 Chromatographic conditions"* from the *"Chapter 1"* (MAIA et al., 2018). The samples were diluted considering the linear range. The chromatograms were obtained using the mobile phase as a solvent. The liposomes were previously solubilized in isopropyl alcohol in the ratio of 1:10 for complete disruption of the vesicles. The results were expressed as the mean ± SD of three different batches of each formulation.

2.2.5 Storage stability study

The determination of the storage stability of liposomes was performed at 7, 15, 30, 60, 90, 120, and 180 days after preparation. The formulations were maintained at 4 °C, under a nitrogen atmosphere. The parameters evaluated included mean diameter, polydispersity index, zeta potential, and drug entrapment. The determination of the Gd-DTPA-BMA content into the liposomes was performed by HILIC employing the chromatographic conditions described in section *"2.2 Chromatographic conditions"* from the *"Chapter 1"* (MAIA et al., 2018). For this, in each time of study, the samples were again purified using the ultrafiltration procedure: centrifugation at 14,000 x *g* for 20 min (Centrifugal Heraeus Multifuge X1R, Thermo Fisher Scientific, Massachusetts, USA), using a centrifugal filter device (Amicon® Ultra-4 10 kDa MWCO, Millipore, Billerica, USA). The mean values of the parameters evaluated were compared with those obtained at time zero. The results were expressed as the mean ± SD of three different batches of each formulation.

2.2.6 Morphological characterization

The morphological examination of liposomes was carried out by transmission electron microscopy (TEM) using a negative staining method (LOPES et al., 2013b). Images were acquired using a Tecnai G2 12 microscope Spirit Biotwin FEI Company with an acceleration potential of 200 kV (Centro de Microscopia, Universidade Federal de Minas Gerais, Belo

Horizonte, Brazil). The liposomes were placed on a formvar-coated copper grid and stained with a 2% (w/v) phosphotungstic acid solution containing 0.5% (w/v) bovine serum albumin and 0.5% (w/v) saccharose. TEM examinations were performed at 24 h after the preparation of the liposomes, enabling complete drying of the samples.

2.2.7 Thermal characterization

The liposomes thermosensitivity was evaluated in a preliminary study by DLS. The measurements were performed, in triplicate, using a Nano ZS 90 Zetasizer (Malvern Instruments, England). Samples were diluted in FBS at a ratio of 1:20 and heated in a range of temperature from 37 °C to 45 °C, using a heating rate of 1 °C/min. The parameters evaluated included mean diameter and particle derived count rate in terms of kilo counts per second (Kcps) (MALVERN INSTRUMENTS, 2013). The results were expressed as the mean ± SD of three different batches of each formulation.

The liposomes *Tc* values were assessed by Differential scanning calorimetry (DSC) analyses using a Microcal VP-DSC Malvern Instruments microcalorimeter (Laboratório Multiusuário de Análises Biomoleculares, Universidade Federal do Espírito Santo, Vitória, Brazil). In brief, liposomes were diluted in HEPES buffer, to a concentration of 1 mg/mL. The heat capacity (Cp), at constant pressure in units of cal/°C was then measured from 15 °C to 65 °C with a heating rate of 1 °C/min (WANG et al., 2008).

Small-angle X-ray scattering (SAXS) measurements were performed as previously described (LOPES et al., 2014; MONTEIRO et al., 2016; RUI-GUANG et al., 2012). Analyses were carried out at D1B-SAXS1 beamline of the Brazilian Synchrotron Light Laboratory (Campinas, Brazil), at a fixed x-ray wavelength (λ) of 0.1488 nm. SAXS patterns were detected using a 300 K Pilatus detector providing a q range of 0.15 to 4.00 nm^{-1}, where q is calculated using Equation 2:

$$q = (4\pi/\lambda) \sin \theta \quad (2)$$

Where: q is the momentum transfer, and θ is the scattering angle.

The samples were deposited on metal rings, which were sealed by a polyimide film (Kapton®). A sample holder with a DSC-linkam heating system was also used for

temperature control (± 0.1 °C) and the heating rate was 1 °C/min, in a heating range from 25 °C to 50 °C. The liposomes samples were prepared by ultracentrifugation, using the same conditions described in the section *"2.2.3 Preparation of liposomes"*. The SAXS measurements were performed in the pellet formed after the ultracentrifugation procedure.

2.2.8 *In vitro* release analyses and *in vitro* release kinetics

In vitro release analyses were performed using the dilution method and an adapted protocol from previously studies (HOSSAN et al., 2007; HOSSAN et al., 2012; HUANG et al., 2017; LI et al., 2010; LIMMER et al., 2014; OLIVEIRA et al., 2016).

The influence of temperature on TTSL-Gd and LTSL-Gd release rate was determined. The content of Gd-DTPA-BMA release from the liposomes was measured after 5 and 10 min of incubation in FBS, at temperatures from 37 °C to 45 °C. For this, each liposome was diluted at a ratio of 1:50 in FBS at room temperature, and added in a heat resistant vial. Then, the vial was incubated in a pre-heated thermoshaker (KS 4,000 I control, IKA, Wilmington, USA), and kept under stirring at 150 rpm. After incubation, during the pre-set time, each vial was quickly immersed into an ice bath to stop the release and was immediately transferred to a centrifugal filter device (Amicon® Ultra-4 10 kDa MWCO, Millipore, Billerica, USA) and centrifuged at 14,000 x *g* for 20 min (Centrifugal Heraeus Multifuge X1R, Thermo Fisher Scientific, Massachusetts, USA). The Gd-DTPA-BMA released from liposomes was measured by HILIC and the percentage was calculated using Equation 3:

$$\textit{Gd-DTPA-BMA release percentage (\%)} = [Gd_R] / [Gd_E] \times 100 \quad (3)$$

Where: Gd_R is the concentration of Gd-DTPA-BMA released (μmol/mL) (determined in the filtrated) and Gd_E is the concentration of Gd-DTPA-BMA entrapped (μmol/mL) in the liposome.

In vitro Gd-DTPA-BMA release from the liposomes, over time, was also monitored. The optimal temperature for release achieved from temperature-dependent Gd-DTPA-BMA release study was adopted as fixed temperature for time-dependent Gd-DTPA-BMA release experiments. The samples were diluted in FBS as described above and incubated in the pre-

heated thermoshaker for 1 h. The Gd-DTPA-BMA released from liposomes was determined by HILIC and the percentage was calculated using Equation 3.

In vitro Gd-DTPA-BMA release from liposomes at 37°C was also determined. The samples were diluted in FBS as described above and incubated in the pre-heated thermoshaker for 24 h. The Gd-DTPA-BMA released from liposomes was determined by HILIC and the percentage was calculated using Equation 3.

From the results obtained in the release study, the reaction kinetics were calculated with the purpose of inferring the release mechanism of Gd-DTPA-BMA. The release constants were obtained by equations of zero-order (Equation 4), first-order (Equation 5), second-order (Equation 6), and Higuchi (Equation 7) kinetic models (CÉSAR, 2015; COSTA; LOBO, 2001; JAIN, A.; JAIN, S. K., 2016).

$$1 - ([A]/[A_0] = mt \quad (4)$$

$$ln([A]/[A_0] = -mt \quad (5)$$

$$(1/[A]) - (1/[A_0]) = mt \quad (6)$$

$$1 - ([A]/[A_0]) = m\sqrt{t} \quad (7)$$

Where: $[A]$ is the percentage of Gd-DTPA-BMA released (%) at time t, $[A_0]$ is the concentration of Gd-DTPA-MBA at time 0, m is the angular coefficient of linear regression.

The more probable kinetics were determined based on the quality of the linear regression obtained, in the time interval under study. For this, the r^2 values obtained were evaluated.

2.2.9 Cell cultures and cytotoxic evaluation

4T1, MDA-MB-231, and WI-26 VA4 cell lines were grown and maintained in RPMI medium, pH 7.4, supplemented with 10% (v/v) FBS and 1% (v/v) of antibiotics (100 μg/mL streptomycin and 100 UI/mL penicillin). All cultures were kept in a humidified incubator with

a controlled atmosphere of 5% CO_2 (v/v) at 37 °C (MAIA et al., 2016; OLIVEIRA et al., 2016).

MTT assay was carried out to evaluate the cytotoxicity of free drug and liposomes containing or not Gd-DTPA-BMA against 4T1 and MDA-MB-231 cancer cell lines as previously described in protocols from the literature (BARBOSA et al., 2015; JOSE et al., 2018; MAIA et al., 2016). Cytotoxicity studies were also conducted against WI-26 VA4 normal cells to evaluate selectivity. MTT assay is based on the reduction of tetrazolium salt to formazan, which is possible only in living cells (MOSMANN, 1983). The treated groups were constituted by free Gd-DTPA-BMA, TTSL-Gd, and LTSL-Gd associated or not with hyperthermia. The control groups were constituted by blank liposomes (TTSL and LTSL) associated or not with hyperthermia. After reaching an adequate confluence, aliquots containing 1 x 10^6 cells/plates were seeded into 96-well plates. The plates were incubated for 24 h in 5% CO_2 at 37 °C. Then, freshly prepared solutions with respective treatments or controls were added to the wells. Seven concentrations were diluted in RPMI medium to obtain the concentrations 0.004; 0.015; 0.060; 0.242; 0.969; 3.875; 15.500 mmol/L of Gd-DTPA-BMA. Blank liposomes were diluted in the same proportion as Gd-DTPA-BMA-loaded liposomes. The plates, in which hyperthermia was used, were incubated at 37 °C, in 5% CO_2, for 6 h prior to heating, to allow the internalization of the liposomes into the cells. After this time, they were heated at the same temperature used in the time-dependent Gd-DTPA-BMA release assay, for 1 h. Then, the plates returned to the humidified incubator. The plates, in which hyperthermia was not used, were maintained during all time, in incubation at 37 °C and 5% CO_2. After 48 h of incubation at 5% CO_2 and 37 °C, the RPMI medium was removed and discarded. MTT reagent was added and kept in each well for 3 h. After this, formazan crystals were solubilized in 50 μL of DMSO. The plates were stirred at 50 rpm for complete solubilization of the crystals. Absorbances were measured in a SpectraMax Plus 384 microplate reader (Molecular Devices, CA, USA), at 550 nm, using the same solvent as control. Absorbance values of the wells in which the cells were maintained in medium alone were measured. Their absorbances were considered as 100% of cell viability.

The concentration capable to reduce the cell viability in 50% of growth, of the tumor cells (IC_{50}, inhibitory concentration) and of WI-26 VA4 cells (CC_{50}, cytotoxic concentration) were calculated by means of a non-linear regression model, using GraphPad Prism 5.0 software for all performed treatments. IC_{50} of free Gd-DTPA-BMA was calculated from MTT assay using highest concentrations (0.10; 0.39; 1.56; 6.25; 25.00; 100.00; 400.00 mmol/L).

The selectivity index (SI) was calculated by the ratio CC_{50}/IC_{50}. At least three independent experiments were performed for each evaluated group.

2.2.10 Statistical analyses

Normality and homogeneity of variance analyses were performed by Lilliefor's and Bartlett's tests, respectively. Data of liposome characterization were evaluated using the ANOVA test followed by Tukey's test. Data of the cytotoxicity study were tested using ANOVA followed by the Bonferroni test. For all analyses, differences were considered significant when the *p*-value was lower than 0.05. All statistical analyses were performed using the GraphPad Prism 5.0 computer program (GraphPad Software Inc., CA, USA).

3 RESULTS AND DISCUSSION

3.1 Thermal stability of Gd-DTPA-BMA

The thermal stability evaluation of Gd-DTPA-BMA was performed to verify the influence of heating, used during the preparation of thermosensitive liposomes, on drug degradation. The Gd-DTPA-BMA samples were heated at 55 °C for 30 and 60 min and compared to a sample of the drug that had not undergone any type of heating. The times of 30 and 60 min were selected because they correspond to the times in which Gd-DTPA-BMA is heated at 55 °C in the extrusion and lipid film hydration steps (by the BANGHAM method), respectively.

Infrared spectroscopy analysis was performed using lyophilized samples of the injectable aqueous solution of Gd-DTPA-BMA, since the hydroxyls present in the water molecules could generate signals that overlap the bands characteristic of the drug.

From the infrared spectra obtained (**Figure 2**), it was observed that there was no thermal degradation of Gd-DTPA-BMA, since all analyzed samples showed bands of absorption at the same wavelengths, with similar intensities. The main absorption bands obtained, as well as the attribution related to the functional groups of the complex, were presented in **Table 1**.

Figure 2 – Infrared absorption spectra of Gd-DTPA-BMA lyophilized samples, Gd-DTPA-BMA without heating (black line), Gd-DTPA-BMA after 30 min of heating at 55 ° C (blue line) and Gd-DTPA-BMA after 60 min of heating at 55 °C (red line).

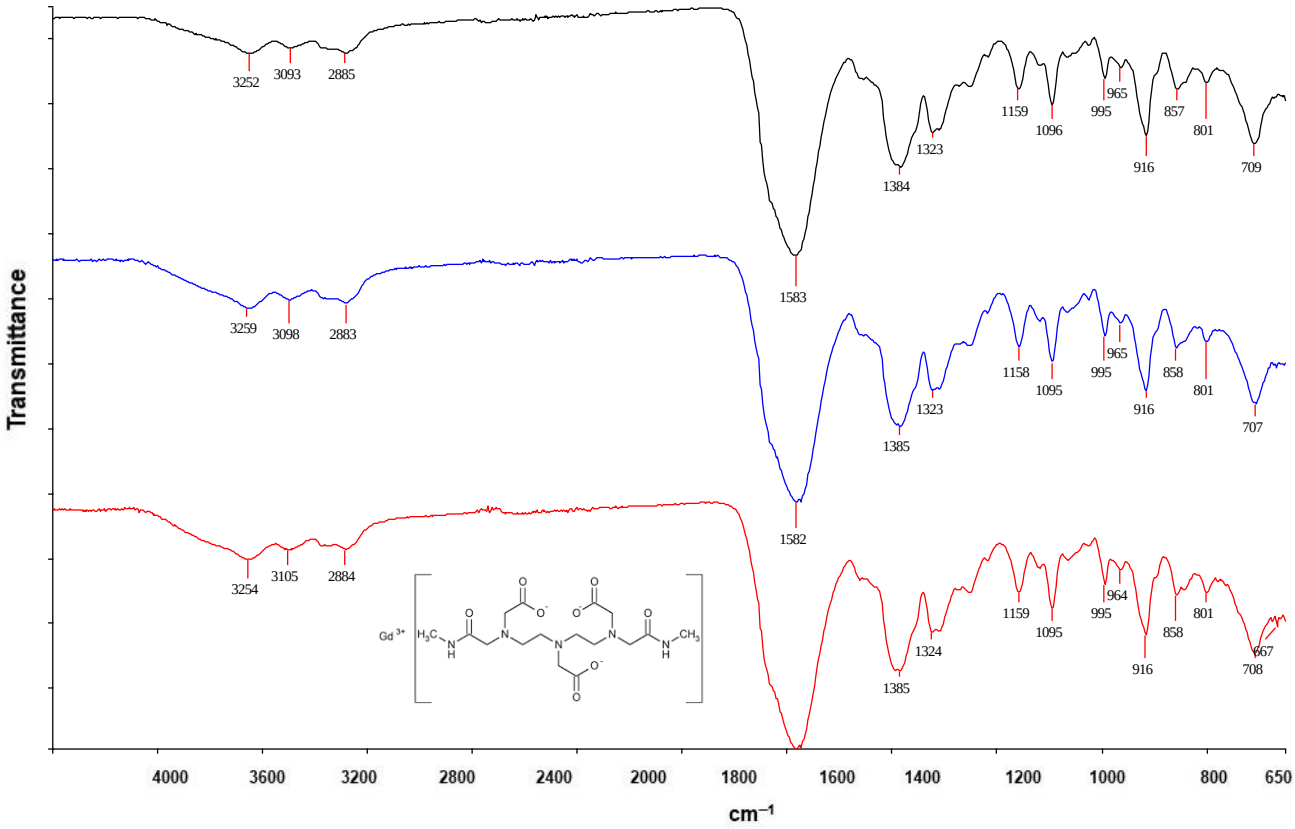

Table 1 – Wave numbers and attribution of the absorption bands obtained in the infrared spectrum of Gd-DTPA-BMA.

Wave number (cm^{-1})	Attribution and functional group
1095	Carbon-oxygen bond stretch of carboxylate
1384	Angular deformation of the carbon-hydrogen bond
1582	Stretch of carbon-oxygen bond of amide Carbon-oxygen double bond stretch of carboxylate
2885	Stretch of carbon-hydrogen bond of aliphatic carbon
3252	Stretch of nitrogen-hydrogen bond of amide

Adapted from: BARBOSA et al., 2011; PAVIA et al., 2010.

Spectra obtained from ultraviolet absorption confirm the thermal stability of Gd-DTPA-BMA under the heating conditions used (**Figure 3**). All analyzed samples showed similar spectral profile with maximum absorption at 210 nm.

Figure 3 – Absorption spectra, in the ultraviolet region, of aqueous solutions of Gd-DTPA-BMA at 0.5 μmol/mL, Gd-DTPA-BMA without heating (black line), Gd-DTPA-BMA after 30 min of heating at 55 °C (blue line) and Gd-DTPA-BMA after 60 min of heating at 55 °C (red line).

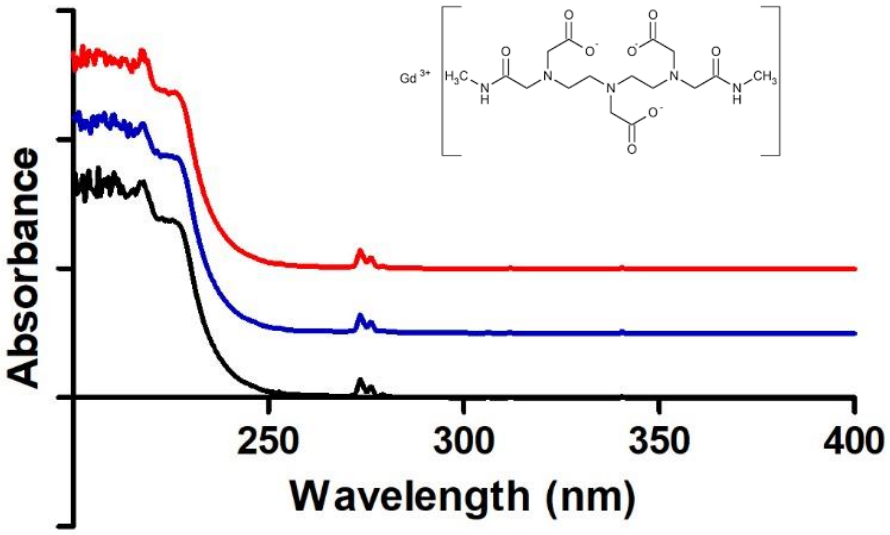

The chromatograms obtained by HILIC also confirm the thermal stability of Gd-DTPA-BMA under the conditions evaluated (**Figure 4**). The heated samples presented elution at 7.1 minutes, as well as the sample that did not undergo heating. No degradation peaks were observed in any of the obtained chromatograms. In addition, the purity of the Gd-DTPA-BMA peak, measured by DAD, was 100% in all samples.

These results confirm that Gd-DTPA-BMA is a suitable drug for encapsulation in thermosensitive liposomes since that complex remains stable during the heating conditions used in the preparation of such formulations. The obtained data are in accordance with studies in the literature, which used analyses by thermogravimetry and DSC, that concluded that Gd-DTPA-BMA presents thermal stability up to about 300 °C (AUKRUST et al., 1997; GE HEALTHCARE, 2013).

Figure 4 – Chromatograms of aqueous solutions of Gd-DTPA-BMA at 0.5 μmol/mL, Gd-DTPA-BMA without heating (black line), Gd-DTPA-BMA after 30 min of heating at 55 ° C (blue line) and Gd-DTPA-BMA after 60 min of heating at 55 °C (red line).

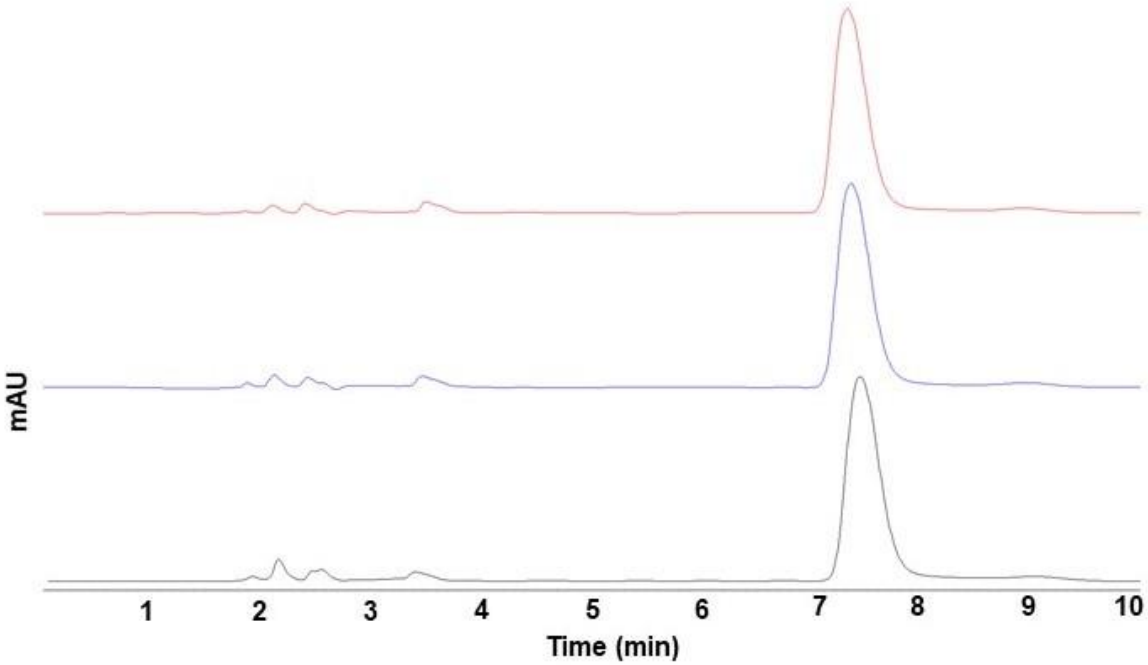

3.2 Preparation of liposomes by REV and BANGHAM methods

Physical properties (size, shape, and structure) and chemical characteristics (charge, surface binders) may affect the biological performance of various nanostructures, including liposomes (BARBOSA et al., 2015; SACCHETTI et al., 2013). Therefore, these parameters need to be adequately planned and characterized in order to guarantee their therapeutic success. Vesicle size and polydispersity index are properties directly related to liposomes biodistribution (LOPES et al., 2013a). Its well known that nanoparticles with an average diameter in the range from 100 to 150 nm are opsonized more slowly and in a minor extent than larger particles. Moreover, these nanoparticles preferentially accumulate in the tumor region by passive targeting (LOPES et al., 2013b; SHARMA, A.; SHARMA, U., 1997).

Passive targeting occurs due to the characteristics of the tumor microenvironment, which presents intense and accelerated autonomic angiogenesis, resulting in a deformed vascular architecture. Thus, unlike blood vessels present in healthy tissues, tumor vascular tissue presents large fenestrations between adjacent endothelial cells. These fenestrations associated with inefficient lymphatic perfusion allow vesicles of adequate size to remain in the neoplastic region due to enhanced permeability and retention effect (EPR) (FERREIRA et

al., 2013; MAEDA, 2001; MAIA, 2015). On the other hand, it is well known that liposomes having an average diameter greater than 400 nm are unable to diffuse through the tumor interstitium in a concentration sufficient to have any therapeutic effect (STEICHEN et al., 2013). The liposomes used in antitumor therapy are administered intravenously, so the mean diameter of the vesicles should be controlled not only to modulate *in vivo* behavior but also to ensure that vascular occlusions or pulmonary embolism do not occur as a result of the treatment. In this context, The United States Pharmacopoeia recommends, based on the diameter of the blood capillaries (around 4 to 9 μm), that injectable lipid formulations should have an average diameter of less than 500 nm, measured in terms of intensity. In addition, the percentage of vesicles greater than 500 nm should be less than 0.05%, when assessing the volume distribution of the vesicles in terms of volume (DRISCOLL, 2006; THE UNITED, 2013).

In this study, thermosensitive liposomes were prepared by REV and BANGHAM methods. The physicochemical characteristics of each formulation were evaluated during the three stages of the preparation: (*1*) formation of vesicles by REV or BANGHAM; (*2*) calibration of vesicle size by extrusion; (*3*) purification of vesicles by ultracentrifugation. The results of this evaluation for TTSL and TTSL-Gd liposomes are set out in **Table 2**. **Table 3** shows the results obtained for LTSL and LTSL-Gd.

From the results of **Tables 2** and **3** it can be observed that in general TTSL-Gd and LTSL-Gd presented similar physicochemical characteristics, as well as their respective blank formulations. By analyzing the three stages of preparation, it is identified that the extrusion procedure was essential for obtaining liposomes with adequate diameter, polydispersity index, and vesicles diameter distribution. Prior to the extrusion, mean diameter values ranged from 1,347 to 1,850 nm for the liposomes obtained by BANGHAM method, while formulations obtained by the REV method showed a mean diameter between 500 and 967 nm. These values are consistent with the type of liposome obtained by each method. The BANGHAM method produces MLV liposomes, while by the REV method LUV liposomes are obtained (DELATTRE et al., 1993; LAOUINI et al., 2012; LOPES et al., 2013a). Considering the results, independent of the vesicle formation method, the extrusion procedure allowed to obtain monodispersed liposomes (polydispersity index <0.3), with mean diameter values between 109 nm and 128 nm. In addition, in all extruded formulations, no particles larger than 300 nm were observed, as shown in the data of the distribution of vesicles diameter.

Table 2 – Physicochemical characteristics of TTSL and TTSL-Gd obtained by REV and BANGHAM methods.

Formulation	Method of vesicle formation [a]	Preparation step [b]	Mean diameter (nm) [c]	Polydispersity index	Distribution of vesicles diameter (%) [d]				Zeta potential (mV)	Mobility electrophoretic (µmcm/Vs)
					≤ 100 nm	≤ 200 nm	200 – 300 nm	≥ 300 nm		
TTSL	REV	1	573 ± 346	0.26 ± 0.04	9.1 ± 15.3	18.3 ± 29.6	2.1 ± 3.5	79.7 ± 33.0	– 1.5 ± 0.3	– 0.12 ± 0.02
		2	113 ± 2	0.08 ± 0.01	58.1 ± 5.4	98.7 ± 1.0	1.2 ± 1.1	0.0 ± 0.0	– 1.7 ± 0.4	– 0.13 ± 0.03
		3	115 ± 3	0.08 ± 0.03	54.5 ± 3.4	98.7 ± 0.7	1.3 ± 0.8	0.0 ± 0.0	– 1.7 ± 0.6	– 0.13 ± 0.05
TTSL-Gd	REV	1	967 ± 99	0.44 ± 0.09	0.0 ± 0.0	0.1 ± 0.2	0.0 ± 0.0	99.9 ± 0.4	– 1.9 ± 0.1	– 0.15 ± 0.01
		2	126 ± 1	0.08 ± 0.01	42.9 ± 2.1	96.8 ± 0.4	3.2 ± 0.5	0.0 ± 0.0	– 2.5 ± 0.4	– 0.19 ± 0.03
		3	128 ± 1	0.08 ± 0.01	40.1 ± 4.4	96.8 ± 0.5	3.3 ± 0.4	0.0 ± 0.0	– 2.3 ± 0.4	– 0.18 ± 0.03
TTSL	BANGHAM	1	1,718 ± 542	0.62 ± 0.36	0.0 ± 0.0	0.0 ± 0.0	0.0 ± 0.0	99.9 ± 0.1	– 1.8 ± 0.5	– 0.14 ± 0.04
		2	109 ± 4	0.07 ± 0.01	60.1 ± 4.8	99.3 ± 0.3	0.6 ± 0.3	0.0 ± 0.0	– 1.7 ± 0.3	– 0.13 ± 0.02
		3	109 ± 4	0.06 ± 0.01	58.0 ± 6.9	99.5 ± 0.1	0.5 ± 0.1	0.0 ± 0.0	– 1.7 ± 0.9	– 0.13 ± 0.07
TTSL-Gd	BANGHAM	1	1,850 ± 677	0.79 ± 0.20	0.0 ± 0.0	0.0 ± 0.0	0.0 ± 0.0	100.0 ± 0.0	– 1.6 ± 0.6	– 0.12 ± 0.05
		2	115 ± 17	0.06 ± 0.02	53.4 ± 24.2	98.6 ± 1.4	1.4± 1.5	0.0 ± 0.0	– 1.7 ± 0.3	– 0.13 ± 0.02
		3	114 ± 16	0.07 ± 0.01	55.2 ± 17.6	98.4 ± 2.0	1.6 ± 2.1	0.0 ± 0.0	– 2.8 ± 1.3	– 0.22 ± 0.10

Note: [a] The denominations REV and BANGHAM refers to the reverse phase evaporation and lipid film hydration methods, respectively; [b] The steps, 1, 2, and 3 refer to the REV or BANGHAM methods, extrusion, and ultracentrifugation, respectively; [c] Values expressed in terms of intensity; [d] Values expressed in terms of volume. Values are expressed as mean ± SD (n = 3 batches).
Abbreviations: TTSL, traditional temperature-sensitive liposomes; TTSL-Gd, traditional temperature-sensitive liposome containing Gd-DTPA-BMA.

Table 3 – Physicochemical characteristics of LTSL and LTSL-Gd obtained by REV and BANGHAM methods.

Formulation	Method of vesicle formation [a]	Preparation step [b]	Mean diameter (nm) [c]	Polydispersity index	Distribution of vesicles diameter (%) [d]				Zeta potential (mV)	Mobility electrophoretic (µmcm/Vs)
					≤ 100 nm	≤ 200 nm	200 – 300 nm	≥ 300 nm		
LTSL	REV	1	555 ± 220	0.39 ± 0.18	4.7 ± 4.2	6.7 ± 5.2	3.6 ± 3.6	89.6 ± 7.5	– 1.4 ± 0.2	– 0.11 ± 0.01
		2	115 ± 3	0.07 ± 0.03	56.0 ± 3.4	98.7 ± 0.9	1.3 ± 1.0	0.0 ± 0.0	– 1.3 ± 0.1	– 0.10 ± 0.01
		3	111 ± 3	0.10 ± 0.02	64.1 ± 6.3	98.6 ± 0.1	1.4 ± 0.1	0.0 ± 0.0	– 2.1 ± 0.3	– 0.16 ± 0.02
LTSL-Gd	REV	1	500 ± 137	0.35 ± 0.12	5.0 ± 4.0	7.8 ± 6.3	5.5 ± 8.7	86.7 ± 14.9	– 1.4 ± 0.3	– 0.11 ± 0.02
		2	128 ± 9	0.08 ± 0.01	41.5 ± 8.9	96.1 ± 2.6	3.7 ± 2.4	0.0 ± 0.0	– 1.3 ± 0.4	– 0.10 ± 0.03
		3	128 ± 8	0.08 ± 0.02	42.5 ± 9.6	96.3 ± 1.7	3.7 ± 1.6	0.0 ± 0.0	– 1.9 ± 0.2	– 0.15 ± 0.02
LTSL	BANGHAM	1	1,347 ± 121	0.85 ± 0.25	0.0 ± 0.0	0.0 ± 0.0	0.0 ± 0.0	99.9 ± 0.1	– 1.6 ± 0.5	– 0.12 ± 0.04
		2	119 ± 3	0.09 ± 0.02	53.8 ± 1.1	97.7 ± 1.1	2.2 ± 1.1	0.0 ± 0.0	– 0.9 ± 0.4	– 0.07 ± 0.03
		3	119 ± 3	0.08 ± 0.02	50.4 ± 5.5	98.2 ± 0.4	1.8 ± 0.4	0.0 ± 0.0	– 1.9 ± 0.5	– 0.15 ± 0.04
LTSL-Gd	BANGHAM	1	1,536 ± 232	0.44 ± 0.19	0.0 ± 0.0	0.0 ± 0.0	0,1 ± 0.2	99.7 ± 0.2	– 2.1 ± 0.3	– 0.16 ± 0.02
		2	118 ± 12	0.09 ± 0.02	52.5 ± 17.3	97.8 ± 1.7	2.2 ± 1.6	0.0 ± 0.0	– 2.1 ± 0.1	– 0.16 ± 0.01
		3	118 ± 12	0.08 ± 0.01	53.2 ± 12.2	97.9 ± 2.1	2.2 ± 2.1	0.0 ± 0.0	– 2.0 ± 0.1	– 0.15 ± 0.01

Note: [a] The denominations REV and BANGHAM refers to the reverse phase evaporation and lipid film hydration methods, respectively; [b] The steps, 1, 2, and 3 refer to the REV or BANGHAM methods, extrusion, and ultracentrifugation, respectively; [c] Values expressed in terms of intensity; [d] Values expressed in terms of volume. Values are expressed as mean ± SD (n = 3 batches).

Abbreviations: LTSL, lysolipid-containing temperature-sensitive liposome; LTSL-Gd, lysolipid-containing temperature-sensitive liposome containing Gd-DTPA-BMA.

These results are in accordance with the requirements defined by The United States Pharmacopeia and are within the range of the mean diameter (100 - 150 nm) most susceptible to the EPR effect, thus being able to contribute to an adequate biodistribution in future studies.

The zeta potential and the electrophoretic mobility were also evaluated since these parameters allow to predict the storage stability and the *in vivo* behavior of liposomes (MAIA et al., 2016). Generally, formulations with zeta potential values higher than 30 mV (in modulus) have satisfactory stability due to the high surface charge, which prevents, by electrostatic repulsion, the aggregation and coalescence of the vesicles (MORA-HUERTAS et al., 2010). It is important to emphasize that the incorporation of PEG to the liposomal surface can also be beneficial for the storage stability of these nanosystems. The PEG acts as a stabilizing agent, preventing the formation of aggregates and the destabilization of liposomes by means of steric repulsions (MAIA et al., 2016; WOLFRAM et al., 2014). This strategy was used in the present study by the addition of phospholipid DSPE-PEG_{2000} in the composition of liposomes.

In **Tables 2** and **3** are shown negative zeta potentials close to neutrality in all formulations evaluated. In addition, the electrophoretic mobility values obtained are in agreement with values described in the literature for liposomal formulations presenting between 5 and 10% of DSPE-PEG_{2000} in their composition (WOODLE et al., 1992). In general, liposomes containing PEG on their surface have low zeta potential values due to their reduced electrophoretic mobility probably caused by the high hydrodynamic resistance conferred by this polymer (BARROS et al., 2013; MAIA et al., 2016). The zeta potential near neutrality, obtained in this study, may be important to increase the circulation time of these formulations. It has been shown in previous studies that neutral particles bind less to plasma proteins than charged particles, circulating longer in the bloodstream (FERTSCH-GAPP et al., 2011; WOLFRAM et al., 2014).

The data of **Tables 2** and **3** also revealed that the ultracentrifugation performed after the extrusion did not cause changes in the physicochemical parameters evaluated, showing a suitable method for purification of the liposomes proposed in this study. The purification by centrifugation or ultracentrifugation may be infeasible if the encapsulated drug exhibits high values of density, concentration or molar mass, rendering the density of the liposome dispersion medium equal to or greater than the density of the phospholipids present in the formulation (NEW, 1990). Gd-DTPA-BMA in the hydrated form has a molar mass of 591.67 g/mol. This value is lower than the molar mass presented by several chemotherapeutics

commonly encapsulated in liposomes, whose purification is performed by centrifugation (BARBOSA et al., 2015; BISWAS et al., 2012; OTO et al., 1995). The density of the injectable solution of Gd-DTPA-BMA (Omniscan®), used in this study, is 1.15 g/cm³ at 20 °C (GE HEALTHCARE, 2013). This value is higher than the density of liposomes composed of phosphatidylcholines, whose density value is 1.01 g/cm³ at 20 °C (DELATTRE et al., 1993). This was probably the reason, that prevented the pellet formation when ultracentrifugation was performed using the conditions reported in section *"2.2.2. Preparation of liposomes"*, without using any previous samples preparation. This inconvenience was bypassed by diluting the liposomes in purified water, which has a lower density than the injectable Gd-DTPA-BMA solution. Thus, the Gd-DTPA-BMA-loaded liposome presented a higher density than the surrounding medium and, therefore, its sedimentation could occur properly. The dilution factor was determined experimentally and corresponded to the lowest value capable of allowing the formation of the pellets. The dilution employed could be corrected after ultracentrifugation, since the liposomes were reconstituted in HEPES buffer considering the initial concentration of the formulations.

The influence of the method used to form vesicles (REV or BANGHAM) on the encapsulation of Gd-DTPA-BMA was also evaluated. The concentration of Gd-DTPA-BMA entrapment and the encapsulation percentage are shown in **Table 4**. The drug/lipid molar ratio was also evaluated as this is an important parameter for the development of liposomal formulations for clinical application (BARBOSA et al. al., 2015). This relationship should be maximized so that smaller amounts of lipids are administered to the patient, thus reducing the risks of side effects associated with these compounds (FRÉZARD et al., 2005).

Table 4 – Influence of the vesicle formation method on the encapsulation of Gd-DTPA-BMA in TTSL-Gd and LTSL-Gd.

Formulation	Method of vesicle formation [a]	Gd-DTPA-BMA entrapment (μmol/mL)	Gd-DTPA-BMA entrapment (mg/mL)	Encapsulation percentage (%)	Drug-to-lipid molar ratio
TTSL-Gd	REV	26.4 ± 4.0	15.2 ± 2.3	10.6 ± 1.6	0.66 ± 0.10
	BANGHAM	25.7 ± 2.0	14.7 ± 1.1	10.3 ± 0.8	0.64 ± 0.05
LTSL-Gd	REV	22.9 ± 3.1	13.2 ± 1.8	9.2 ± 1.2	0.57 ± 0.08
	BANGHAM	23.8 ± 3.3	13.7 ± 1.9	9.5 ± 1.3	0.59 ± 0.07

Note: [a] The denominations REV and BANGHAM refer to the reverse phase evaporation and lipid film hydration methods, respectively; Values are expressed as mean ± SD (n = 3 batches).
Abbreviations: TTSL-Gd, traditional temperature-sensitive liposome containing Gd-DTPA-BMA; LTSL-Gd, lysolipid-containing temperature-sensitive liposome containing Gd-DTPA-BMA.

Regardless of the method used for vesicle formation, no significant differences were observed between the concentration of Gd-DTPA-BMA entrapped into the TTSL-Gd and LTSL-Gd formulations, probably because they have a similar composition. The REV method is described in the literature as the most suitable procedure for the encapsulation of hydrophilic substances, due to the production of liposomes that have large internal aqueous space, thus being able to accommodate larger amounts of the drug (LAOUINI et al., 2012). However, in the present study, no significant differences in drug load capacity were observed between the formulations obtained by REV and BANGHAM methods. This result might be explained by the fact that liposomes obtained by REV were prepared at room temperature while the liposomes obtained by BANGHAM were produced at a temperature higher than the T_c of the phospholipids DPPC and DSPC. In this case, the high fluidity presented by the lipid membrane of the liposomes, due to the heating used during the preparation, may have facilitated the hydration, resulting in percentages of encapsulation similar to the percentages obtained by REV. Another explanation that justifies the lack of significant difference between the results of Gd-DTPA-BMA entrapment is that MLV liposomes prepared by the lipid film hydration method became LUV after the extrusion step. Thus, like the liposomes obtained by REV, these liposomes also have a large internal aqueous space. It is well described in the literature the transformation of MLV liposomes into LUV as a result of extrusion (WANG et al., 2008; LOPES et al., 2013a). The lamellarity of these formulations will be confirmed in the morphological analysis by TEM. In the last eight years, our research group has performed studies on the development and characterization of conventional, pH-sensitive and stealth pH-sensitive liposomes containing Gd-DTPA-BMA for the treatment of cancer (MAIA, 2015; MAIA et al., 2015; MAIA et al., 2016; SOARES et al., 2011a; SOARES et al., 2011b; SOARES et al., 2012; SOARES et al., 2013). In these studies, all formulations developed were prepared by the REV method because of the high hydrophilic character of Gd-DTPA-BMA. The results obtained in the present study, however, demonstrated that the BANGHAM method allows obtaining the same encapsulation efficiency provided by REV, with the advantage of being simpler, faster, and economical. In view of this, the BANGHAM method was selected for use in the vesicle formation stage, in the next studies.

The level of Gd-DTPA-BMA entrapment obtained in this study, in terms of μmol/mL, is similar to the concentration determined in pH-sensitive and stealth pH-sensitive formulations developed in previous studies by our group (MAIA et al., 2015; MAIA et al., 2016). The encapsulation percentage values found are in agreement with values obtained in thermosensitive formulations containing Gd-DTPA-BMA, developed for use in magnetic

resonance (HOSSAN et al., 2010). The drug-to-lipid molar ratio was also evaluated and presented results similar to those found by Hossann et al. However, the formulations of the mentioned study present a total lipid concentration (50 mmol/L) higher than the lipid concentration of the liposomes developed in the present study (40 mmol/L). Considering the IC_{50} values described in the literature and the dose required for treatment, Gd-DTPA-BMA entrapment was considered satisfactory in both formulations (GE HEALTHCARE, 2013; MAIA, 2015; MAIA et al., 2016; SOARES et al., 2010; SOARES et al., 2011a; SOARES et al., 2011b; SOARES et al., 2012; SOARES et al., 2013).

At the beginning of this study, it was planned that the two proposed liposomal formulations would have equal lipid molar ratios differing only in relation to DSPC and MSPC lipids in order to obtain structurally comparable nanosystems. Thus, the TTSL-Gd and LTSL-Gd liposomes would be composed of DPPC/DSPC/DSPE-PEG_{2000} (80:15:5) and DPPC/MSPC/DSPE-PEG_{2000} (80:15:5), respectively. In this lipid ratio, the physicochemical characterization results obtained for the TTSL-Gd formulation were satisfactory, regardless of the preparation method used. Thus, this proportion was maintained. On the other hand, the proportion defined for LTSL-Gd had to be modified, since it resulted in an unstable formulation, with bimodal size distribution, being composed mainly by micelles. These characteristics are related to the proportion of MSPC used. MSPC is a single-chain lysophospholipid that has a critical micellar concentration (CMC) of 0.4 μmol/L (STAFFORD et al., 1989). The phase changes occurring in lysophospholipids, such as MSPC, are induced primarily by changes in the water content of the dispersion medium, and consequently by their concentration in aqueous dispersions (DELATTRE et al., 1993). In this case, when the lipid concentration increases, the lysophospholipids are organized into unstable structures, as observed in the present study. Thus, the modification performed in the LTSL-Gd composition consisted of reducing the MSPC concentration from 6 mmol/L to 4 mmol/L. The new lipid ratio defined, DPPC/MSPC/DSPE-PEG_{2000} (85:10:5), allowed to obtain liposomes with adequate physicochemical characteristics. The **Figure 5** confirms that the two lipid ratios evaluated for LTSL have resulted in formulations with different characteristics, including their visual aspects.

Figure 5 – LTSL (DPPC/MSPC/DSPE-PEG$_{2000}$, 80:15:5) and LTSL (DPPC/MSPC/DSPE-PEG$_{2000}$, 85:10:5) before the extrusion (A) and after the extrusion (B).

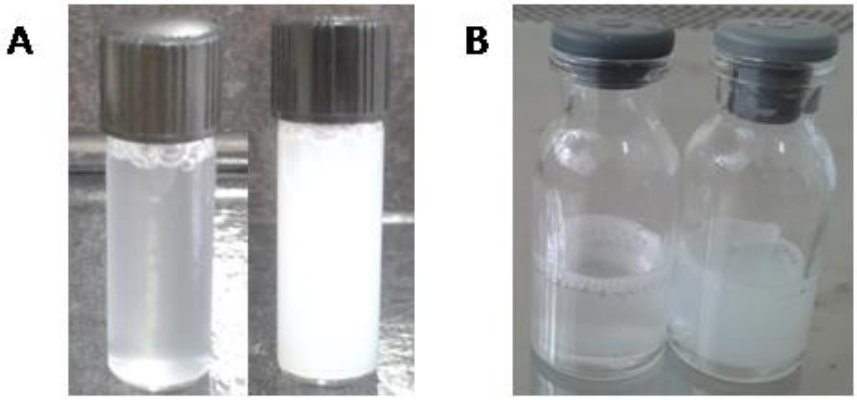

3.3 Optimization of Gd-DTPA-BMA entrapment

Although the level of Gd-DTPA-BMA entrapment in the prepared liposomes has been adequate, tests to improve encapsulation percentage were performed, aiming to reduce the expense of drug employed in the process.

The TTSL-Gd and LTSL-Gd liposomes used in all previous studies of this work were prepared using a solution of Gd-DTPA-BMA, diluted in HEPES buffer, at a concentration of 250 μmol/mL. This concentration was defined from literature studies on the development of thermosensitive liposomes containing Gd-DTPA-BMA for diagnostic purposes (FOSSHEIM et al., 2000; HOSSANN et al., 2010; WANG et al., 2008). To assess the influence between Gd-DTPA-BMA concentration added in the preparation and the entrapment of this drug in the proposed liposomes, TTSL-Gd and LTSL-Gd were again prepared using Gd-DTPA-BMA at a 125 μmol/mL and 500 μmol/mL. The liposomes were obtained by the BANGHAM method as defined previously and the results of this evaluation are exposed in **Table 5**.

The encapsulation percentage (%) remained practically unchanged, independent of the concentration of Gd-DTPA-BMA added during the preparation of the liposomes, being always within the encapsulation range (5-15%), typically obtained for hydrophilic substances, by the BANGHAM method (SHARMA, A.; SHARMA, U., 1997). Consequently, when the Gd-DTPA-BMA concentration added during the preparation was reduced to half (125 μmol/mL), the amount of encapsulated drug (in terms of μmol/mL) and the drug-to-lipid molar ratio were also reduced in the same proportion. The formulations prepared with Gd-DTPA-BMA at 500 μmol/mL resulted in higher Gd-DTPA-BMA entrapment values but remained stable for only one week. After this time, only half of the drug content remained in

both liposomes. A probable explanation for the instability is related to the high osmolarity of the Gd-DTPA-BMA solution at 500 μmol/mL (780 mOsm/kg), which may have caused osmotic stress on the vesicle membrane (GE HEALTHCARE, 2013; HOSSAN et al., 2013). Osmotic stress destabilizes the membrane of liposomes and leads to unwanted leakage or vesicle aggregation (HALLETT et al., 1993; HUPFELD et al., 2010). The formulations prepared with Gd-DTPA-BMA at 250 μmol/ml were selected for the use in the next studies since they presented high values of Gd-DTPA-BMA entrapment and remained stable for a longer time. In this case, osmotic stress was not observed because Gd-DTPA-BMA was diluted in HEPES buffer, resulting in a solution with osmolarity (323 mOs / kg) close to that found in body fluids.

Table 5 – Influence of the drug concentration added in the preparation, on the Gd-DTPA-BMA entrapment in the liposomes.

Formulation	Gd-DTPA-BMA added in the preparation (μmol/mL)	Gd-DTPA-BMA entrapment (μmol/mL)	Gd-DTPA-BMA entrapment (mg/mL)	Encapsulation percentage (%)	Drug-to-lipid molar ratio
TTSL-Gd	125	13.8 ± 0.9*	7.9 ± 0.5*	11.0 ± 0.7	0.35 ± 0.02*
	250	25.7 ± 2.0	14.7 ± 1.1	10.3 ± 0.8	0.64 ± 0.05
	500	44.7 ± 3.5*	25.7 ± 2.0*	8.9 ± 0.7	1.12 ± 0.08*
LTSL-Gd	125	14.0 ± 2.1*	8.1 ± 1.2*	11.2 ± 1.6	0.35 ± 0.06*
	250	23.8 ± 3.3	13.7 ± 1.9	9.5 ± 1.3	0.59 ± 0.07
	500	35.8 ± 1.4*	20.5 ± 0.8*	7.2 ± 0.3	0.89 ± 0.03*

Note: * asterisks represent significant difference when compared with the corresponding 250 μmol/mL; *P*-values lower than 0.05 were set as the significance level (Tukey's test). Values are expressed as mean ± SD (n = 3 batches).
Abbreviations: TTSL-Gd, traditional temperature-sensitive liposome containing Gd-DTPA-BMA; LTSL-Gd, lysolipid-containing temperature-sensitive liposome containing Gd-DTPA-BMA.

The physicochemical characteristics of the formulations analyzed in this optimization stage were also evaluated. The results of mean diameter, polydispersity index, vesicles diameter distribution, zeta potential, and electrophoretic mobility did not change significantly as a function of Gd-DTPA-BMA concentration added during preparation (**Table 6** and **Table 7**).

Table 6 – Physicochemical characteristics of TTSL-Gd prepared employing different Gd-DTPA-MBA concentrations.

Formulation	Gd-DTPA-BMA added in the preparation (µmol/mL) [a]	Preparation step [b]	Mean diameter (nm) [c]	Polydispersity index	Distribution of vesicles diameter (%) [d]				Zeta potential (mV)	Mobility electrophoretic (µmcm/Vs)
					≤ 100 nm	≤ 200 nm	200 – 300 nm	≥ 300 nm		
TTSL-Gd	125	1	2,278 ± 435	1.00 ± 0.00	0.0 ± 0.0	0.0 ± 0.0	0.0 ± 0.0	100.0 ± 0.2	– 1.0 ± 0.4	– 0.07 ± 0.04
		2	117 ± 7	0.06 ± 0.01	52.0 ± 9.3	98.8 ± 0.7	1.4 ± 0.7	0.0 ± 0.0	– 0.9 ± 0.5	– 0.07 ± 0.04
		3	116 ± 7	0.09 ± 0.01	57.6 ± 8.5	98.2 ± 0.9	1.9 ± 0.9	0.0 ± 0.0	– 1.1 ± 0.6	– 0.08 ± 0.05
TTSL-Gd	250	1	1,850 ± 677	0.79 ± 0.20	0.0 ± 0.0	0.0 ± 0.0	0.0 ± 0.0	100.0 ± 0.0	– 1.6 ± 0.6	– 0.12 ± 0.05
		2	115 ± 17	0.06 ± 0.02	53.4 ± 24.2	98.6 ± 1.4	1.4 ± 1.5	0.0 ± 0.0	– 1.7 ± 0.3	– 0.13 ± 0.02
		3	114 ± 16	0.07 ± 0.01	55.2 ± 17.6	98.4 ± 2.0	1.6 ± 2.1	0.0 ± 0.0	– 2.8 ± 1.3	– 0.22 ± 0.10
TTSL-Gd	500	1	1,830 ± 262	1.00 ± 0.00	0.0 ± 0.0	0.0 ± 0.0	0.0 ± 0.0	100.0 ± 0.1	– 1.6 ± 0.2	– 0.12 ± 0.02
		2	122 ± 7	0.08 ± 0.01	47.8 ± 7.8	97.6 ± 1.2	2.4 ± 1.1	0.0 ± 0.0	– 2.1 ± 0.1	– 0.16 ± 0.01
		3	120 ± 7	0.07 ± 0.03	47.8 ± 9.4	98.1 ± 1.2	1.9 ± 1.3	0.0 ± 0.0	– 2.1 ± 0.5	– 0.17 ± 0.04

Note: [a] Refers to the concentration of Gd-DTPA-BMA added during the preparation of the formulation; [b] The steps, 1, 2, and 3 refer to the BANGHAM method, extrusion, and ultracentrifugation, respectively; [c] Values expressed in terms of intensity; [d] Values expressed in terms of volume. Values are expressed as mean ± SD (n = 3 batches).
Abbreviation: TTSL-Gd, traditional temperature-sensitive liposome containing Gd-DTPA-BMA.

Table 7 – Physicochemical characteristics of LTSL-Gd prepared employing different Gd-DTPA-MBA concentrations.

Formulation	Gd-DTPA-BMA added in the preparation (µmol/mL) [a]	Preparation step [b]	Mean diameter (nm) [c]	Polydispersity index	Distribution of vesicle diameter (%) [d]				Zeta potential (mV)	Mobility electrophoretic (µmcm/Vs)
					≤ 100 nm	≤ 200 nm	200 – 300 nm	≥ 300 nm		
LTSL-Gd	125	1	1,620 ± 61	0.99 ± 0.02	0.0 ± 0.0	0.0 ± 0.0	0.0 ± 0.0	100.0 ± 0.1	– 1.4 ± 0.3	– 0.11 ± 0.02
		2	119 ± 8	0.07 ± 0.02	49.7 ± 10.2	98.1 ± 1.2	1.8 ± 1.1	0.0 ± 0.0	– 1.5 ± 0.2	– 0.12 ± 0.01
		3	119 ± 9	0.08 ± 0.01	50.4 ± 7.8	97.9 ± 1.4	2.1 ± 1.4	0.0 ± 0.0	– 1.7 ± 0.5	– 0.13 ± 0.04
LTSL-Gd	250	1	1,536 ± 232	0.44 ± 0.19	0.0 ± 0.0	0.0 ± 0.0	0.1 ± 0.2	99.7 ± 0.2	– 2.1 ± 0.3	– 0.16 ± 0.02
		2	118 ± 12	0.09 ± 0.02	52.5 ± 17.3	97.8 ± 1.7	2.2 ± 1.6	0.0 ± 0.0	– 2.1 ± 0.1	– 0.16 ± 0.01
		3	118 ± 12	0.08 ± 0.01	53.2 ± 12.2	97.9 ± 2.1	2.2 ± 2.1	0.0 ± 0.0	– 2.1 ± 0.1	– 0.15 ± 0.01
LTSL-Gd	500	1	1,698 ± 543	0.78 ± 0.19	0.0 ± 0.0	0.0 ± 0.0	0.0 ± 0.0	100.0 ± 0.1	– 1.7 ± 0.5	– 0.13 ± 0.04
		2	114 ± 6	0.07 ± 0.02	55.7 ± 10.1	98.8 ± 0.4	1.1 ± 0.4	0.0 ± 0.0	– 1.3 ± 0.3	– 0.10 ± 0.03
		3	114 ± 5	0.07 ± 0.01	57.3 ± 8.1	98.8 ± 0.4	1.2 ± 0.6	0.0 ± 0.0	– 1.8 ± 1.1	– 0.14 ± 0.09

Note: [a] Refers to the concentration of Gd-DTPA-BMA added during the preparation of the formulation; [b] The steps, 1, 2, and 3 refer to the BANGHAM method, extrusion, and ultracentrifugation, respectively; [c] Values expressed in terms of intensity; [d] Values expressed in terms of volume. Values are expressed as mean ± SD (n = 3 batches).
Abbreviation: LTSL-Gd, lysolipid-containing temperature-sensitive liposome containing Gd-DTPA-BMA.

3.4 Storage stability study

A storage stability study at 4 °C within a 180-day period was performed by accompanying the alterations of physicochemical properties of TTSL-Gd and LTSL-Gd. No significant variation was found in mean diameter and polydispersity index values of both formulations throughout the assessed period (**Table 8** and **Table 9**).

Table 8 – Data of storage stability study of TTSL-Gd.

Time (days)	Mean diameter (nm)	Polydispersity index	Zeta potential (mV)	Gd-DTPA-BMA entrapment (µmol/mL)
0	121 ± 5	0.06 ± 0.02	– 1.9 ± 0.3	21.9 ± 2.8
7	121 ± 4	0.05 ± 0.01	– 2.4 ± 0.5	22.2 ± 2.3
15	121 ± 3	0.07 ± 0.02	– 1.9 ± 0.3	20.8 ± 1.4
30	122 ± 4	0.06 ± 0.01	– 1.7 ± 0.3	21.9 ± 1.0
60	121 ± 2	0.06 ± 0.02	– 2.0 ± 0.4	24.9 ± 1.3
90	120 ± 4	0.06 ± 0.01	– 1.6 ± 0.1	22.1 ± 1.4
120	119 ± 3	0.06 ± 0.01	– 2.7 ± 0.4	23.5 ± 1.5
180	121 ± 3	0.07 ± 0.04	– 3.2 ± 0.2*	15.8 ± 1.7*

Note: * asterisks represent significant difference when compared with the 0-day. 0-day represent the day of TTSL-Gd preparation. *P*-values lower than 0.05 were set as the significance level (Tukey's test). Values are expressed as mean ± SD (n = 3 batches).
Abbreviations: TTSL-Gd, traditional temperature-sensitive liposome containing Gd-DTPA-BMA.

Table 9 – Data of storage stability study of LTSL-Gd.

Time (days)	Mean diameter (nm)	Polydispersity index	Zeta potential (mV)	Gd-DTPA-BMA entrapment (µmol/mL)
0	105 ± 7	0.05 ± 0.01	– 1.9 ± 0.8	18.6 ± 0.8
7	104 ± 7	0.06 ± 0.01	– 2.3 ± 0.3	18.8 ± 0.8
15	106 ± 7	0.05 ± 0.01	– 1.3 ± 1.0	17.6 ± 0.4
30	106 ± 7	0.05 ± 0.01	– 2.4 ± 0.4	18.1 ± 0.4
60	104 ± 6	0.07 ± 0.03	– 3.2 ± 0.3	22.4 ± 2.0
90	101 ± 7	0.06 ± 0.01	– 3.1 ± 0.5	19.8 ± 0.7
120	104 ± 6	0.07 ± 0.03	– 4.9 ± 1.3	19.7 ± 0.7
180	106 ± 7	0.08 ± 0.01	– 8.0 ± 2.2*	12.1 ± 0.7*

Note: * asterisks represent significant difference when compared with the 0-day. 0-day represent the day of LTSL-Gd preparation. *P*-values lower than 0.05 were set as the significance level (Tukey's test). Values are expressed as mean ± SD (n = 3 batches).
Abbreviations: LTSL-Gd, lysolipid-containing temperature-sensitive liposome containing Gd-DTPA-BMA.

Concerning the zeta potential and Gd-DTPA-BMA concentration, significant alterations were observed only at 180 days of storage. A probable explanation for the change in zeta potential values may be the hydrolysis of the lipids that composed the liposomal bilayer. This instability mechanism may also have been responsible for the reduction in Gd-DTPA-BMA content.

The maintenance of the physicochemical characteristics of TTSL-Gd and LTSL-Gd, for a period of approximately four months, may have occurred due to the steric repulsion caused by the PEG chains on the surface of the liposomes, which can prevents the aggregation and fusion of vesicles (BARBOSA et al., 2015; MAIA et al., 2016; WOLFRAM et al., 2014). Another factor that may have contributed to the stability of the formulations is the dispersant phase of the formulations (HEPES buffer). The HEPES buffer is composed of 10 mmol/L HEPES, 145 mmol/L sodium chloride and 2 mmol/L EDTA. This dispersion medium was chosen because it could contribute to the stability of the proposed liposomes. HEPES is an antioxidant that can prevent lipid peroxidation of the components of the formulations. EDTA is able to form stable complexes with metals, such as Gd, if Gd-DTPA-BMA dissociates, releasing Gd^{3+} ion. The sodium chloride component is required in the formulation since intravenous administration preparations need to be isotonic (MAIA et al., 2016).

3.5 Morphological characterization

TEM was performed to assess the morphology, lamellarity, and size of liposomes (**Figure 6**). **Figures 6A** and **Figure 6B** show the spherical form of blank liposomes, which present mean size around to 100 nm, consistent with data obtained from DLS analyses. The photomicrographs of TTSL and LTSL confirm the unilamellar nature of liposomes, corroborating for the information that extrusion produces LUV liposomes. In **Figure 6B** is possible to observe that the presence of the lysophospholipid MSPC causes a small irregularity in the liposomal bilayer.

Figures 6C and **Figures 6D** show TTSL-Gd and LTSL-Gd, respectively. These liposomes present a unilamellar structure with non-spherical form when compared with blank liposomes. Besides that, the inner aqueous core of TTSL-Gd and LTSL-Gd show a high electron density and low light transmittance, when compared with blank liposomes. This high electron density observed can be attributed to the Gd-DTPA-BMA entrapped into these liposomes. This observation is in accordance with results from the literature (ZHANG et al., 2013). The size of TTSL-Gd and LTSL-Gd obtained by TEM was lower than that obtained by

DLS. A possible explanation for this is related to the MET technique principle, the paramagnetic characteristics of Gd-DTPA-BMA, and the thermosensitive nature of liposomes.

Figure 6 – TEM photomicrographs obtained for the liposomes, TTSL (A), LTSL (B), TTSL-Gd (C), and LTSL-Gd (D).

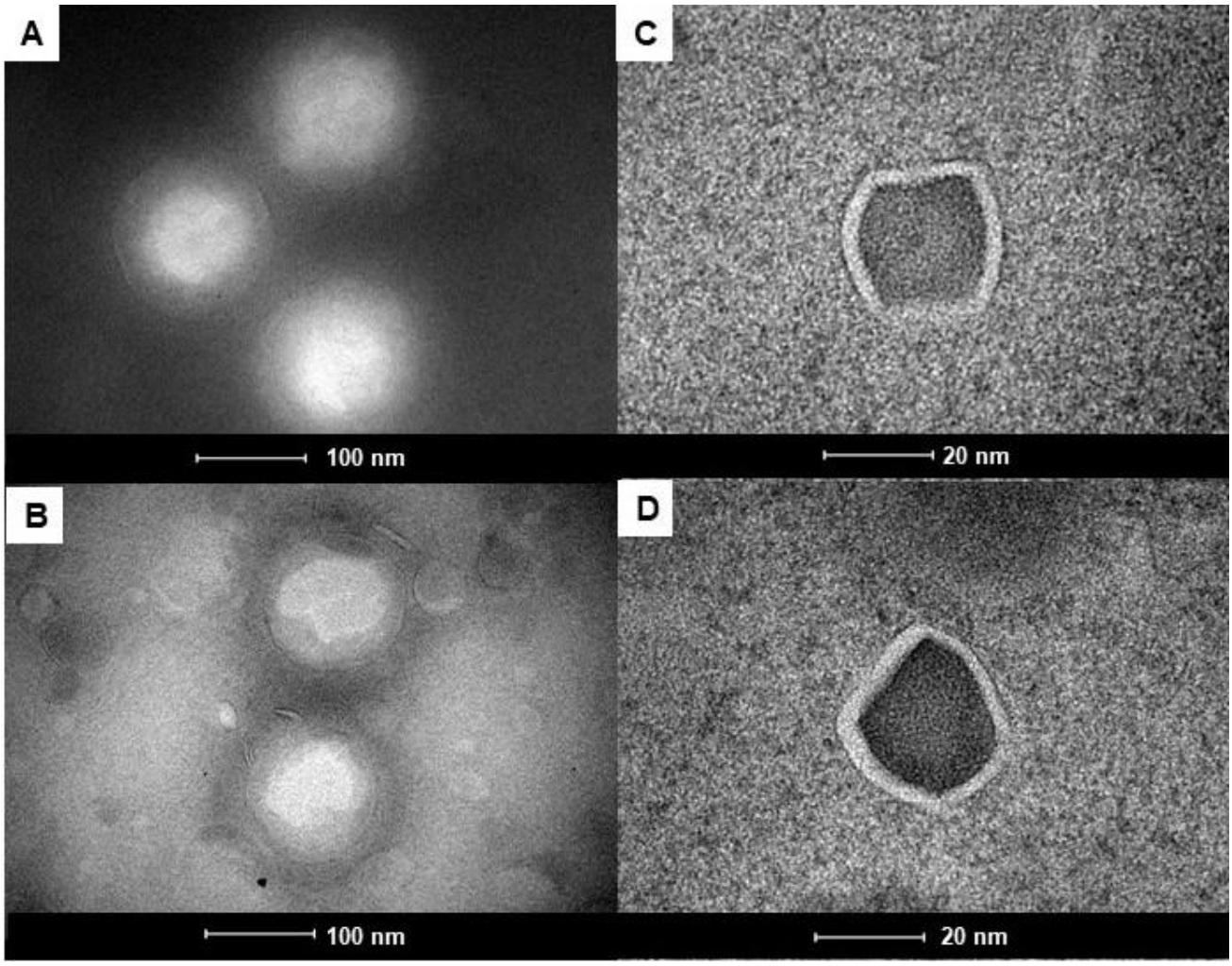

The principle of TEM analysis consists of bombarding the sample with electrons generated from a tungsten filament. These electrons are accelerated by a potential difference of the order of kV in a high vacuum column. The electron beam passes through a system of lenses (condensers, objective, intermediate and projectors), before and after reaching the sample. In modern microscopes, only the electron gun is an electrostatic lens, the other lenses are magnetic (ANDRADE, 2015; BIBI et al., 2011). Magnetic materials, such as Gd-DTPA-BMA, are capable of generating heat when subjected to a magnetic field (LAURENT et al., 2011; LIMA-TENÓRIO et al., 2015; SALUNKHE et al., 2014; SINGH; SAHOO, 2014). If

sample heating occurred during TEM analysis, this would cause destabilization of the liposomes, which could result in the release of the encapsulated contents and decrease in the size of the nanostructures.

3.6 Thermal characterization

3.6.1 DLS analyses

The thermosensitive formulations developed in this study were designed for use in the treatment of cancer and to allow an image-guided drug delivery. The image-guided drug delivery can be visualized by MRI since Gd-DTPA-BMA is a contrast agent widely used in this technique (BELLIN, 2006; LINDNER et al., 2015). The antitumor treatment can be performed by means of moderate hyperthermia. This clinical modality consists of heating the tumor region at temperatures in the range between 41 °C and 45 °C (KUMAR; MOHAMMAD, 2011). The heating used, may promote the release of drugs encapsulated in thermosensitive liposomes, if the temperature employed is equal to or close to the T_c of the liposomal lipid composition (KNEIDL et al., 2014). In this context, a preliminary thermosensitivity study was proposed to determine the temperature range at which the Lβ → Lα phase transition occurs. The results of this evaluation are exposed in **Figure 7**.

It is possible to observe that all formulations remained stable between 37 °C and 40 °C since no significant differences were visualized in the values of mean diameter and Kcps, evaluated in this temperature range. This result is relevant because it indicates that probably the liposomes will remain stable, at body temperature (37 °C). This is important to avoid nonspecific releases following administration. From 40 °C to 41 °C, it is observed that the mean diameter of the liposomes and Kcps decrease. The decrease in size may be related to the release of Gd-DTPA-BMA and to the change that occurs in the lipid bilayer during the Lβ → Lα phase transition. This transition has a pre-transition state denominated rippled gel phase (Pβ') (**Figure 8**) (JUNG, 2000; RUI-GUANG et al., 2012). The pre-transition, which corresponds to the conversion Lβ → Pβ' is mainly related to the polar region of phosphatidylcholines bilayers, while the main phase transition Pβ' → Lα is closely related to the acyl chains of phosphatidylcholines bilayers (RUI-GUANG et al., 2012). Vesicles in the Lα phase have a smaller bilayer thickness than vesicles in the Lβ and Pβ' phases (JUNG,

2000; NEW, 1990). The decrease in the kcps, can be related to the fact that liposomes may be disrupted by the heat, resulting in lower particle counts.

Figure 7 – Variation of the mean diameter (bars) and particle derived count rate (line and points) of the liposomes, as a function of temperature.

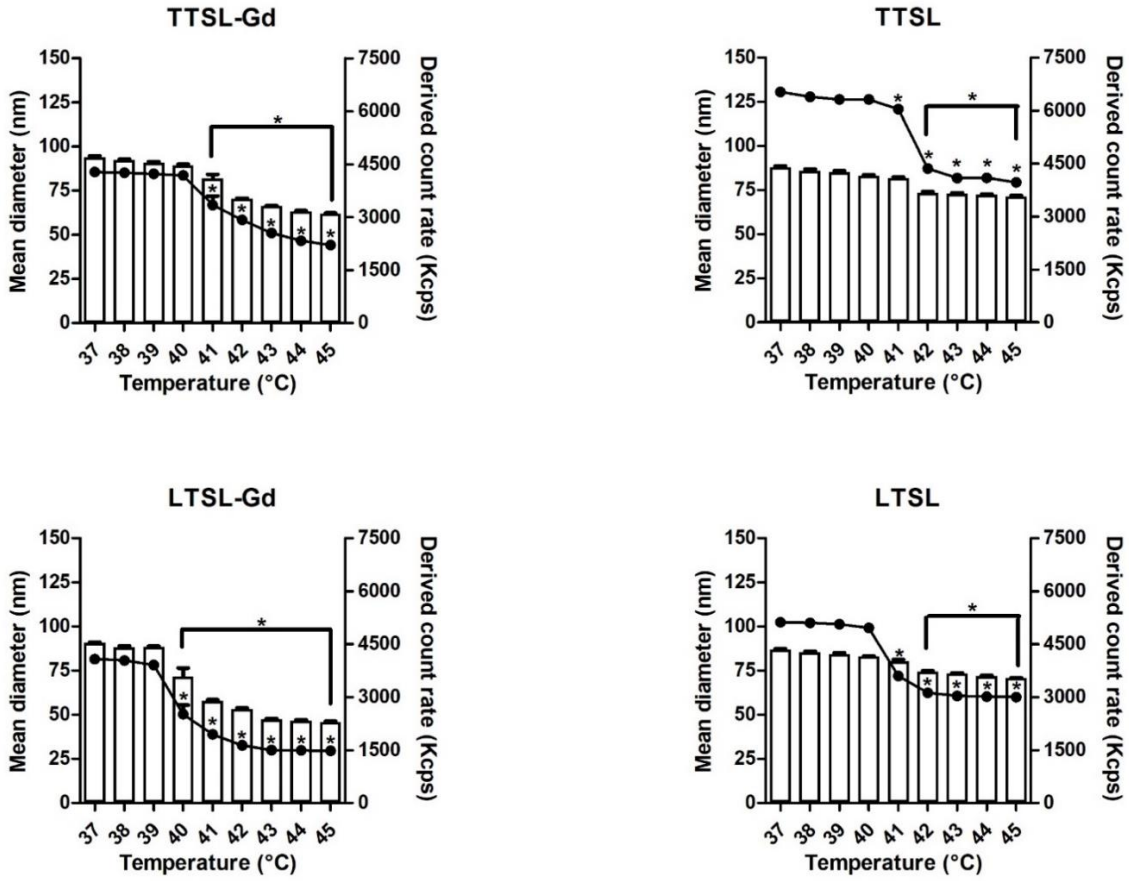

Note: * asterisks represent significant difference when compared with the 37 °C. *P*-values lower than 0.05 were set as the significance level (Tukey's test). Values are expressed as mean ± SD (n = 3 batches).
Abbreviations: TTSL-Gd, traditional temperature-sensitive liposome containing Gd-DTPA-BMA; TTSL, traditional temperature-sensitive liposomes; LTSL-Gd, lysolipid-containing temperature-sensitive liposome containing Gd-DTPA-BMA; LTSL, lysolipid-containing temperature-sensitive liposome.

Figure 8 – Schematic representation of Lβ → Lα phase transition.

Adapted from JUNG, 2000.
Abbreviations: Lβ, lammellar gel order phase; Pβ', pre-transition rippled gel phase; Lα, fluid lamellar phase.

3.6.2 Differential scanning calorimetry analyses (DSC)

The DSC analysis was performed to confirm the T_c value for each formulation developed in this study. In this technique the transition Lβ → Lα is visualized by means of an endothermic peak. In the thermograms, the temperature of the maximum *Cp* corresponds to the T_c (BASTOS, 2016; SMITH; DEA, 2013). The T_c values obtained by DSC (**Figure 9**) were higher than obtained by DLS probably due to the difference in sensitivity between the techniques.

Figure 9 – Thermograms of the liposomes obtained by DSC.

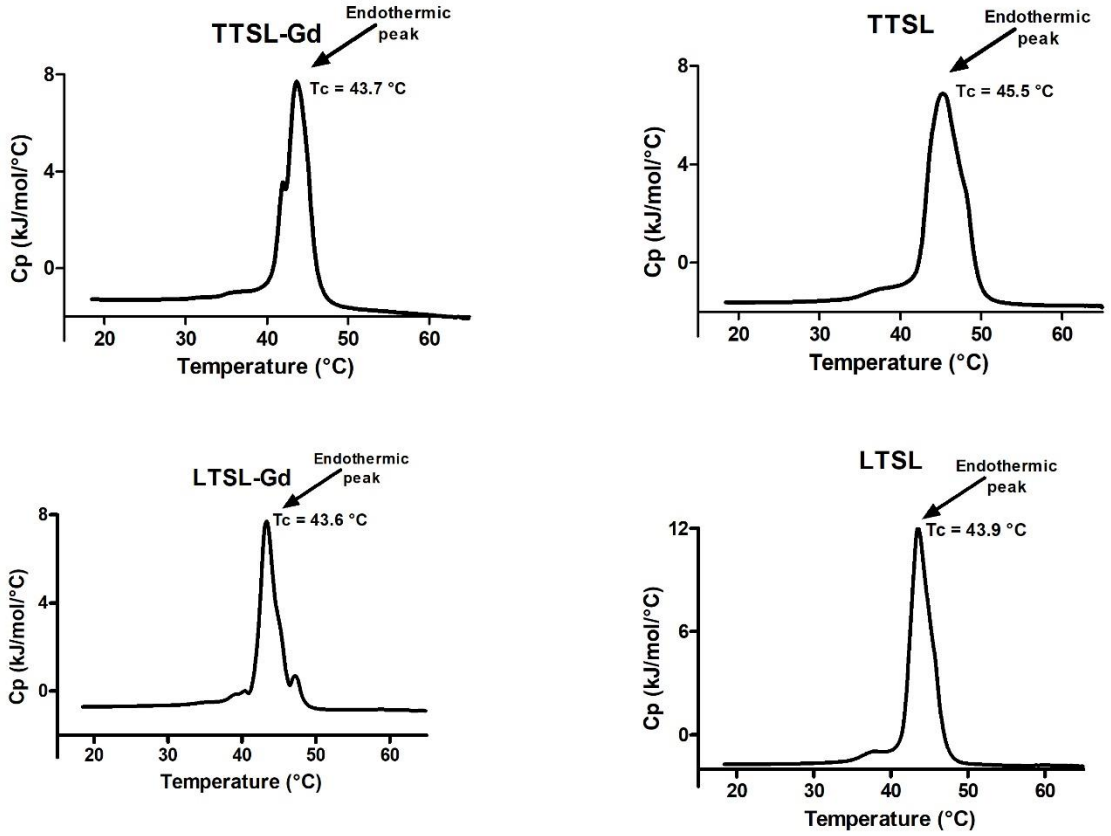

Abbreviations: T_c, Chain melting temperature (temperature of the transition Lβ → Lα phase); TTSL-Gd, traditional temperature-sensitive liposome containing Gd-DTPA-BMA; TTSL, traditional temperature-sensitive liposomes; LTSL-Gd, lysolipid-containing temperature-sensitive liposome containing Gd-DTPA-BMA; LTSL, lysolipid-containing temperature-sensitive liposome.

The DSC results confirm that the lipid composition chosen for both formulations was adequated, since T_c values obtained (TTSL: 45.5 °C, TTSL-Gd: 43.7 °C, LTSL: 43.7 °C, and LTSL-Gd: 43.6 °C) are in accordance with T_c values of thermosensitive liposomes used in the

treatment of cancer, as well as within the specified range of moderate hyperthermia (KUMAR; MOHAMMAD, 2011; LI et al., 2013; WILLERDING et al., 2016).

3.6.3 Small-angle X-ray scattering (SAXS)

Diffraction patterns of the formulations showed by SAXS indicate Bragg indexes of 1,2 and 1,2,3, which characterizes the presence of lamellar phases (LOPES et al., 2014; MONTEIRO et al., 2016; RUI-GUANG et al., 2012) (**Figure 10**).

Figure 10 – Diffractograms of the liposomes obtained by SAXS.

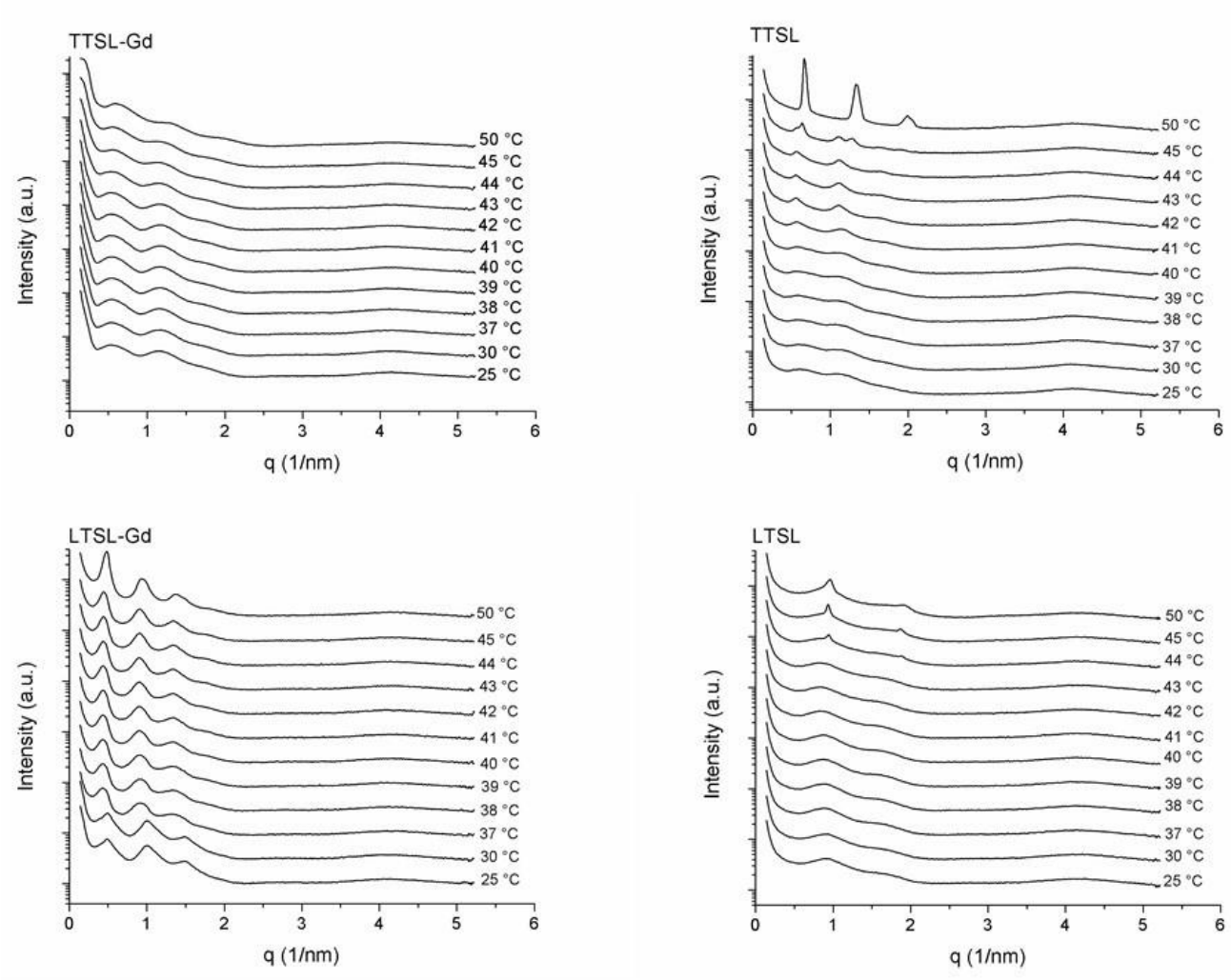

Abbreviations: TTSL-Gd, traditional temperature-sensitive liposome containing Gd-DTPA-BMA; TTSL, traditional temperature-sensitive liposomes; LTSL-Gd, lysolipid-containing temperature-sensitive liposome containing Gd-DTPA-BMA; LTSL, lysolipid-containing temperature-sensitive liposome.

Visually, it is easier to identify changes in the diffractograms of blank formulations. The thermosensitivity of the TTSL and the LTSL formulations can be confirmed by the appearance of new peaks at 45 °C and 44 °C, respectively. These results are in agreement with data obtained by DSC. In the formulations containing Gd-DTPA-BMA, the thermosensitivity can be visualized by means of the enlargement of the peaks, which occurs when the temperature is increased.

3.7 *In vitro* release analyses

In vitro release studies were performed as a function of temperature and time in SFB to simulate the *in vivo* conditions. The *in vivo* stability of the liposomes is strongly influenced by the serum components. In the nanosystems, in general, following intravenous administration, a corona protein may be formed on the surface of the particle, which prevents the release and impairs active targeting to the target regions (MIRSHAFIEE et al., 2013). In the specific case of thermosensitive liposomes, the serum components may accelerate the release. There is evidence that albumin and cholesterol promote release due to interaction with the liposomal bilayer (HOSSANN et al., 2012; MITTAG et al., 2017). Results obtained in buffer medium are highly reproducible but do not allow predicting the *in vivo* behavior of the formulation. On the other hand, the use of serum as a release medium allows establishing *in vivo* correlations (HUANG et al., 2017; MITTAG et al., 2017).

The release study was performed using the dilution method. Generally, in nanocarrier systems, the release by dilution method results in an initial burst effect, followed by a controlled release. On the other hand, the release by dialysis presents a controlled profile during the entire analysis time. The dilution method was selected for use in the present study, as it allows simulating the dilution and the stress that the formulation undergoes following intravenous administration (OLIVEIRA et al., 2016).

The results of the temperature-dependent Gd-DTPA-BMA release are shown in **Figure 11**. At a fixed time of 5 min, TTSL-Gd showed no release at any of the evaluated temperatures. On the other hand, LTSL-Gd showed significant release at 43 °C (27%). At a fixed time of 10 min, LTSL-Gd presented higher release (68% at 43 °C), at lower temperature than TTSL-Gd (43% at 45 °C). This difference might be explained by the phospholipids that compose each formulation. TTSL-Gd has DSPC in its composition, which presents high T_c value (54.9 °C), which may have contributed to a higher rigidity in this formulation, making it difficult to release, when compared to LTSL-Gd (GRÜLL; LANGEREIS, 2012). On the other

hand, LTSL-Gd has a lysophospholipid (MSPC) in its composition, which makes its membrane more fluid and more responsive to heating (KNEIDL et al., 2014).

Figure 11 – Temperature dependent Gd-DTPA-BMA release from TTSL-Gd and LTSL-Gd

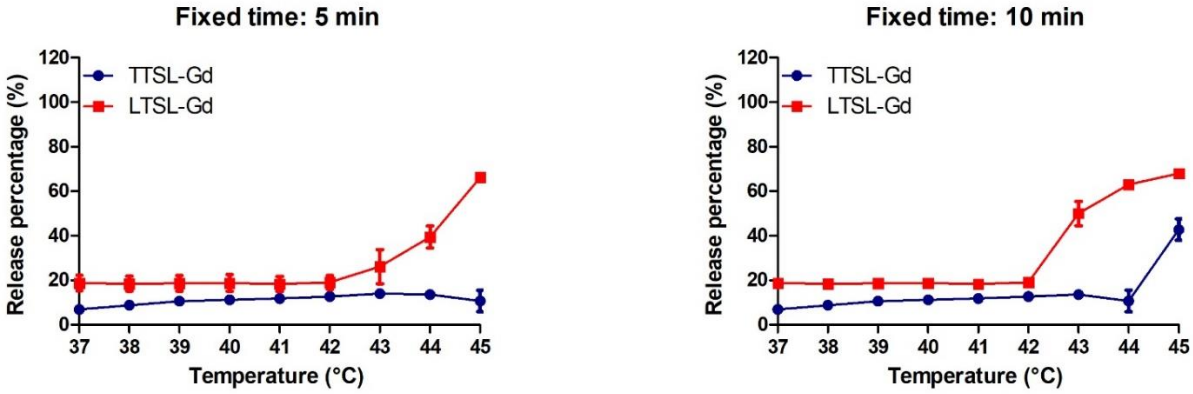

Abbreviations: TTSL-Gd, traditional temperature-sensitive liposome containing Gd-DTPA-BMA; LTSL-Gd, lysolipid-containing temperature-sensitive liposome containing Gd-DTPA-BMA.

The same profile was observed in the time-dependent Gd-DTPA-BMA release study (**Figure 12**). To perform this analysis, the temperature was set at 45 °C for TTSL-Gd and at 43 °C for LTSL-Gd. The set temperature was determined experimentally and corresponded to the lowest value capable of allowing the Gd-DTPA-BMA release. This lowest value was chosen so that smaller aumounts of heat are administered to the patient, thus reducing the risks of side effects associated with this procedure. In this analysis, the formulations were heated for 1 h, since this is the maximum time used for moderate hyperthermia treatment (HOSSANN et al., 2012). At the end of this time, TTSL-Gd had released only 47% of the Gd-DTPA-BMA entrapped, while LTSL-Gd released 100% of the drug.

Figure 12 – Time-dependent Gd-DTPA-BMA release from TTSL-Gd and LTSL-Gd

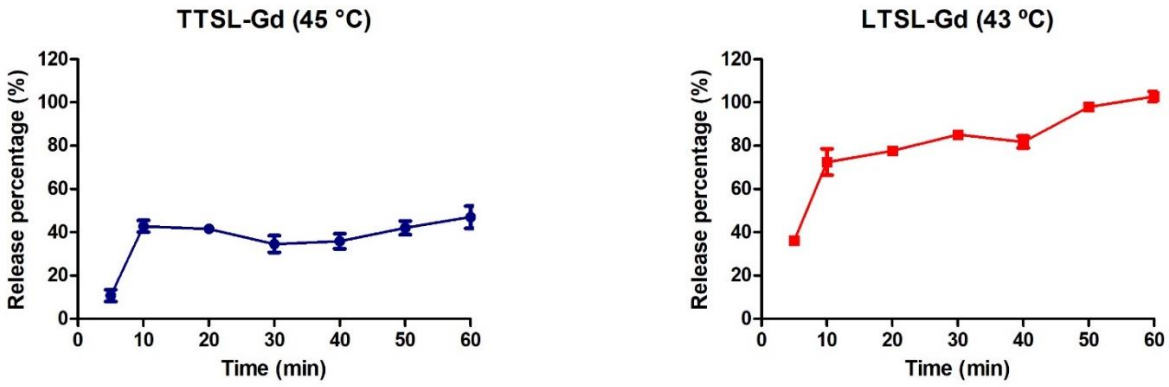

Abbreviations: TTSL-Gd, traditional temperature-sensitive liposome containing Gd-DTPA-BMA; LTSL-Gd, lysolipid-containing temperature-sensitive liposome containing Gd-DTPA-BMA.

The stability of liposomes at corporal temperature (37 °C) was also evaluated (**Figure 13**). This analysis is important to determine how long the thermosensitive liposome remains stable after intravenous administration without release in nonspecific regions. The ideal behavior for this type of formulation is that it releases as little as possible until it reaches the tumor region (HOSSANN et al., 2007; LI et al., 2010). It is possible to observe that due to greater membrane fluidity, LTSL-Gd remained stable at 37 °C for a shorter time, than TTSL-Gd over the 24 h time analysis.

Figure 13 – TTSL-Gd and LTSL-Gd stability at corporal temperature

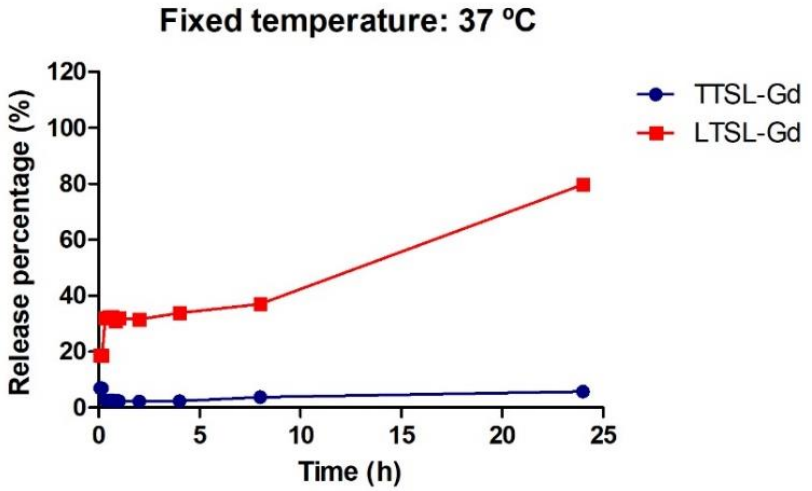

Abbreviations: TTSL-Gd, traditional temperature-sensitive liposome containing Gd-DTPA-BMA; LTSL-Gd, lysolipid-containing temperature-sensitive liposome containing Gd-DTPA-BMA.

From the data obtained in the release studies, calculations of reaction kinetics were performed. The results of this analysis are exposed in **Table 10**.

Table 10 – Data of *in vitro* release kinetics study

Mathematical model	r ² of the linear regression		
	TTSL-Gd (release at 45 °C)	LTSL-Gd (release at 43 °C)	LTSL-Gd (release at 37 °C)
Zero-order	0.36	0.87	0.35
First-order	0.40	0.12	0.32
Second-order	0.36	0.76	0.33
Higuchi	0.42	0.89	0.47

Note: It was not possible to test the mathematical models for TTSL-Gd at 37 ° C since the formulation did not show release at this temperature.
Abbreviations: TTSL-Gd, traditional temperature-sensitive liposome containing Gd-DTPA-BMA; LTSL-Gd, lysolipid-containing temperature-sensitive liposome containing Gd-DTPA-BMA.

The r^2 values obtained for the linear regressions of each mathematical model evaluated, suggest that the formulations present release kinetics according to the Higuchi model, in which the release of the drug occurs by diffusion based on the Law of Fick's Law (JAIN. A.; JAIN, S. K, 2016). This information is consistent with the mechanism of drug release described in the literature for thermosensitive liposomes (KNEIDL et al., 2014).

3.8 *In vitro* cytotoxicity evaluation

To evaluate the effects of liposomes containing Gd-DTPA-BMA on breast cancer cell lines, an MTT assay was employed. In general, the groups evaluated showed the same cytotoxicity profile, regardless of whether hyperthermia was used or not, in the two analyzed cell lines (4T1 and MDA-MB-231).

It was expected that control liposomes without Gd-DTPA-BMA (TTSL and LTSL) presented some toxicity since they had 40 mmol/L total lipid concentration, however, the toxicity observed was low and negligible, with values of cellular viability consistent with biocompatible compounds, at all examined concentrations (ISO, 2009).

Free Gd-DTPA-BMA showed cytotoxicity similar to that observed by the blank liposomes. Gd-DTPA-BMA is an extracellular contrast, extremely hydrophilic, with low cellular internalization, which justifies its low cytotoxicity (LIU; ZHANG, 2012; MAIA et al., 2016).

Treatments employing TTSL-Gd, LTSL-Gd, and LTSL-Gd associated with hyperthermia resulted in IC_{50} values about 100 times lower than treatments using Gd-DTPA-BMA in the free form (**Table 11**). The IC_{50} values obtained for these liposomes did not present significant differences. Higher activity of Gd-DTPA-BMA encapsulated in liposomes compared to the free form occurs because the vesicles may have facilitated the intracellular internalization of the drug. The low activity of TTSL-Gd associated with hyperthermia at 45 °C compared with the activity of the other groups of liposomes containing Gd-DTPA-BMA might be explained by the hyperthermia protocol used. TTSL-Gd presents a more rigid lipid bilayer than LTSL-Gd, due to the presence of DSPC in its composition. Probably because of this, the time of 6 h was not enough for the internalization of liposomes into the cells, prior to the hyperthermia procedure. Therefore, when the plates of this group were heated, Gd-DTPA-BMA may have released in the extracellular space, which reflected in lower activity and higher IC_{50} values, when compared to the other liposomal treatments, in the two cell lines evaluated (**Table 11**). Recent studies confirm that it is important to understand and coordinate

the stimuli-responsive drug release after cell uptake to achieve a better therapeutic response (JOSE et al., 2018).

Table 11 – *IC_{50}*, *CC_{50}* and *SI* values for cancer e and normal cell lines.

Samples	4T1		MDA-MB-231		WI-26 VA 4
	IC_{50} (mmol/L)	*SI*	*IC_{50}* (mmol/L)	*SI*	*CC_{50}*
TTSL-Gd	2.2 ± 1.7	290.00	1.0 ± 0.3	638.00	638.0 ± 81.5
TTSL-Gd 45 °C	17.5 ± 0.9	8.86	43.5 ± 21.2	3.56	155.1 ± 15.5
LTSL-Gd	1.4 ± 1.6	37.50	1.4 ± 1.1	37.50	52.5 ± 16.5
LTSL-Gd 43 °C	1.5 ± 0.1	29.80	1.5 ± 0.3	29.80	44.7 ± 24.6
Gd-DTPA-BMA	173.7 ± 43.9	0.07	155.0 ± 10.3	0.07	11.5 ± 18.4
Gd-DTPA-BMA 43 °C	178.8 ± 1.2	0.03	128.6 ± 44.5	0.04	5.1 ± 0.1
Gd-DTPA-BMA 45 °C	143.1 ± 71.5	0.03	150.7 ± 6.1	0.03	0.4 ± 0.1

Note: Values are expressed as mean ± SD (n =3).
Abbreviations: *IC_{50}*, inhibitory concentration; *CC_{50}*, cytotoxic concentration; *SI*, selectivity index; 4T1, murine breast adenocarcinoma cell line; MDA-MB-231, human breast adenocarcinoma cell line; WI-26 VA4, normal human lung fibrosblast cell line; TTSL-Gd, traditional temperature-sensitive liposome containing Gd-DTPA-BMA; LTSL-Gd, lysolipid-containing temperature-sensitive liposome containing Gd-DTPA-BMA; Gd-DTPA-BMA, gadodiamide; 43 °C, represents the use of hyperthermia at 43 °C; 45 °C, represents the use of hyperthermia at 45 °C.

In order to investigate the selectivity of the treatment proposed in this study, cytotoxicity was also evaluated in a normal cell line (WI-26 VA 4). The *CC_{50}* results show that treatment with Gd-DTPA-BMA in the free form was much more toxic than treatment with this drug encapsulated in liposomes (**Table 11**). The *SI* values for all treatments was also calculated. It is desirable that the proposed treatment present a high SI value, giving maximum antitumoral activity with minimal normal cell toxicity (BARBOSA et al., 2015). This was observed for all liposomal treatments, except for TTSL-Gd associated with hyperthermia, which although presented high *CC_{50}* value, also showed high *IC_{50}* values.

These findings revealed that the incorporation of Gd-DTPA-BMA into liposomes could improve cytotoxic activity in 4T1 e MDA-MB-231 breast cancer cell lines and minimal toxicity to WI-26 VA 4 normal cell line.

CONCLUSIONS

In the present study two liposomal formulations (TTSL-Gd and LTSL-Gd) containing Gd-DTPA-BMA were successfully prepared in terms of mean vesicle size, zeta potential, and Gd-DTPA-BMA entrapment. These liposomes presented suitable features for future *in vivo*

studies and high physicochemical stability for four months. This work also investigated the cytotoxicity of the formulations against breast cancer cell lines (4T1, MDA-MB-231) In additon, selectivity was evaluated against a fibroblast cell line (WI-26 VA4). Results from these experiments indicate that the liposomal formulations present higher activity in tumor cells and lower toxicity in normal cells than free Gd-DTPA-BMA. Therefore, the data obtained in this study suggest that the incorporation of Gd-DTPA-BMA into liposomes can improve cytotoxicity on breast cancer cell lines evaluated, as well can enable greater safety and selectivity against normal cells.

ACKNOWLEDGEMENTS

The authors would like to thank CNPq (Conselho Nacional de Desenvolvimento Científico e Tecnológico), FAPEMIG (Fundação de Amparo à Pesquisa do Estado de Minas Gerais) and CAPES (Coordenação de Aperfeiçoamento de Pessoal de Nível Superior) for their financial support. The authors also thank the Centro de Microscopia of Universidade Federal de Minas Gerais (*http://www.microscopia.ufmg.br*), the Laboratório Multiusuário de Análises Biomoleculares of Universidade Federal do Espiríto Santo (*http://labiom.ufes.br/)*, and, Brazilian Synchrotron Light Laboratory (Campinas, Brazil) for providing the equipment and technical support for experiments involving microscopy, microcalorimetric, and SAXS analysis, respectively.

REFERENCES

ANDRADE, V. M. C. S. Manganitas nanoestruturadas: um estudo do efeito magnetocalórico. 2015. 78 f. Dissertação (Mestrado em Física, Universidade Federal Fluminense, Rio de Janeiro, 2015.

AUKRUST, A.; RAKNES, Å; SJØGREN, C. E.; SYDNES, L. K. Polymorphism of gadolinium diethylenetriaminepentaacetic acid bis (methylamide) (GdDTPA-BMA) and dysprosium diethylenetriaminepentaacetic acid bis (methylamide) (DyDTPA-BMA). *Acta Chem. Scand.*, v. 51, p. 918-926, 1997.

BANGHAM, A. D.; STANDISH, M. M.; WATKINS, J. C. Diffusion of univalent ions across the lamellae of swollen phospholipids. *J. Mol. Biol.*, v. 13, p. 238-252, 1965.

BARBOSA, L. C. A. *Espectroscopia no infravermelho na caracterização de compostos orgânicos*. 1ª ed. Viçosa: Editora UFV, 2011, 189 p.

BARBOSA, M. V.; MONTEIRO, L. O. F.; CARNEIRO, G.; MALAGUTTI, A. R.; VILELA, J. M. C.; ANDRADE, M. S.; OLIVEIRA, M. C.; CARVALHO-JÚNIOR, A. D.; LEITE, E. A. Experimental design of a liposomal lipid system: a potential strategy for paclitaxel-based breast cancer treatment. *Colloids Surf B Biointerfaces*, v. 136, p. 553-561, 2015.

BARROS, A. L. B.; MOTA, L. G.; SOARES, D. C. F.; SOUZA, C. M.; CASSALI, G. D.; OLIVEIRA, M. C.; CARDOSO, V. N. Long-circulating, pH-sensitive liposomes *versus* long-circulating, non-pH-sensitive liposomes as a delivery system for tumor identification. *J. Biomed. Nanotechnol.*, v. 9, n. 9, p. 1636-1643, 2013.

BASTOS, M. *Using DSC to characterize thermotropic phase transitions in lipid bilayer membranes*. Application Note. Malvern Instruments Limited, 2016.

BELLIN, M. F. MR contrast agents, the old and the new. *Eur. J. Radiol.*, v. 60, p. 314-323, 2006.

BIBI, S.; KAUR, R.; HENRIKSEN-LACEY, M.; McNEIL, S. E.; WILKHU, J.; LATTMANN, E.; CHRISTENSEN, D.; MOHAMMED, A. R.. PERRIE, Y. Microscopy imaging of liposomes: from coverslips to environmental SEM. *Int. J. Pharm.*, v. 417, p. 138-150, 2011.

BISWAS, S.; NAMITA, S.; DODWADKAR; DESHPANDE, P. P.; TORCHILIN, V. P. Liposomes loaded with paclitaxel and modified with novel triphenylphosphonium-PEG-PE conjugate possess low toxicity, target mitochondria and demonstrate enhanced antitumor effects *in vitro* and *in vivo*. *J. Control. Release*, v. 159, n. 3, p. 393-402, 2012.

CÉSAR, A. L. A. Preparação e caracterização de dispositivo polimérico para liberação controlada de 5-ASA. 2015. 102 f. Dissertação (Mestrado em Ciências Farmacêuticas). Faculdade de Farmácia, Universidade Federal de Minas Gerais, Belo Horizonte, 2015.

CHAFFER, C. L.; WEINBERG, R. A. A perspective on cancer cell metastasis. *Science*, v. 331, p. 1559-1564, 2011.

COSTA, P.; LOBO, J. M. S. Modeling and comparison of dissolution profiles. *Eur J Pharm Sci*., v. 13, p. 123-133, 2001.

DELATTRE, J.; COUVREUR, P.; PUISIEUX, F.; PHILIPPOT, J. R.; SCHUBER, F. Méthodes de preparation des liposomes. In: Les liposomes – *Aspects technologiques, biologiques et pharmacologiques.* 1ª ed., Paris: Les éditions INSERM, 1993, p. 43-57.

DELATTRE, J.; COUVREUR, P.; PUISIEUX, F.; PHILIPPOT, J. R.; SCHUBER, F. Polymorphisme des lipids. Contraintes stériques et élastiques. In: Les liposomes – *Aspects technologiques, biologiques et pharmacologiques.* 1ª ed., Paris: Les éditions INSERM, 1993, p. 7-36.

DRISCOLL, D. F. Lipid injectable emulsions: Pharmacopeial and safety issues. *Pharm. Res.*, v. 23, n. 9, p. 1959-1969, 2006.

FDA – Food and Drug Administration. Informations for Healthcare Professionals: Gadolinium-based constrast agents for magnetic resonance imaging scans. Disponível em: http://www.fda.gov/Drugs/DrugSafety/ucm223966.htm. Page last updated: 02/06/2018. Acesso em: 20 de abril de 2019.

FERREIRA, D. S.; LOPES, S. C. A.; FRANCO, M. S.; OLIVEIRA, M. C. pH-sensitive liposomes for drug delivery in cancer treatment. *Therapeutic Delivery*, v. 4, p. 1099-1123, 2013.

FERTSCH-GAPP, S.; SEMMLER-BEHNKE, M.; WENK, A.; KREVLING, W. G. Binding of polystyrene and carbon black nanoparticles to blood serum proteins. Inhal. Toxicol., v. 23, n. 8, p. 468-475, 2011.

FOSSHEIM, S. L.; II'YASOV, K. A.; HENNING, J.; BJØRNERUD, A. Thermosensitive paramagnetic liposomes for temperature control during MR imaging-guided hyperthermia. *In vitro* feasibility studies. *Acad. Radiol.*, v. 7, p. 1107-1115, 2000.

FRÉZARD, F.; SCHETTINI, D. A.; OLGUITA, G. F. R.; DEMICHELLI, C. Lipossomas: propriedades físico-químicas e farmacológicas, aplicações na quimioterapia à base de antimônio. *Quím. Nova*, v. 28, p. 511-518, 2005.

GARELLO, F.; TERRENO, E. Sonosensitive MRI nanosystems as cancer theranostics: a recente update. *Front Chem*, v. 6, n. 157. p. 1-7, 2018.

GE HEALTHCARE. Product monograph: Omniscan^{TM} (gadodiamide injection USP), Control No.: 169935, p. 1-36, 2013.

GRAHN, A. Y.; BANKIEWICZ, K. S.; DUGICH-DJORDJEVIC, M.; BRINGAS, J. R.; HADACZEK, P.; JOHNSON, G. A.; EASTMAN, S.; LUZ, M. Non-PEGylated liposomes for convection-enhanced delivery of topotecan and gadodiamide in malignant glioma: initial experience. *J. Neurooncol.*, v. 95, n. 2, p. 185-197, 2009.

GRÜLL, H.; LANGEREIS, S. Hyperthermia-triggered drug delivery from temperature-sensitive liposomes using MRI-guided high intensity focused ultrasound. *J. Control. Release*, v. 161, p. 317-327, 2012.

HAEMMERICH, D.; MOTAMARRY, A. Thermosensitive liposomes for image-guided drug delivery. *Adv Cancer Res.*, v. 139, p. 121-146, 2018.

HALLET, F. R.; MARSH, J.; NICKEL, B. G.; WOOD, J. M. Mechanical properties of vesicles. II. A model for osmotic swelling and lysis. *Biophys J.*, v. 64, n. 2, p. 435-442, 1993.

HUPFELD, S.; MOEN, H. H.; AUSBACHER, D.; HAAS, H.; BRANDL, M. Liposomes fractionation and size analysis by asymmetrical flow field-flow fractionation/multi-angle light scattering: influence of ionic strength and osmotic pressure of the carrier liquid. Chem. Phys. Lipids., v. 163, n. 2, p. 141-147, 2010.

HIJNEN, N.; KNEEPKENS, E.; DE SMET, M.; LANGEREIS, S.; HEIJMAN, E.; GRÜLL, H. Thermal combination therapies for local drug delivery by magnetic resonance-guided high-intensity focused ultrasound. *Proc Natl Acad Sci USA*, v. 114, n. 24, p. E4802-E4811, 2017.

HILDEBRANDT, B.; WUST, P.; AHLERS, O.; DIEING, A.; SREENIVASE, G.; KERNER, T.; FELIZ, R.; RIESS, H. The cellular and molecular basis of hyperthermia. *Crit. Rev. Oncol. Hematol.*, v. 43, p. 33-56, 2002.

HOSSANN, M.; SYUNYAEVA, Z.; SCHMIDT, R.; ZENGERLE, A.; EIBL, H.; ISSELS, R. D.; LINDNER, L. H. *J. Control. Release*, v. 162, p. 400-406, 2012.

HOSSANN, M.; WANG, T.; WIGGENHORN, M.; SCHMIDT, R.; ZENGERLE, A.; WINTER, G.; EIBL, H.; PELLER, M.; REISER, M.; ISSELS, R. D.; LINDNER, L. H. Size of thermosensitive liposomes influences content release. *J. Control. Release*, v. 147, p. 436-443, 2010.

HOSSANN, M.; WANG, T.; SYUNYAEVA, Z.; WIGGENHORN, M.; ZENGERLE, A.; ISSELS, R. D.; REISER, M.; LINDNER, L. H.; PELLER, M. Non-ionic Gd-based MRI contrast agents are optimal for encapsulation into phosphatidyl glycerol-based thermosensitive liposomes. *J. Control. Release*, v. 166, p. 22-29, 2013.

HOSSANN, M.; WIGGENHORN, M.; SCHWERDT, A.; WACHHOLZ, K.; TEICHERT, N.; EIBL, H.; ISSELS, R. D.; LINDNER, L. H. *In vitro* stability and content release properties of phosphatidylglyceroglycerol containing thermosensitive liposomes. *Biochim. Biophys. Acta.*, v. 1768, p. 2491-2499, 2007.

HUANG, X.; LI, M.; BRUNI, R.; MESSA, P.; CELLESI, F. The effect of thermosensitive liposomal formulations on loading and release of high molecular weight biomolecules. *Int. J. Pharm.*, v. 524, n. 1-2, p. 279-289, 2017.

INCA – Instituto Nacional do Câncer José Alencar Gomes da Silva. 2018. Disponível em: <http://www1.inca.gov.br/estimativa/2018/>. Acesso em: 09 de abril de 2019.

ISSELS, R. D. Hyperthermia adds to chemotherapy. *Eur. J. Cancer*, v. 44, p. 2546-2554, 2008.

ISSELS, R.; KAMPMANN, E.; KANAAR, R.; LINDNER, L. H. Hallmarks of hyperthermia in driving the future of clinical hyperthermia as targeted therapy: translation into clinical application. *Int. J. Hyperthermia*, v. 32, n. 1, p. 89-95, 2016.

ISO 10993-5. International Standard: biological evaluation of medical devices. Part 5: tests for *in vitro* cytotoxicity. ISO 10993-5, 2009.

JAIN, A.; JAIN, S. K. *In vitro* release kinetics model fitting of liposomes: an insight. *Chem. Phys. Lipids.*, v. 201, p. 28-40, 2016.

JOSE, A.; NINAVE, K. M.; KARNAM, S.; VENUGANTI, V. V. K. Temperature-sensitive liposomes for co-delivery of tamoxifen and imatinib for synergistic breast cancer treatment. *J. Liposome Res.*, v. 11, p. 1-10, 2018.

JUNG, M. Introduction. In: Polymerisation in bilayers. Eindhoven: Technische Universiteit Eindhoven. DOI: 10.6100/IR531044.

NEW, R. R. C. Introduction. In: *Liposomes a practical approach.* 1ª ed. England: Oxford University Press, 1990, p. 1-31.

KAELIN JR, W. G. The concept of synthetic lethality in the context of anticancer therapy. *Nat. Rev. Cancer*, v. 5, p. 689-698, 2005.

KIM, W.; KIM, E-G.; LEE, S.; KIM, D.; CHUN, J.; PARK, K. H.; YOUN, H-S; YOUN, B-H. TFAP2C-mediated upregulation of TGFBR1 promotes lung tumorigenesis and epithelial-mesenchymal transition. *Exp. Mol. Med.*, v 48, n. 11, doi:10.1038/emm.2016.125, 2016.

KNEIDL, B.; PELLER, M.; WINTER, G.; LINDNER, L. H., HOSSAN, M. Thermosensitive liposomal drug delivery systems: state of the art review. *Int. J. Nanomed.***,** v. 9, p. 4387-4398, 2014.

KUMAR, C. S. S. R,; MOHAMMAD, F. Magnetic nanomaterials for hyperthermia-based therapy and controlled drug delivery. *Adv. Drug Delivery Rev.*, v. 63, p. 789-808, 2011.

LAMICHHANE, N.; UDAYAKUMAR, T. S.; D'SOUZA, W. D.; SIMONE, C. B.; RAGHAVAN, S. R.; POLF, J.; MAHMOOD, J. Liposomes: clinical applications and potential for image-guided drug delivery. *Molecules*, v. 23, n. 2, E288, p. 1-17, 2018.

LAOUINI, A.; JAAFAR-MAALEJ, C.; LIMAYEM-BLOUZA, I.; SFAR, S.; CHARCOSSET, C.; FESSI, H. Preparation, characterization and applications of liposomes: state of the art. *J. Colloid Sci. Biotechnol.*, v.1, p. 147-168, 2012.

LAURENT, S.; DUTZ, S.; HÄFELI, U. O.; MAHMOUDI, M. Magnetic fluid hyperthermia: focus on superparamagnetic iron oxide nanoparticles. *Adv. Colloid Interface Sci*., v. 166, p. 8-23, 2011.

LI, L. HAGEN, T. L. M. T.; SCHIPPER, D.; WIJNBERG, T. M.; RHOON, G. C. V.; EGGERMONT, A. M. M.; LINDNER, L. H.; KONING, G. A. Triggered content release from optimized stealth thermosensitive liposomes using mild hyperthermia. *J. Control. Release*, v. 143, p. 274-279, 2010.

LI, L.; HAGEN, T. L. M. T.; HOSSANN, M.; SÜSS, R.; RHOON, G. C. V.; EGGERMONT, A. M. M.; HAEMMERICH, D.; KONING, G.A. Mild hyperthermia triggered doxorubicin release from optimized stealth thermosensitive liposomes improves intratumoral drug delivery and efficacy. *J. Control. Release*, v. 168, n. 2, p. 142-150, 2013.

LIMA-TENÓRIO, M. K.; PINEDA, E. A.; AHMAD, N. M.; FESSI, H.; ELAISSARI, A. Magnetic nanoparticles: *in vivo* cancer diagnosis and therapy. *Int. J. Pharm*., v. 493, p. 313-327, 2015.

LIMMER, S.; HAHN, J.; SCHMIDT, R.; WACHHOLZ, K.; ZENGERLE, A.; LECHNER, K.; EIBL, H.; ISSELS, R. D.; HOSSANN, M.; LINDNER, L. H. Gemcitabine treatment of rat soft tissue sarcoma with phosphatidyldiglycerol-based thermosensitive liposomes. *Pharm. Res.*, v. 31, n. 9, p. 2276-2286, 2014.

LINDNER, U.; LINGOTT, J.; RICHTER, S.; JIANG, W.; JAKUBOWSKI, N.; PANNE, U. Analysis of gadolinium-based constrast agents in tap water with a new hydrophilic interaction chromatography (ZIC-cHILIC) hyphenated with inductively coupled plasma mass spectrometry. *Anal. Bioanal. Chem.,* v. 407, p. 2425-2422, 2015.

LIU, K.; NEWBURY, P. A.; GLICKSBERG, B. S.; ZENG, W. Z. D.; ANDRECHEK, R.; CHEN, B. Evaluating cell lines as models for metastatic cancer through integrative analysis of open genomic data. *Bio Rx IV*, doi: https://doi.org/10.1101/337287, 2018.

LIU, Y.; ZHANG, N. Gadolinium loaded nanoparticles in theranostic magnetic resonance imaging. *Biomaterials,* v. 33, p. 5363-5375, 2012.

LOPES, S. C. A.; GIUBERTI, C. S.; ROCHA, T. G. R.; FERREIRA, D. S.; LEITE, E. A.; OLIVEIRA, M. C. Lipossomes as carriers of anticancer drugs. In: *Liposomes as carriers of anticancer drugs.* Letícia Rangel. Org. 1. Ed. Rijeka: In Tech Open Scienc/Open Minds, 2013a, p. 85-124a.

LOPES, S. C. A.; NOVAIS, M. V. M.; FERREIRA, D. S.; BRAGA, F. C.; PANIAGO-MAGALHÃES, R.; MALACHIAS, Â.; OLIVEIRA, M. C. Ursolic acid incorporation does not prevent the formation of a non-lamellar phase in pH-sensitive and long-circulating liposomes. *Langmuir*, v. 30, n. 50, p. 15083-15090, 2014.

LOPES, S. C. A.; NOVAIS, M. V. M.; TEIXEIRA, C. S.; HONORATO-SAMPAIO, K.; PEREIRA, M. T.; FERREIRA, L. A. M.; BRAGA, F. C.; OLIVEIRA, M. C. Preparation, physicochemical characterization, and cell viability evaluation of long-circulating and pH-sensitive liposomes containing ursolic acid. *BioMed Res. Int.,* v. 1, p. 1-7, 2013b.

MAEDA, H. The enhanced permeability and retention (EPR) effect in tumor vasculature: the key role of tumor-selective macromolecular drug targeting. *Adv. Biol. Regul.*, v. 41, p. 189-207, 2001.

MAIA, A. L. C. Lipossomas contendo gadodiamida: aspectos analíticos, farmacotécnicos e avaliação da atividade citotóxica *in vitro*. 2015. 118 f. Dissertação (Mestrado em Ciências Farmacêuticas). Faculdade de Farmácia, Universidade Federal de Minas Gerais, Belo Horizonte, 2015.

MAIA, A. L. C.; FERNANDES, C.; SILVA, T. D.; OLIVEIRA, C. N. P.; SILVEIRA, J. N.; RAMALDES, G. A. Development and validation of high performance liquid chromatographic and derivative spectrophotometric methods for determination of gadodiamide in liposomal formulations. *Anal Methods*, v. 7, p. 8315-8325, 2015.

MAIA, A. L. M.; FERNANDES, C.; OLIVEIRA, C. N. P.; TEIXEIRA, C. S.; OLIVEIRA, M. S.; SOARES, D. C. F.; RAMALDES, G. A. Liposomes containing gadodiamide: preparation, physicochemical characterization, and *in vitro* cytotoxic evaluation. *Current Drug Delivery*, v. 13, p. 1-9, 2016.

MALVERN INSTRUMENTS. Size theory. In: *Zetasizer Nano User Manual – MAN 0485*. v. 1.1, Inglaterra, 2013, p. 11.1 – 11.8

MANZOOR, A. A.; LINDNER, L. H.; LANDON, C. D.; PARK, J.-Y.; SIMNICK, A. J.; DREHER, M. R.; DAS, S.; HANNA, G.; PARK, W.; CHILKOTI, A.; KONING, G. A.; TEN HAGEN, T. L. M.; NEEDHAM, D.; DEWHIRST, M. W. Overcoming limitations in nanoparticle drug delivery: triggered, intravascular release to improve drug penetration into tumors. *Cancer Res.* v. 72, p. 5566-5575, 2012.

MIRSHAFIEE, V.; MAHMOUDI, M.; LOU, K.; CHENG, J.; KRAFT, M. L. Protein corona significantly reduces active targeting yield. *Chem Commun (Camb)*, v. 49, n. 25, p. 2557-2559, 2013.

MITTAG, J. J.; KNEIDL, B.; PREIβ, T.; HOSSANN, M.; WINTER, G.; WUTTKE, S.; ENGELK H.; RÄDLER, J. O. Impact of plasma protein binding on cargo release by thermosensitive liposomes probed by fluorescence correlation spectroscopy. *Eur. J. Pharm. Biopharm.* v. 119, p. 215-223, 2017.

MONTEIRO, L. O. F.; LOPES, S. C. A.; BARROS, A. L. B.; MAGALHÃES-PANIAGO, R.; MALACHIAS, Â.; OLIVEIRA, M. C.; LEITE, E. A. Phase behavior of dioleyphosphatidylethanolamine molecules in the presence of components of pH-sensitive liposomes and paclitaxel. *Colloids Surf B Biointerfaces.* v. 144, p. 276-283, 2016.

MORA-HUERTAS, C. E.; FESSI, H.; ELAISSARI, A. Polymer-based nanocapsules of drug delivery. *Int. J. Pharm.,* v. 385, p. 113-142, 2010.

MOSMANN, T. Rapid colorimetric assay for cellular growth and survival: application to proliferation and cytotoxicity assays. *J. Immunol. Methods*. v. 65, n. 1-2, p. 55-63, 1983.

MROSS, K; KRATZ, F. Limits of conventional cancer chemotherapy. In: *Drug Delivery in Oncology*. New Jersey: John Wiley & Sons, 2011, p. 1-30.

NEW, R. R. C. Introduction. In: *Liposomes a practical approach.* 1ª ed. England: Oxford University Press, 1990, p. 1-31.

OLIVEIRA, M. S.; MUSSI, S. V.; GOMES, D. A.; YOSHIDA, M. I.; FRÉZARD, F.; CARREGAL, V. M.; FERREIRA, L. A. M. α-Tocopherol succinate improves encapsulation and anticancer activity of doxorubicin loaded in solid lipid nanoparticles. *Colloids Surf B Biointerfaces,* v. 140, p. 246-253, 2016.

OTO, E. K.; ZALIPSKY, S.; QUINN, Y. P.; ZHU, G. Z.; USTER, P. S. Poly(methacrylic acid)-induced liposome aggregation for measuring drug entrapment. *Anal. Biochem.*, v. 229, n. 1, p. 106-111, 1995).

PAVIA, D. L.; LAMPMAN, G. M.; KRIZ, G. S.; VYVYAN, J. R. *Introdução à espectroscopia*. 4ª ed., São Paulo: Cengage Learning, 2010, 700 p.

PRADHAN, P.; GIRI, J.; RIEKEN, F.; KOCH, C.; MYKHAYLYK, O.; DÖBLINGER, M.; BANERIEE, R.; BAHADUR, D.; PLANK, C. Targeted temperature sensitive magnetic liposomes for thermo-chemotherapy. *J. Control. Release*, v. 142, p. 108-121, 2010.

PULASKI, B. A.; OSTRAND-ROSENBERG, S. Mouse 4T1 breast tumor model. *Curr. Protoc. Immunol.* Chapter 20: Unit 20.2. doi: 10.1002/0471142735.im2002s39, 2001.

RUI-GUANG, W.; JUN-DONG, D.; FU-GEN, W.; XIAO-HUA, Z.; WEI-FENG, L.; YU-RONG, W. Competitive molecular interaction among paenol-loaded liposomes: differential scanning calorimetry and synchrotron X-ray diffraction studies. *Int J Pharm*, v. 438, p. 91-97, 2012.

SAADEH, Y.; LEUNG, T.; VYAS, A.; CHATURVEDI, L. S.; PERUMAL, O.; VYAS, D. Applications of nanomedicine in breast cancer detection, imaging, and therapy. *J. Nanosci. Nanotechnol.*, v. 14, n. 1, p. 913-923, 2014.

SACCHETTI, C.; MOTMEDCHABOKI, K.; MAGRINI, A.; PALMIERI, G.; MATTEI, M.; BERNARDINI, S.; ROSATO, N.; BOTTINI, N.; BOTTINI, M. Surface polyethylene glycol conformation influences the protein corona of polyethylene glycol-modified single-walled carbon nanotubes: potential implications on biological performance. *ACS Nano*, v. 7, n. 3, p. 1974-1989, 2013.

SALUNKHE, A. B.; KHOT, V. M.; PAWAR, S. H. Magnetic hyperthermia with magnetic nanoparticle: a status review. *Curr. Top. Med. Chem.*, v. 14, n. 5, p. 572-594, 2014.

SHELLOCK, F. G.; KANAL, E. Safety of magnetic resonance imaging contrast agents. *J Magn Reson Imaging*, v. 10, p. 477-484, 1999.

SHARMA, A.; SHARMA, U. Liposomes in drug delivery: progress and limitations. *Int. J. Pharm.*, v. 154, p. 123-140, 1997.

SINGH, A. SAHOO, S. K. Magnetic nanoparticles: a novel platform for cancer theranostics. *Drug Discov. Today*, v. 19, n. 4, p. 474-481, 2014.

SMITH, E. A.; DEA, P. K. Differential scanning calorimetry studies of phospholipid membranes: the interdigitated gel phase. In: *Application of calorimetry in a wide context – differential scanning calorimetry, isothermal titration calorimetry and microcalorimetry*. Amal Ali Elkordy, IntechOpen, 2013. DOI: 10.5772/51882.

SOARES, D. C. F.; MENEZES, M. A. B. C.; SANTOS, R. G.; RAMALDES, G. A. ^{159}Gd: preparation and preliminary evaluation as a potential antitumoral radionuclide. *J. Radioanal. Nucl. Chem.* v. 284, p. 315-320, 2010.

SOARES, D.C.F.; OLIVEIRA, M.C.; SANTOS, R.G.; ANDRADE, M.S.; VILELA, J.M.C.; CARDOSO, V.N.; RAMALDES, G.A. Liposomes radiolabeled with 159Gd-DTPA-BMA: Preparation, physicochemical characterization, release profile and *in vitro* cytotoxic evaluation. *Eur J Pharm Sci*., v. 42, n. 5, p. 462-469, 2011a.

SOARES, D.C.F.; OLIVEIRA, M.C.; BARROS, A.L.B.; CARDOSO, V.N.; RAMALDES, G.A. Liposomes radiolabeled with 159Gd: *In vitro* antitumoral activity, biodistribution study and scintigraphic image in Ehrlich tumor bearing mice. *Eur J Pharm Sci*., v. 43, n. 4, p. 290-296, 2011b.

SOARES, D.C.F.; CARDOSO, V. N.; BARROS, A.L.B.; SOUZA, C.M.; CASSALI, G.D.; OLIVEIRA, M.C.; RAMALDES, G.A. Antitumoral activity and toxicity of PEG-coated and PEG-folate-coated pH-sensitive liposomes containing 159Gd-DTPA-BMA in Ehrlich tumor bearing mice. *Eur J Pharm Sci*., v. 45, n. 1-2, p. 58-64, 2012.

SOARES, D.C.F.; BARROS, A.L.B.; SANTOS, R.G.S.; SOUSA, E.M.B.; RAMALDES, G.A. Apoptosis mediated by caspase-3 and p53-dependent anticancer effects of 159Gd-DTPA-BMA complex. *J Radioanal Nucl Chem.*, v. 295, n. 1, p. 63-66, 2013.

STAFFORD, R. E.; FANNI, T.; DENNIS, E. A. Interfacial properties and critical micelle concentration of lysophospholipids. *Biochemistry*, v. 28, n. 12, p. 5113-5120, 1989.

STEICHEN, S. D.; CALDORERA-MOORE, M.; PEPPAS, N. A. A review of current nanoparticle and targeting moieties for the delivery of cancer therapeutics. *Eur. J. Pharm. Sci.*, v. 48, p. 416-427, 2013.

SZOKA JR, F.; PAPAHADJOPOULOS, D. Procedure for preparation of liposomes with large internal aqueous space and high capture by reverse-phase evaporation. *Proc. Natl. Acad. Sci.*, v. 75, n. 9, p. 4194-4198, 1978.

THE UNITED States Pharmacopeia. 36 ed. Rockville: *The United States Pharmacopeial Convention*, 2013. Chapter 729 Globule size distribution in lipid injectable emulsions. p. 321-323.

WANG, T.; HOSSANN, M.; REINL, H. M.; PELLER, M.; EIBL, H.; REISER, M.; ISSELS, R. D.; LINDNER, L. H. *In vitro* characterization of phosphatidylglyceroglycerol-based thermosensitive liposomes with encapsulated ^{1}H MR T_1-shortening gadodiamide. *Contrast Media Mol. Imaging*, v. 3, p. 19-26, 2008.

WHO – World Health Organization. 2018. Disponível em: < https://www.who.int/en/news-room/fact-sheets/detail/cancer>. Acesso em: 9 de abril de 2019.

WILLERDING, L.; LIMMER, S.; HOSSANN, M.; ZENGERLE, A.; WACHHOLZ, K.; TEN HAGEN, T. L. M.; KONING, G. A.; SROKA, R.; LINDNER, L. H.; PELLER, M. Method of hyperthermia and tumor size influence effectiveness of doxorubicin release from thermosensitive liposomes in experimental tumors. *J. Control. Release*, v. 222, p. 47-55, 2016.

WOLFRAM, J.; SURI, K.; YANG, Y.; SHEN, J.; CELIA, C.; FRESTA, M.; ZHAO, Y.; SHEN, H.; FERRARI, M. Shrinkage of pegylated and non-pegylated liposomes in serum. *Colloids Surf B Biointerfaces*, v. 114, p. 294-300, 2014.

WOODLE, M. C.; COLLINS, L. R.; SPONSLER, E.; KOSSOVISKY, N.; PAPAHAJOPOULOS, D. MARTIN, F. J. Sterically stabilized liposomes. Reduction in electrophoretic mobility but not electrostatic surface potential. *Biophys J.*, v. 61, p. 902-910, 1992.

YINGCHONCHAROEN, P.; KALINOWSKI, D. S.; RICHARDSON, D. R. Lipid-based drug delivery systems in cancer therapy: what is available and what is yet to come. *Pharmacol Rev.*, v. 68, n. 3, p. 701-787, 2016.

ZHANG, Y.; ZHOU, J.; GUO, D.; AO, M.; ZHENG, Y.; WANG, Z. Preparation and characterization of gadolinium-loaded PLGA particles surface modified with RGDS for the detection of thrombus. *Int. J. Nanomedicine.*, v. 8, p. 3745-3756, 2013.

ZUGAZAGOITIA, J.; GUEDES, C.; PONCE, S.; FERRER, I.; MOLINA-PINELO, S; PAZ-ARES, L. Current Challenges in Cancer Treatment. *Clin Ther.*, v. 38, n. 7, p. 1551-1566, 2016.

CONCLUSÃO GERAL E PERSPECTIVAS

Esta tese foi dividida em duas partes. Na primeira parte foi realizada uma revisão de literatura, apresentando a fundamentação teórica da utilização de Gd-DTPA-BMA em lipossomas termossensíveis para o tratamento do câncer. A segunda parte, onde o trabalho experimental é apresentado, foi dividida em dois capítulos.

No capítulo 1 foram descritos o desenvolvimento e a validação de método analítico por HILIC, para determinação de Gd-DTPA-BMA em lipossomas e em outras amostras mais complexas. Neste estudo, os seguintes resultados foram obtidos:

- Foram identificadas, com base em uma revisão da literatura, as variáveis independentes críticas para o desenvolvimento de métodos por HILIC para a determinação de Gd-DTPA-BMA. Essas variáveis são: (*i*) tipo de tampão, (*ii*) proporção de ACN, (*iii*) concentração de tampão e (*iv*) pH do componente aquoso da fase móvel;
- Foram identificadas, por meio de experimento preliminar, as faixas de variação e os níveis em que as variáveis independentes deveriam ser avaliadas em um planejamento fatorial. Os resultados encontrados foram: (*i*) pH do tampão NH_4FA (nível –1 = 3,7; nível 0 = 4,2; nível +1 = 4,7), (*ii*) proporção de ACN na fase móvel (%) (nível –1 = 60; nível 0 = 65; nível +1 = 70), (*iii*) concentração do tampão NH_4FA (mmol/L) (nível –1 = 5; nível 0 = 15; nível +1 = 25);
- Foram definidas as condições ótimas das variáveis independentes, por meio de análises de superfície de resposta e planejamento fatorial do tipo Box-Behnken, sendo elas: fase móvel composta por 60% de ACN, NH_4FA em concentração de 5 mmol/L e pH do componente aquoso da fase móvel igual 4,5;
- A vazão da fase móvel foi otimizada, por meio de uma curva de Van Deemter. A vazão de 0,6 mL/min permitiu aumentar 29% da eficiência (*N*) e 12% da detectabilidade e R_s do método proposto;
- O método desenvolvido mostrou-se seletivo, preciso, exato e linear na faixa entre 40 e 120 nmol/L;
- Os limites de detecção e quantificação obtidos foram 4,56 e 6,78 nmol/L, respectivamente;
- A robustez do método desenvolvido foi demonstrada por meio do teste de Youden. O método mostrou-se robusto frente a todas as variações realizadas: (*i*) proporção de ACN na fase móvel, (*ii*) pH do componente aquoso da fase móvel (*iii*) concentração

do tampão NH_4FA, (*iv*) temperatura da coluna, (*v*) vazão da fase móvel, (*vi*) marca da ACN, (*vii*) marca do tampão.

No capítulo 2 foram descritos o desenvolvimento e a caracterização de duas formulações (TTSL-Gd e LTLS-Gd), com diferentes composições, contendo Gd-DTP-BMA. Também foi descrita a avaliação da citotoxicidade dessas formulações em linhagens de células tumorais (4T1 e MDA-MB-231) e sadias (WI-26 VA 4). Os resultados obtidos neste capítulo são:

- Foi demonstrado, por espectrometria nas regiões do infravermelho e ultravioleta e por HILIC, que Gd-DTPA-BMA é um fármaco adequado para encapsulação em lipossomas termossensíveis, uma vez que esse complexo permaneceu estável durante as condições de aquecimento utilizadas no preparo dessas formulações;
- Foi demonstrado que ao utilizar o método BANGHAM para o preparo dos lipossomas, obtém-se as mesmas taxas de encapsulação que as taxas obtidas pelo método REV, que é mais demorado, complexo e dispendioso;
- Foi demonstrado que a quantidade de fármaco adicionado durante o preparo influencia na taxa de encapsulação e estabilidade dos lipossomas. Ao adicionar 250 μmol/mL de Gd-DTPA-BMA durante o preparo foi possível obter formulações com alto teor de fármaco e adequada estabilidade. O valor de fármaco encapsulado em cada lipossoma (TTSL-Gd = 25,7 ± 2,0 μmol/mL; LTSL-Gd = 23,8 ± 3,3 μmol/mL) é adequado para o tratamento antitumoral, considerando valores de IC_{50} descritos na literatura;
- Os lipossomas desenvolvidos apresentaram adequadas características físico-químicas, em termos de diâmetro médio (TTSL-Gd = 114 ± 16 nm; LTSL-Gd = 118 ± 12 nm), índice de polidispersão (TTSL-Gd = 0,07 ± 0,01; LTSL-Gd = 0,08 ± 0,01) e potencial zeta (TTSL-Gd = –2,8 ± 1,3 mV; LTSL-Gd = –2,1 ± 0,1 mV). Os valores obtidos podem contribuir para a estabilidade de armazenamento e biodistribuição adequadas dos nanosistemas;
- A estabilidade de armazenamento das formulações, a 4 °C por 120 dias, foi demonstrada pela manutenção das seguintes características: diâmetro médio, índice de polidispersão, potencial zeta e quantidade de Gd-DTPA-BMA encapsulada;
- A caracterização morfológica das formulações, realizada por microscopia eletrônica de transmissão, revelou vesículas esféricas e unilamelares. As amostras contendo Gd-DTPA-BMA apresentaram alto contraste no núcleo aquoso interno, evidenciando a encapsulação do fármaco;

- Análises térmicas foram realizadas por DLS, DSC e SAXS. Os resultados das diferentes análises foram consistentes e evidenciaram valores de T_c (TTSL-Gd = 43,7 °C; LTSL-Gd = 43,6 °C) compatíveis com tratamento empregando hipertermia moderada (41 °C a 45 °C);
- Estudos de liberação *in vitro* revelaram que a formulação LTSL-Gd apresenta maior liberação e em menor temperatura que TTSL-Gd, devido a sua maior fluidez. Por este motivo, também foi observado que LTSL-Gd se manteve estável, a 37 °C, por um tempo inferior a TTSL-Gd. As análises sugerem que as formulações apresentam cinética de liberação conforme modelo de Higuchi, no qual a liberação do fármaco ocorre por difusão, baseada na Lei de Fick.
- Os estudos de citotoxicidade revelaram que todos os grupos avaliados apresentaram perfis semelhantes, independente da utilização de hipertermia ou não, nas linhagens 4T1 e MDA-MB-231. Nestas células, os lipossomas brancos e Gd-DTPA-BMA não apresentaram citotoxicidade significativa. TTSL-Gd e LTSL-Gd apresentaram valores de IC_{50}, aproxidamente 100 vezes menores que aqueles para o fármaco livre. As análises na linhagem de células normais evidenciaram a seletividade do tratamento proposto.

Portanto, os resultados apresentados nesta tese, possibilitam concluir que lipossomas termossensíveis constituem um interessante sistema nanocarreador para Gd-DTPA-BMA, e podem representar uma alternativa adequada e vantajosa para o tratamento do câncer de mama.

A partir do estudo realizado foi possível propor as seguintes perspectivas:

- Investigar de forma mais aprofundada o mecanismo de ação citotóxica de Gd-DTPA-BMA por meio de análises de citometria de fluxo;
- Realizar estudos de biodistribuição, por ressonância magnética, para confirmar o potencial das formulações para liberação de fármaco monitorada por imagem;
- Realizar estudos de atividade antitumoral *in vivo*, em camundongos BALB/c portadores de adenocarcinoma mamário 4T1;
- Realizar estudos de toxicidade *in vivo*, por meio da determinação do peso dos animais, mortalidade, sinais clínicos, exames hematológicos, bioquímicos e histopatológicos.
- Realizar estudo de liofilização dos lipossomas, afim de viabilizar comercialmente as formulações desenvolvidas.

REFERÊNCIAS GERAIS

ALMEIDA, V. L.; LEITÃO, A.; REINA, L. C. B.; MONTANNARI, C. A.; DONNICI, C. L.; LOPES, M. T. P. Câncer e agentes antineoplásicos ciclo-celular específicos e ciclo-celular não específico que interagem com o DNA: Uma introdução. *Quim. Nova,* v. 28, p. 118-129, 2005.

ARISAWA, E. A. L.; SILVA, C. M. O. M.; CARDOSO, C. A. C.; LEMOS, N. R. P.; PINTO, M. C. Efeitos colaterais da terapia antitumoral em pacientes submetidos à químio e à radioterapia. *Rev. Biociênc.*, v. 11, p. 55-61, 2005.

BANGHAM, A. D.; STANDISH, M. M.; WATKINS, J. C. Diffusion of univalent ions across the lamellae of swollen phospholipids. *J. Mol. Biol.*, v. 13, p. 238-252, 1965.

BATISTA, C. M.; CARVALHO, C. M. B.; MAGALHÃES, N. S. S. Lipossomas e suas aplicações terapêuticas: Estado da arte. *Rev. Bras. Cienc. Farm.*, v. 43, p. 167-179, 2007.

DELATTRE, J.; COUVREUR, P.; PUISIEUX, F.; PHILIPPOT, J. R.; SCHUBER, F. Méthodes de preparation des liposomes. In: Les liposomes – *Aspects technologiques, biologiques et pharmacologiques.* 1ª ed., Paris: Les éditions INSERM, 1993, p. 43-57.

DEMEL, R. A.; DE KRUYFF, B. The function of sterols in membranes. *Biochim. Biophys. Acta*, v. 457, p. 109-132, 1976.

DUROCHER, J.R.; PAYNE, R. C.; CONRAD, M. E. Role of sialic acid in erythrocyte survival. *Blood*, v. 45, n. 1, p. 11-20, 1975.

FALK, M. H.; ISSELS, R. D. Hyperthermia in oncology. *Int. J. Hyperthermia,* v. 17, p. 1-18, 2001.

FERREIRA, D. S.; LOPES, S. C. A.; FRANCO, M. S.; OLIVEIRA, M. C. pH-sensitive liposomes for drug delivery in cancer treatment. *Therapeutic Delivery*, v. 4, p. 1099-1123, 2013.

FRÉZARD, F. Liposomes: from biophysics to the design of peptide vaccines. *Braz. J. Med. Biol. Res.*, v. 32, p. 181-189, 1999.

FRÉZARD, F.; SCHETTINI, D. A.; OLGUITA, G. F. R.; DEMICHELLI, C. Lipossomas: propriedades físico-químicas e farmacológicas, aplicações na quimioterapia à base de antimônio. *Quím. Nova*, v. 28, p. 511-518, 2005.

GABER, M. H.; HONG, K. L.; HUANG, S. K.; PAPAHADJOPOULOS, D. Thermosensitive sterically stabilized liposomes – formulation and *in vitro* studies on mechanism of doxorubicin release by bovine serum and human plasma. *Pharm. Res.*, v. 12, p. 1407-1416, 1995.

GOORLEY, T.; NIKJOO, H. Electron and photon spectra for three gadolinium-based cancer therapy approaches. *Radiat. Res.*, v.154, p. 556-563, 2000.

GRAHN, A. Y.; BANKIEWICZ, K. S.; DUGICH-DJORDJEVIC, M.; BRINGAS, J. R.; HADACZEK, P.; JOHNSON, G. A.; EASTMAN, S.; LUZ, M. Non-PEGylated liposomes for

convection-enhanced delivery of topotecan and gadodiamide in malignant glioma: initial experience. *J. Neurooncol.*, v. 95, n. 2, p. 185-197, 2009.

GRÜLL, H.; LANGEREIS, S. Hyperthermia-triggered drug delivery from temperature-sensitive liposomes using MRI-guided high intensity focused ultrasound. *J. Control. Release*, v. 161, p. 317-327, 2012.

HABASH, R. W. Y.; BANSAL, R.; KREWSKI, D.; ALHAFID, H. Thermal therapy, part 2: hyperthermia techniques. *Crit. Rev. Biomed. Eng.*, v. 34, p. 491-542, 2006.

HILDEBRANDT, B.; WUST, P.; AHLERS, O.; DIEING, A.; SREENIVASE, G.; KERNER, T.; FELIZ, R.; RIESS, H. The cellular and molecular basis of hyperthermia. *Crit. Rev. Oncol. Hematol.*, v. 43, p. 33-56, 2002.

HOSSANN, M.; WANG, T.; WIGGENHORN, M.; SCHMIDT, R.; ZENGERLE, A.; WINTER, G.; EIBL, H.; PELLER, M.; REISER, M.; ISSELS, R. D.; LINDNER, L. H. Size of thermosensitive liposomes influences content release. *J. Control. Release*, v. 147, p. 436-443, 2010.

HOSSANN, M.; WANG, T.; SYUNYAEVA, Z.; WIGGENHORN, M.; ZENGERLE, A.; ISSELS, R. D.; REISER, M.; LINDNER, L. H.; PELLER, M. Non-ionic Gd-based MRI contrast agents are optimal for encapsulation into phosphatidyl glycerol-based thermosensitive liposomes. *J. Control. Release*, v. 166, p. 22-29, 2013.

HUWYLER, J.; DREWE, J.; KRÄHENBÜHL, S. Tumor targeting using liposomal antineoplastic drugs. *Int. J. Nanomedicine*, v. 3, p. 21-29, 2008.

INCA – Instituto Nacional do Câncer José Alencar Gomes da Silva. 2018. Disponível em: <http://www1.inca.gov.br/estimativa/2018/>. Acesso em: 09 de abril de 2019.

ISMAEL, G. F. V.; ROSA, D. D.; MANO, M. S.; AWADA, A. Novel cytotoxic drugs: Old challenges, new solutions. *Cancer Treat. Rev.*, v. 34, p. 81– 91, 2008.

ISSELS, R.; KAMPMANN, E.; KANAAR, R.; LINDNER, L. H. Hallmarks of hyperthermia in driving the future of clinical hyperthermia as targeted therapy: translation into clinical application. *Int. J. Hyperthermia*, v. 32, n. 1, p. 89-95, 2016.

KAELIN JR, W. G. The concept of synthetic lethality in the context of anticancer therapy. *Nat. Rev. Cancer*, v. 5, p. 689-698, 2005.

KARP, G. Técnicas em biologia celular e molecular. In: *Biologia celular e molecular, conceitos e experimentos.* 3ª Ed. Barueri: Manole, 2005.

KLIBANOV, A. L.; MARUYAMA, K.; TORCHILIN, V. P.; HUANG, L. Amphipathic polyethyleneglycols effectively prolong the circulation time of liposomes. *FEBS Letters*, v. 268, n. 1, p. 235-237, 1990.

KNEIDL, B.; PELLER, M.; WINTER, G.; LINDNER, L. H., HOSSAN, M. Thermosensitive liposomal drug delivery systems: state of the art review. *Int. J. Nanomed.*, v. 9, p. 4387-4398, 2014.

KUMAR, C. S. S. R,; MOHAMMAD, F. Magnetic nanomaterials for hyperthermia-based therapy and controlled drug delivery. *Adv. Drug Delivery Rev.*, v. 63, p. 789-808, 2011.

LAOUINI, A.; JAAFAR-MAALEJ, C.; LIMAYEM-BLOUZA, I.; SFAR, S.; CHARCOSSET, C.; FESSI, H. Preparation, characterization and applications of liposomes: state of the art. *J. Colloid Sci. Biotechnol.*, v.1, p. 147-168, 2012.

LASIC, D. D. Novel applications of liposomes. *Trends Biotechnol.*, v. 16, p.307-321, 1998.

LASIC, D. D. The mechanism of vesicle formation. *Biochem. J.*, v. 256, p. 1-11, 1988.

LIU, Y.; ZHANG, N. Gadolinium loaded nanoparticles in theranostic magnetic resonance imaging. *Biomaterials*, v. 33, p. 5363-5375, 2012.

LOPES, S. C. A.; GIUBERTI, C. S.; ROCHA, T. G. R.; FERREIRA, D. S.; LEITE, E. A.; OLIVEIRA, M. C. Lipossomes as carriers of anticancer drugs. In: *Liposomes as carriers of anticancer drugs.* Letícia Rangel. Org. 1. Ed. Rijeka: In Tech Open Scienc/Open Minds, 2013a, p. 85-124a.

LOPES, S. C. A.; NOVAIS, M. V. M.; TEIXEIRA, C. S.; HONORATO-SAMPAIO, K.; PEREIRA, M. T.; FERREIRA, L. A. M.; BRAGA, F. C.; OLIVEIRA, M. C. Preparation, physicochemical characterization, and cell viability evaluation of long-circulating and pH-sensitive liposomes containing ursolic acid. *BioMed Res. Int.*, v. 1, p. 1-7, 2013b.

MAIA, A. L. C. Lipossomas contendo gadodiamida: aspectos analíticos, farmacotécnicos e avaliação da atividade citotóxica *in vitro*. 2015. 118 f. Dissertação (Mestrado em Ciências Farmacêuticas). Faculdade de Farmácia, Universidade Federal de Minas Gerais, Belo Horizonte, 2015.

MAIA, A. L. C.; FERNANDES, C.; SILVA, T. D.; OLIVEIRA, C. N. P.; SILVEIRA, J. N.; RAMALDES, G. A. Development and validation of high performance liquid chromatographic and derivative spectrophotometric methods for determination of gadodiamide in liposomal formulations. *Anal Methods*, v. 7, p. 8315-8325, 2015.

MAIA, A. L. M.; FERNANDES, C.; OLIVEIRA, C. N. P.; TEIXEIRA, C. S.; OLIVEIRA, M. S.; SOARES, D. C. F.; RAMALDES, G. A. Liposomes containing gadodiamide: preparation, physicochemical characterization, and *in vitro* cytotoxic evaluation. *Current Drug Delivery*, v. 13, p. 1-9, 2016.

MANZOOR, A. A.; LINDNER, L. H.; LANDON, C. D.; PARK, J.-Y.; SIMNICK, A. J.; DREHER, M. R.; DAS, S.; HANNA, G.; PARK, W.; CHILKOTI, A.; KONING, G. A.; TEN HAGEN, T. L. M.; NEEDHAM, D.; DEWHIRST, M. W. Overcoming limitations in nanoparticle drug delivery: triggered, intravascular release to improve drug penetration into tumors. *Cancer Res.*, v. 72, p. 5566-5575, 2012.

MROSS, K; KRATZ, F. Limits of conventional cancer chemotherapy. In: *Drug Delivery in Oncology*. New Jersey: John Wiley & Sons, 2011, p. 1-30.

MURA, S.; COUVREUR, P. Nanotheranostics for personalized medicine. *Adv. Drug. Deliv. Rev.*, v. 64, p. 1394-1416, 2012.

NCI – National Cancer Institute, 2011. Disponível em: <https://www.cancer.gov/about-cancer/treatment/types/surgery/hyperthermia-fact-sheet>. Acesso em: 09 de abril de 2019.

NEEDHAM, D.; ANYARAMBHATLA, G.; KONG, G.; DEWHIRST, M. W. A new temperature-sensitive liposome for use with mild hyperthermia: characterization and testing in a human tumor xenograft model. *Cancer Res.*, v. 60, p. 1197-1201, 2000.

NEVES, M.; KLING, A.; OLIVEIRA, A. Radionuclides used for therapy and suggestion for new candidates. *J. Radioanal. Nucl. Chem.*, v. 266, p. 377-384, 2005.

NEW, R. R. C. Introduction. In: *Liposomes a practical approach*. 1ª ed. England: Oxford University Press, 1990, p. 1-31.

OLIVEIRA, R.; SANTOS, D.; FERREIRA, D.; COELHO, P.; VEIGA, F. Preparações radiofarmacêuticas e suas aplicações. *Braz. J. Pharm. Sci.*, v. 42, p. 151-164, 2006.

PAPAHADJOPOULOS, D.; GABIZON, A. Liposomes designed to avoid the reticulo endothelial system. *Prog. Clin. Biol. Res.*, v. 343, p. 85-93, 1990.

RUNGE, V. M. Safety of approved MR contrast media for intravenous injection. *J. Magn. Reson. Imagin*, v. 12, p. 205-213, 2000.

SAHA, G. B. Fundamentals of nuclear pharmacy. 6ª Ed. New York: Springer, 2010.

SEMPKOWSKI, M.; LOCKE, T.; STRAS, S.; ZHU, C.; SOFOU, S. Liposome-based approaches for delivery of mainstream chemotherapeutics: preparation methods, liposome designs, therapeutic efficacy. *Crit. Rev. Oncog.*, v. 19, n. 3-4, p. 177-221, 2014.

SHARMA, A.; SHARMA, U. Liposomes in drug delivery: progress and limitations. *Int. J. Pharm.*, v. 154, p. 123-140, 1997.

SHI, J.; KANTOFF, P. W.; WOOSTER, R.; FAROKHZAD, O. C. Cancer nanomedicine: progress, challenges and opportunities. *Nat. Rev. Cancer*, v. 17, n. 1, p. 20-37, 2017.

SINGH, A. T. K.; EVENS, A. M.; PRACHAND, S. N.; GORDON, L. I. Motexafin gadolinium enhances p53-Mdm2 interactions, reducing p53 and downstream targets in lymphoma cell lines. *Anticancer Res.*, v. 30, p. 1131-1136, 2010.

SOARES, D. C. F.; MENEZES, M. A. B. C.; SANTOS, R. G.; RAMALDES, G. A. ^{159}Gd: preparation and preliminary evaluation as a potential antitumoral radionuclide. *J. Radioanal. Nucl. Chem.* v. 284, p. 315-320, 2010.

SOARES, D.C.F.; OLIVEIRA, M.C.; SANTOS, R.G.; ANDRADE, M.S.; VILELA, J.M.C.; CARDOSO, V.N.; RAMALDES, G.A. Liposomes radiolabeled with 159Gd-DTPA-BMA: Preparation, physicochemical characterization, release profile and *in vitro* cytotoxic evaluation. *Eur J Pharm Sci*., v. 42, n. 5, p. 462-469, 2011a.

SOARES, D.C.F.; OLIVEIRA, M.C.; BARROS, A.L.B.; CARDOSO, V.N.; RAMALDES, G.A. Liposomes radiolabeled with 159Gd: *In vitro* antitumoral activity, biodistribution study

and scintigraphic image in Ehrlich tumor bearing mice. *Eur J Pharm Sci*., v. 43, n. 4, p. 290-296, 2011b.

SOARES, D.C.F.; CARDOSO, V. N.; BARROS, A.L.B.; SOUZA, C.M.; CASSALI, G.D.; OLIVEIRA, M.C.; RAMALDES, G.A. Antitumoral activity and toxicity of PEG-coated and PEG-folate-coated pH-sensitive liposomes containing 159Gd-DTPA-BMA in Ehrlich tumor bearing mice. *Eur J Pharm Sci*., v. 45, n. 1-2, p. 58-64, 2012.

SOARES, D.C.F.; BARROS, A.L.B.; SANTOS, R.G.S.; SOUSA, E.M.B.; RAMALDES, G.A. Apoptosis mediated by caspase-3 and p53-dependent anticancer effects of 159Gd-DTPA-BMA complex. *J Radioanal Nucl Chem*., v. 295, n. 1, p. 63-66, 2013.

SZOKA JR, F.; PAPAHADJOPOULOS, D. Procedure for preparation of liposomes with large internal aqueous space and high capture by reverse-phase evaporation. *Proc. Natl. Acad. Sci.*, v. 75, n. 9, p. 4194-4198, 1978.

SZOKA, F.; PAPAHADJOPOULOS, D. Comparative properties and methods of preparation of lipid vesicles (liposomes). *Annu. Rev. Biophys. Bioeng.*, v. 9, p. 467-508, 1980.

TA, T.; PORTER, T. M. Thermosensitive liposomes for localized delivery and triggered release of chemotherapy. *J. Control. Release,* v.169, p. 112-125, 2013.

TELGMANN, L; SPERLING, M.; KARST, U. Determination of gadolinium-base MRI contrast agents in biological and environmental samples: A review. *Anal Chim. Acta*, v. 764, p. 1-16, 2013.

THERMOSOME. Heating technologies. Various medical devices from different manufacturers are usable for triggering of Thermosomes in clinical applications. Disponível em: <http://www.thermosome.com/heating-technologies/>. Acesso em: 09 de abril de 2019.

TORCHILIN, V. P.; OMELYANENKO, V. G.; PAPISOV, M. I.; BOGDANOV, A. A. JR.; TRUBETSKOY, V. S.; HERRON, J. N.; GENTRY, C. A. Poly(ethyleneglycol) on the liposome surface: on the mechanism of polymer-coated liposome longevity. *Biochim. Biophys. Acta*, v. 1195, p. 11-20, 1994.

ULRICH, A. S. Biophysical aspects of using liposomes as delivery vehicles. *Biosci.Rep.*, v. 22, p. 129-150, 2002.

US NATIONAL LIBRARY OF MEDICINE. *Clinical Trials*. Disponível em: <http://www.clinicaltrials.gov>. Acesso em: 09 de abril de 2019.

VEMURI, S.; RHODES, C. T. Preparation and characterization of liposomes as therapeutic delivery systems: a review. *Pharm. Acta Helv.*, v. 70, n. 2, p. 95-111, 1995.

WHO – World Health Organization. 2018. Disponível em: < https://www.who.int/en/news-room/fact-sheets/detail/cancer>. Acesso em: 09 de abril de 2019.

YATVIN, M. B.; WEINSTEIN, J. N.; DENNIS, W. H.; BLUMENTHAL, R. Design of liposomes for enhanced local release of drugs by hyperthermia. *Science*, v. 202, p. 1290-1293, 1978.

ZUGAZAGOITIA, J.; GUEDES, C.; PONCE, S.; FERRER, I.; MOLINA-PINELO, S; PAZ-ARES, L. Current Challenges in Cancer Treatment. *Clin Ther.*, v. 38, n. 7, p. 1551-1566, 2016.

ANEXO A

Artigo científico publicado (requisito parcial para obtenção do grau de Doutora)

http://dx.doi.org/10.21577/0103-5053.20180120

J. Braz. Chem. Soc., Vol. 29, No. 11, 2426-2440, 2018
Printed in Brazil - ©2018 Sociedade Brasileira de Química

Article

Chemometric-Assisted Hydrophilic Interaction Chromatographic Method for the Determination of Gadolinium-Based Magnetic Resonance Imaging Contrast Agent in Liposomes

Ana Luiza C. Maia,[a] Pedro Henrique R. da Silva,[a] Christian Fernandes,[a] Aline T. M. e Silva,[a] André Luís B. de Barros,[b] Daniel Cristian F. Soares[a,c] and Gilson A. Ramaldes[a]*

[a]*Departamento de Produtos Farmacêuticos, Faculdade de Farmácia, Universidade Federal de Minas Gerais, 31270-901 Belo Horizonte-MG, Brazil*

[b]*Departamento de Análises Clínicas e Toxicológicas, Faculdade de Farmácia, Universidade Federal de Minas Gerais, 31270-901 Belo Horizonte-MG, Brazil*

[c]*Laboratório de Bioengenharia, Universidade Federal de Itajubá, Campus Itabira, 35903-087 Itabira-MG, Brazil*

Gadodiamide (Gd-DTPA-BMA) is a gadolinium (Gd) chelate composed of two carboxylate groups of diethylenetriaminepentaacetic acid (DTPA) and two amide groups (BMA). Gd complexes are the most widely used contrast agents in nuclear magnetic resonance. Furthermore, our research group has demonstrated the potential of liposomes containing Gd-DTPA-BMA for cancer therapy. The aim of this study was to develop and validate a chemometric-assisted method by hydrophilic interaction liquid chromatography (HILIC) for determination of Gd-DTPA-BMA in liposomes. The chromatographic conditions obtained were: Sequant® ZIC®-HILIC Merck (150 × 4.6 mm, 3.5 µm, 100 Å) column, mobile phase composed of 5 mmol L^{-1} ACN/NH_4FA, pH 4.5 (60:40 v/v) at 0.6 mL min^{-1}, injection volume of 20 µL, temperature of 30 °C, and detection at 210 nm. The linear range was of 40 to 120 nmol mL^{-1}. The use of chemometrics allowed obtaining optimal chromatographic parameters, in terms of signal-to-noise ratio, resolution, and asymmetry.

Keywords: gadodiamide, liposomes, hydrophilic interaction chromatography, chemometrics, Box-Behnken

Introduction

Gadodiamide (Gd-DTPA-BMA, Figure 1), a gadolinium (Gd) complex, is one of the most commonly used contrast agent in diagnosis by imaging, due to its low chemotoxicity. In addition, several studies have reported that there is no evidence of endogenous transmetalation or *in vivo* metabolism of this complex. Despite this, its administration is contraindicated in patients presenting chronic renal failure due to the risk of developing nephrogenic systemic fibrosis.[1-3] Recently, the European Medicines Agency (EMA)[4] confirmed a review that found that Gd deposition can occur in brain tissues after the use of Gd contrast agents. Until the present date, there is no evidence that Gd deposition in the brain has caused any harm to patients. In order to prevent any risks that could potentially occur, EMA[4] has recommended restrictions and suspensions for use of some intravenous linear agents containing Gd. Several studies have reported the encapsulation of Gd-DTPA-BMA and other Gd complexes in liposomes for diagnostic purposes.[5-7] The antitumor activity of this complex in the liposomal form is also being investigated, since Gd-DTPA-BMA induces the apoptosis of neoplastic cells through the activation of caspase-3.[3,8-12] In this context, thermosensitive liposomes constitute promising nanocarriers since they may contribute to increase the treatment efficacy due to the association with hyperthermia techniques.[13]

The determination of Gd-DTPA-BMA in environmental and biological samples has been performed most often by expensive techniques requiring complex instrumentation, such as inductively coupled plasma optical emission spectrometry and high performance liquid chromatography coupled to mass spectrometry (LC-MS).[14-17] The Gd-DTPA-BMA quantification

*e-mail: soares@unifei.edu.br

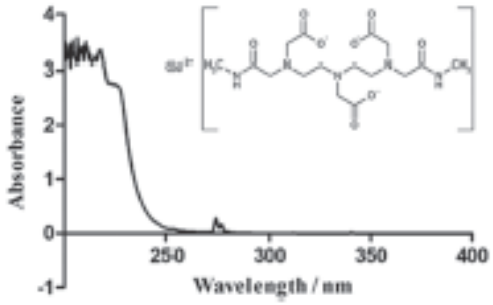

Figure 1. Structure and spectrum in the ultraviolet region of Gd-DTPA-BMA at 57 mg mL^{-1} in purified water.

method described in the United States Pharmacopeia[18] employs LC with post-column derivatization to enable the detection of the complex in the region of the visible spectrum. However, derivatization generally requires special instrumentation and high reagent consumption. In addition, this additional step makes the analysis more time consuming.[2] The determination of Gd-DTPA-BMA by LC using radioactivity detectors has also been described.[17,18] In this case, the main disadvantage is related to the requirement of prior radiolabeling of the complex. In this context, the development of simpler, faster and low cost methods for determination of Gd-DTPA-BMA is extremely useful, mainly for determination of this complex in liposomal formulations. The development of liposomes can be laborious and consists of several stages. Thus, rapid information about the influence of changes in the formulation or in the preparation method on the amount of drug entrapment is required. Our group recently developed methods for quantification of Gd-DTPA-BMA by reverse phase liquid chromatography (RP-LC) and derivative spectrophotometry. In both methods, detection was performed in the ultraviolet region.[2] The spectrophotometric method presented low detectability, while retention of Gd-DTPA-BMA in RP-LC was challenging due to its high polarity. Moreover, RP-LC method is not appropriate for determination of this drug in more complex matrices, such as serum, plasma, culture medium or buffers fortified with blood proteins. In these cases, RP-LC does not present adequate resolution. In addition, due to the impossibility to use any organic solvent in the mobile phase, optimization is limited.

Hydrophilic interaction liquid chromatography (HILIC) has been the technique of choice for the determination of polar compounds, especially metallic complexes.[20] The increased use of HILIC may be related to its ability to resolve limitations of conventional chromatography. An example is the analysis of polar substances that present low retention in RP-LC.[21] In HILIC, several chromatographic parameters can interfere in the retention and separation of the compounds. For this reason, the use of chemometric tools during the development of analytical methods is a useful approach.[21,22] Recently, chemometrics have gained importance in the development of chromatographic methods, as can be observed in the scientific literature.[23,24]

Some methods for Gd-DTPA-BMA determination in biological and environmental samples by HILIC are described in the literature.[20,25-28] However, none of these studies reported the determination of Gd-DTPA-BMA in liposomes, making necessary further investigations. Moreover, few data are presented in these studies concerning method optimization. In addition, to our knowledge, no studies have been reported on the development of method for determination of Gd-DTPA-BMA by HILIC, in which a rational approach has been used.

In this context, the aim of this study was to develop and validate an analytical method for the determination of Gd-DTPA-BMA in liposomes by HILIC. For this, Box-Behnken factorial planning and response surface methodology were used during the method development. The method was validated according to the Brazilian legislation[30] and the ICH validation guidelines for analytical procedures Q2(R1)[31] and applied for determination of Gd-DTPA-BMA entrapment in liposomes.

Experimental

Materials

Gd-DTPA-BMA (Omniscan®, General Electric Healthcare Company, Ireland) was purchased from HDL Logística Hospitalar (Uberlândia, Brazil), batch 12,747,449, content of 99.7%. Dipalmitoylphosphatidylcholine (DPPC), distearoylphosphatidylcholine (DSPC), and distearoylphosphatidylethanolamine-polyethyleneglycol$_{2000}$ (DSP-PEG$_{2000}$) were purchased from Lipoid GmbH (Ludwigshafen, Germany). Monostearoylphosphatidylcholine (MSPC) was purchased from Avanti Lipids (Alabama, USA). HEPES (4-(2-hydroxyethyl)-1-piperazine-ethanesulfonic acid) was purchased from Sigma Chemical Company (St. Louis, USA). Acetonitrile (ACN) HPLC grade was purchased from Tedia Brazil (Rio de Janeiro, Brazil) and from J.T.Baker (Pennsylvania, USA). Hydrochloric acid and chloroform were purchased from LabSynth (São Paulo, Brazil). Diethyl ether, and isopropyl alcohol HPLC grade were purchased from Vetec (Rio de Janeiro, Brazil). The water used to prepare all the solutions and samples was purified on a Milli-Q® Direct-Q3 Millipore system (Billerica, USA). Ammonium

acetate (NH_4Ac) was purchased from Neon (São Paulo, Brazil). Ammonium formate (NH_4FA) was purchased from Spectrum (São Paulo, Brazil) and from Vetec (Rio de Janeiro, Brazil).

Chromatographic conditions

HILIC was performed using a 1260 series chromatograph (Agilent Technologies, California, USA), equipped with a degasser, a quaternary pump (G1311B), a column oven (G1316A), an autosampler (G1329B), and a diode array detector (DAD) (G4212B), coupled to the EzChrom integration program. The chromatographic conditions of the developed method were: Sequant® ZIC®-HILIC Merck (150 × 4.6 mm, 3.5 µm, 100 Å) column (Darmstadt, Germany), mobile phase composed of 5 mmol L^{-1} ACN/NH_4FA, pH 4.5 (60:40 v/v) isocratically eluted at a flow-rate of 0.6 mL min^{-1}, injection volume of 20 µL, temperature of 30 °C, and detection at 210 nm.

Preparation of liposomes

Thermosensitive formulations containing Gd-DTPA-BMA were prepared by reverse-phase evaporation method using the procedure described in a previous study by our research group.[3,32] The total lipid concentration for the two liposomes was 40 mmol L^{-1}. The composition of each formulation was chosen based on the studies of Li *et al.*[33] For the preparation of the traditional thermosensitive liposome (TTSL-Gd), chloroform aliquots of DPPC, DSPC, and DSPE-PEG_{2000}, in a lipid molar ratio of 80:15:5, were transferred to a round-bottomed flask and subjected to solvent evaporation under reduced pressure. The thermosensitive liposome containing lysophospholipid (LTSL-Gd) was prepared from chloroform aliquots of DPPC, MSPC, and DSPE-PEG_{2000}, in lipid molar ratio of 85:10:5. The lipid film obtained in both cases was dissolved in diethyl ether, previously treated with a solution of 10 mmol L^{-1} HEPES buffer. After complete dissolution of the lipids, an aqueous solution of Gd-DTPA-BMA (250 µmol mL^{-1}) was added, maintaining the aqueous:organic phase ratio at 1:3. Then, the dispersion obtained was subjected to vigorous vortexing at 3,000 rpm for 5 min, producing a water in oil (W/O) emulsion. Subsequently, the W/O emulsion was subjected to evaporation under reduced pressure to remove the organic solvent, enabling the formation of lipid vesicles. Then, the obtained liposomes were calibrated employing 10 cycles of extrusion on polycarbonate membranes of 0.4, 0.2, and 0.1 µm pore sizes, under nitrogen pressure, at 55 °C. Non-entrapped Gd-DTPA-BMA was separated from liposomes by ultracentrifugation at 350,000 × g, at 4 °C for 2 h. After ultracentrifugation, the pellet was reconstituted in HEPES buffer to obtain the same initial volume. To obtain the traditional thermosensitive liposomes (TTSL) and thermosensitive liposome containing lysophospholipid (LTSL) without Gd-DTPA-BMA, the same experimental protocol was performed, except for the step of addition of the drug, which was replaced by the addition of HEPES buffer.

HILIC method development

Initially, a review of the literature was carried out to determine the critical independent variables for the development of methods for determination of Gd-DTPA-BMA by HILIC. To determine the detection wavelength, the UV spectrum in the range of 200 to 400 nm of a Gd-DTPA-BMA sample at 57 mg mL^{-1} was obtained. The analyses were performed using a Shimadzu 1800 series UV-Vis spectrophotometer (Tokyo, Japan). Then, 11 experiments were performed as described in Table 1 to investigate the range of variation and levels at which independent variables should be evaluated in a factorial design. In each experiment, nine determinations were performed, being three determinations on a sample of Gd-DTPA-BMA at 0.5 µmol mL^{-1}, three determinations on a sample of TTSL spiked with Gd-DTPA-BMA at 0.5 µmol mL^{-1} and three determinations on a sample of LTSL spiked with Gd-DTPA-BMA at 0.5 µmol mL^{-1}.

The optimization of the chromatographic parameters was performed using Box-Behnken factorial design and response surface methodology.[34] Three independent variables at three levels (−1, 0 and 1) were evaluated: X_1 = buffer pH, level −1 = 3.7, level 0 = 4.2 and level +1 = 4.7; X_2 = ACN ratio in the mobile phase (in percentage), level −1 = 60, level 0 = 65, level +1 = 70; X_3 = buffer concentration (mmol L^{-1}), level −1 = 5, level 0 = 15, level +1 = 25. The dependent variables evaluated as responses were: signal-to-noise ratio, resolution (R_s), and asymmetry (A_s). Fifteen experiments were performed in random order, including three replicates of the central point. Six determinations were performed in each experiment, being three determinations on a sample of Gd-DTPA-BMA at 0.3 µmol mL^{-1} and three determinations on a sample of TTSL and LTSL spiked with Gd-DTPA-BMA at 0.3 µmol mL^{-1}. The coefficients of determination (r^2) and correlation (r) were obtained using the least squares method. The model was evaluated using analysis of variance (ANOVA) and the estimation of the errors was calculated by means of experiments at the central point. The results were evaluated using the software Statistica 7.0.[35]

In order to determine the linear velocity in which the height equivalent to a theoretical plate (H) is minimal, a Van

Table 1. Variables screening for development of method for determination of Gd-DTPA-BMA in liposomes by HILIC

Experiment	Parameter evaluated	Independent variable	Mobile phase composition
1	type of buffer	NH_4Ac	ACN/NH_4Ac 10 mmol L^{-1}, pH 5.8, 70:30 v/v
2		NH_4FA	ACN/NH_4FA 10 mmol L^{-1}, pH 4.7, 70:30 v/v
3	ACN ratio	60%	ACN/NH_4FA 10 mmol L^{-1}, pH 4.7, 60:40 v/v
4		70%	ACN/NH_4FA 10 mmol L^{-1}, pH 4.7, 70:30 v/v
5		75%	ACN/NH_4FA 10 mmol L^{-1}, pH 4.7, 75:25 v/v
6	buffer concentration	5 mmol L^{-1}	ACN/NH_4FA 5 mmol L^{-1}, pH 4.7, 70:30 v/v
7		10 mmol L^{-1}	ACN/NH_4FA 10 mmol L^{-1}, pH 4.7, 70:30 v/v
8		15 mmol L^{-1}	ACN/NH_4FA 15 mmol L^{-1}, pH 4.7, 70:30 v/v
9	the aqueous phase pH of the mobile phase	2.7	ACN/NH_4FA 10 mmol L^{-1}, pH 2.7, 70:30 v/v
10		3.7	ACN/NH_4FA 10 mmol L^{-1}, pH 3.7, 70:30 v/v
11		4.7	ACN/NH_4FA 10 mmol L^{-1}, pH 4.7, 70:30 v/v

Deemter curve was constructed.[36] For this, mobile phase flow-rate was varied as follows: 0.04; 0.06; 0.08; 0.1; 0.2; 0.3; 0.4; 0.5; 0.6; 0.7; 0.8; 0.9; 1.0; 1.5 and 2.0 mL min^{-1}. For each flow-rate its correspondent number of theoretical plates (N) and retention time (t_g) were obtained. The curve was obtained by plotting the H as a function of the linear velocity of the mobile phase (U_g).

Method validation

Selectivity was demonstrated by the separation of Gd-DTPA-BMA from all potentially interfering compounds, with adequate resolution. Gd-DTPA-BMA chromatograms in the lower concentration of analytical curve (40 nmol mL^{-1}) and those from mobile phase, isopropyl alcohol, TTSL/LTSL, and fetal bovine serum were overlapped to demonstrate the absence of interfering peaks in the same t_g of Gd-DTPA-BMA. The fetal bovine serum was previously ultrafiltered in a centrifugal filter device (Amicon® Ultra-4 10 kDa MWCO, Millipore, Billerica, USA) by centrifugation at 14,000 × g for 20 min. All samples were prepared using mobile phase as solvent. The liposomes were previously solubilized in isopropyl alcohol at the ratio of 1:10 for complete disruption of the vesicles. Peak purity was also evaluated.[30,31]

Five concentration levels were used, in triplicate, to determine linearity. The linear range evaluated was 50 to 150% of the working concentration (80 nmol mL^{-1}), which corresponds to the concentrations of 40, 60, 80, 100, and 120 nmol mL^{-1}. The peak areas were used to construct the analytical curve. Linear regression was verified by the least squares method using GraphPad Prism 5.0 software program.[37] The coefficients r and r^2 were evaluated.

The limits of detection (LOD) and quantification (LOQ) were initially determined by evaluating the signal-to-noise ratio. For this, Gd-DTPA-BMA solutions were prepared, using mobile phase as solvent, in decreasing concentrations in the range of 50 to 0.05 nmol mL^{-1}. LOD and LOQ were defined as the concentrations for which signal-to-noise ratios of 3:1 and 10:1, respectively, were obtained. After determination of linearity, LOD and LOQ were also calculated based on the standard deviation (SD) of the y-intercept when $x = 0$ and the slope of the calibration curve of Gd-DTPA-BMA.[38]

Intra-day precision was evaluated by means of nine determinations, being three concentrations (50, 100 and 150% of the working concentration) in triplicate, corresponding to the concentrations of 40, 80 and 120 nmol mL^{-1}. To determine inter-days precision, the same procedure was performed on alternate days. The relative standard deviation (RSD) of the determinations was calculated.

The accuracy was determined by quantification of Gd-DTPA-BMA in the presence of the components of the formulations. TTSL and LTSL, without the drug, were spiked with Gd-DTPA-BMA at 40, 80 and 120 nmol mL^{-1}. Samples were prepared in triplicate and the results were expressed as percentage recovery of the drug added to the placebo.

The robustness was evaluated by means of the Youden test by deliberately modifying seven conditions of the chromatographic method: ACN ratio in the mobile phase, mobile phase aqueous component pH, buffer concentration, column temperature, flow-rate, ACN brand, and buffer brand.[38] The levels of the modified variables as well as the factorial combination of the experimental planning are described in Table 2. The seven parameters and their respective modifications were combined in eight experiments that were performed in random order. Six determinations were performed in each condition, being three determinations on a sample of Gd-DTPA-BMA at 80 nmol mL^{-1}, and three determinations on a sample

Table 2. Experimental planning for robustness assessment by means of Youden test

Analytical parameter	Condition		Factorial combination							
	Nominal	Varied	1	2	3	4	5	6	7	8
ACN ratio in the mobile phase / %	60 (A)	63 (a)	A	A	A	A	a	a	a	a
The aqueous phase pH of the mobile phase	4.5 (B)	4.7 (b)	B	B	b	b	B	B	b	b
Buffer concentration / (mmol L^{-1})	5 (C)	5.5 (c)	C	c	C	c	C	c	C	c
Column temperature / °C	30 (D)	33 (d)	D	D	d	d	d	d	D	D
Flow-rate / (mL min^{-1})	0.6 (E)	0.7 (e)	E	e	E	e	e	E	e	E
ACN brand	Tedia (F)	J.T. Baker (f)	F	f	f	F	F	f	f	F
Buffer brand	Vetec (G)	Spectrum (g)	G	g	g	G	g	G	G	g

of TTSL and LTSL spiked with Gd-DTPA-BMA at 80 nmol mL^{-1}.

Results and Discussion

HILIC method development

In general, the stationary phase and the mobile phase are the most important factors for the development of analytical methods by HILIC.[21,22] In the present study, a SeQuant® ZIC®-HILIC (150 × 4.6 mm, 3.5 µm, 100 Å) column was used. This column was chosen based on the chemical structure and some physical-chemical properties of Gd-DTPA-BMA. ZIC®-HILIC, which contains a sulfobetaine binder, is indicated for the analysis of ionic and non-ionic polar compounds.[21,40] Gd-DTPA-BMA is a non-ionic complex, relatively stable due to its log Ks (logarithm of the complex stability constant) value equal to 16.85.[1] The absence of charges in the complex suggests that the hydrophilic partition is probably the main retention mechanism. The sulfobetaine binder adsorbs a large amount of water on the surface of the stationary phase through hydrogen bonding.[21,40] Thus, Gd-DTPA-BMA will possibly exhibit higher affinity for the stationary phase compared to affinity for the solvent-rich mobile phase. Gd-DTPA-BMA is freely soluble in water and has a log P (logarithm of octanol / water partition coefficient) of −2.13.[41,42] These characteristics support the hypothesis of the hydrophilic partition retention mechanism.

A typical mobile phase employed in HILIC is composed of an organic portion (water miscible polar solvent) in a ratio equal to or higher than 60% and an aqueous portion containing or not some type of buffer in a ratio equal to or higher than 2%.[21,43] ACN and methanol are the most commonly used organic solvents in HILIC. In the present study, ACN was selected since the use of a protic solvent, such as methanol, could drastically reduce the retention of Gd-DTPA-BMA. In this case, the use of a higher amount of solvent would be necessary to obtain the same retention provided by an aprotic solvent.[22,44] Buffers are employed in HILIC if the control of the mobile phase pH is required and when peak asymmetry can be a problem.[22] Commonly, the determination of Gd-DTPA-BMA by RP-LC reveals tailing peaks and high value of A_s.[17,45,46] Therefore, pH control of the mobile phase using buffers was used in the proposed method. The buffers usually used in HILIC are NH_4Ac and NH_4FA, due to the high solubility in organic solvents, even in high concentrations, and due to the volatility they present, being compatible with MS detectors.[21] Although they exhibit similar characteristics, the use of NH_4Ac or NH_4FA may result in different elution profiles.[47,48] For this reason, both buffers were investigated at this initial screening.

To determine the detection wavelength, the UV spectrum in the range of 200 to 400 nm of a Gd-DTPA-BMA sample at 57 mg mL^{-1} was obtained. Due to the lack of extended chromophores in its structure, Gd-DTPA-BMA showed maximum absorption at 210 nm (Figure 1).

After choosing the stationary phase type (ZIC®-HILIC), the organic solvent (ACN), the possible buffers (NH_4Ac and NH_4FA), the detection wavelength (210 nm), the temperature (30 °C), and the injection volume (20 µL), 11 experiments were carried out, in order to define the variables and range of variation to be evaluated in a later factorial design. The results of this step are showed in Table S1 (Supplementary Information (SI) section).

The use of NH_4FA (pH = 4.7) resulted in a signal-to-noise ratio about three times higher than that obtained with NH_4Ac (pH = 5.8), leading to higher detectability. A higher value of N is another advantage observed with the use of NH_4FA. The R_s between Gd-DTPA-BMA and liposomes peaks, obtained with NH_4FA (R_s = 6.9), under the conditions evaluated, was lower than that obtained with NH_4Ac (R_s = 11.8); however, it was adequate ($R_s \geq 2$) according to the validation guides.[49-51] For these reasons, NH_4FA buffer was selected to compose the mobile phase and to be used in the following experiments.

The range selected for evaluation of the percentage of ACN, based on the results of Table S1 (SI section), was between 60 and 70%. The minimum level of 60% was selected because in this condition t_R was appropriate (t_R = 4.3 min) and the value of retention factor (k) obtained (k = 1.7) is within the recommended range 0.5 < k < 20.[31] The maximum level of 70% was also chosen based on t_R and k values obtained (t_R = 8.6 min, k = 4.4). Ratios of ACN above 70% were not considered, since the t_R of Gd-DTPA-BMA becomes very long.

The concentration of NH_4FA buffer was evaluated in the experiments 6, 7, and 8 (Table 1). The range of variation chosen for evaluation in a factorial design was between 5 and 25 mmol L^{-1}. The minimum level of 5 mmol L^{-1} was selected because it is the minimum concentration necessary to obtain symmetrical peaks.[21] The maximum level of 25 mmol L^{-1}, although not tested experimentally, was selected because it is described in the literature as the limit concentration in which there is no probability of precipitation in contact with ACN.[32]

Experiments 9, 10, and 11 were performed to evaluate the mobile phase aqueous component pH (Table 1). The entire NH_4FA buffering range was investigated. Based on the results (Table S1, SI section), pH values between 3.7 and 4.7 were chosen for evaluation in a factorial design. The minimum level of 3.7 was selected, since it corresponded to the lowest pH value in which Gd-DTPA-BMA remained stable. When using pH 2.7, it was not possible to calculate most of the dependent variables expressed in Table S1 (SI section), due to the deformation of the chromatographic peak corresponding to the drug. The maximum level of 4.7 was selected because, in this condition, satisfactory results were obtained. In addition, this value corresponds to the maximum pH of the NH_4FA buffering range.

The variables chosen to compose the factorial planning, based on the initial screening, were: mobile phase aqueous component pH (X_1), ACN ratio (X_2), and buffer concentration (X_3). The other chromatographic conditions were fixed: SeQuant® ZIC®-HILIC (150 × 4.6 mm, 3.5 µm, 100 Å) column, isocratic elution at 1.0 mL. min^{-1}, injection volume of 20 µL, temperature of 30 °C, and detection at 210 nm. The responses chosen to evaluate the efficiency of the method were: signal-to-noise ratio, R_s, and A_s. These dependent variables were selected based on the application of the proposed method. The experimental conditions evaluated, and the responses obtained are presented in Table 3.

The obtained signal-to-noise ratios showed high variation between the experiments (minimum 1645031 and maximum 9622069). With respect to R_s, experiments 3,

Table 3. Results from Box-Behnken experimental design used for optimization of the HILIC method

Independent variable				Level		
				–1	0	1
X_1	pH			3.7	4.2	4.7
X_2	ACN ratio / %			60	65	70
X_3	buffer concentration / (mmol L^{-1})			5	15	25

Experiment	Contrast			Experimental condition			Dependent variable[a]		
	X_1	X_2	X_3	X_1	X_2	X_3	Signal-to-noise ratio	R_s	A_s
1	1	1	0	4.7	70	15	7164899	7.7	1.32
2	1	–1	0	4.7	60	15	7846412	3.7	1.18
3	–1	1	0	3.7	70	15	4029493	1.3	1.31
4	–1	–1	0	3.7	60	15	6040335	0.0	1.21
5	1	0	1	4.7	65	25	1675031	5.1	1.31
6	1	0	–1	4.7	65	5	9622069	5.5	1.25
7	–1	0	1	3.7	65	25	6731611	0.0	1.27
8	–1	0	–1	3.7	65	5	7473207	4.0	1.25
9	0	1	1	4.2	70	25	2324785	7.2	1.30
10	0	1	–1	4.2	70	5	5124660	7.2	1.33
11	0	–1	1	4.2	60	25	3487648	2.7	1.23
12	0	–1	–1	4.2	60	5	6514122	3.5	1.19
13[c]	0	0	0	4.2	65	15	2293381	3.7	1.27

[a]Values are expressed as mean of 3 injections; [b]values are expressed as mean (n = 3 samples, being 3 injections for each sample); [c]central point. R_s: resolution; A_s: asymmetry.

4, and 7 (Table 3) generated results lower than the recommended value, which should be ≥ 2.[49-51] These data suggest that the combination of low pH (3.7) and intermediate (15 mmol L^{-1}) or high (25 mmol L^{-1}) buffer concentration in the mobile phase composition should be avoided, as they may result in inadequate R_s between the Gd-DTPA-BMA peak and the liposome peak. In terms of A_s, the observed results presented low variation (minimum 1.18 and maximum 1.33).

In order to extrapolate the data obtained by the Box-Behnken matrix and calculate the optimal point for the variables X_1, X_2 and X_3, the data presented in Table 3 were used to construct mathematical models. By combining the values of the variables and the responses obtained, the coefficients of the equations which describe the studied system were calculated (Table S2, SI section). These equations were elaborated from the effects of the primary linear and quadratic interactions. Secondary interactions were excluded because they generated experimentally incoherent optimal points. The ANOVA, r, r^2 and pure error data calculated from the central point replicates are described in Table S2 (SI section). The value of r^2 obtained (close to 1) was satisfactory.[53] In addition, the residuals showed random behavior, without tendencies, confirming the fit of the calculated model (Figure S1, SI section). The response surfaces obtained are shown in Figures 2, 3, and 4. The independent variables were grouped two by two to evaluate the influence of the interaction between them, in the responses signal-to-noise ratio, R_s, and A_s. In the Figures 2, 3, and 4, the graphs a-c were obtained employing constant buffer concentration. In the graphs d-f the fixed parameter was the ACN ratio. The g-i graphs were prepared by maintaining the values of the mobile phase aqueous component pH constant. The fixed value of each of these variables is indicated in parentheses above the respective graph.

For signal-to-noise ratio evaluation, shown in Figure 2, it can be seen from the scale of the graphs 2a-2c that the lower the concentration of the buffer, the higher the response. According to graph 2a, higher values of signal-to-noise ratio are obtained when using pH ≥ 4.4, regardless of the ACN ratio used. The results showed in the graphs 2d-2f are in agreement with these observations. The values of the scales of the graphs 2g-2i, demonstrate that the highest responses are obtained when the highest pH of the buffering range of NH_4FA was used (graph 2i). According to graph 2i, regardless of the ACN ratio, the highest signal-to-noise ratio was observed when the buffer concentration was 10 mmol L^{-1} or less. From the analysis of the nine response surfaces presented in Figure 2, mobile phase aqueous component pH (values ranging from 4.4 to 4.7) and the buffer concentration (≤ 10 mmol L^{-1}) are the factors that most influence the signal-to-noise ratio.

The results of R_s are presented in Figure 3. According to graphs 3a-3c, when the lowest concentration of buffer was employed (graph 3a), any combination of pH and ACN ratio results in $R_s \geq 2$. The results showed in the graphs 3d-3f confirm these observations, and show that high pH values produced higher values of R_s. Analyzing the scales of the graphs 3g-3i, the benefit of using high pH was confirmed, since the highest responses were found when pH was fixed at 4.7 (graph 3i). In general, the analysis of the nine response surfaces of Figure 3 shows that higher R_s values were obtained when the following conditions were combined: low buffer concentration, high pH, and high ACN ratio.

The response surfaces presented in Figure 4 were used to evaluate A_s. Analysis of graphs 4a-4c reveals that lower A_s values were obtained when lower buffer concentrations were employed. According to graph 4a, the combination of low ACN ratio and high pH value results in lower A_s values. The analysis of graphs 4d-4f confirms this observation. According to graph 4d, there was a tendency to obtain lower values of A_s when the buffer concentration is ≤ 6 mmol L^{-1} and the pH is ≥ 4.4. In the graphs 4g-4i, regardless of the pH employed, the combination between low ACN ratio and low buffer concentration results in low A_s values.

The results of the response surface methodology are in agreement with the data obtained in the Pareto charts (data not shown). Peak height, baseline noise, N, peak width measured at 5% of the peak height, peak area, t_R and k were also evaluated as responses. From the results of these analyses, showed in Table S3 (SI section), and from their respective response surface (data not shown), it was possible to identify the optimized conditions, considering the individual desirability of each parameter and the global desirability for the proposed method.

In order to verify if the defined optimal conditions result in optimum response values for the Gd-DTPA-BMA chromatographic peak, a new experiment was performed using mobile phase composed of 60% ACN, NH_4FA at 5 mmol L^{-1} and mobile phase aqueous component pH of 4.5. Six determinations were performed in each experiment, being three determinations on a sample of Gd-DTPA-BMA at 0.3 μmol mL^{-1} and three determinations on a sample of TTSL and LTSL spiked with Gd-DTPA-BMA at 0.3 μmol mL^{-1}. Under these conditions, the signal-to-noise ratio obtained was 9594265. This result is in agreement with the highest signal-to-noise ratio found in the Box-Behnken planning experiments (experiment 6, Table 3). The value of R_s obtained using the optimized conditions was equal to 3.2. This result was considered

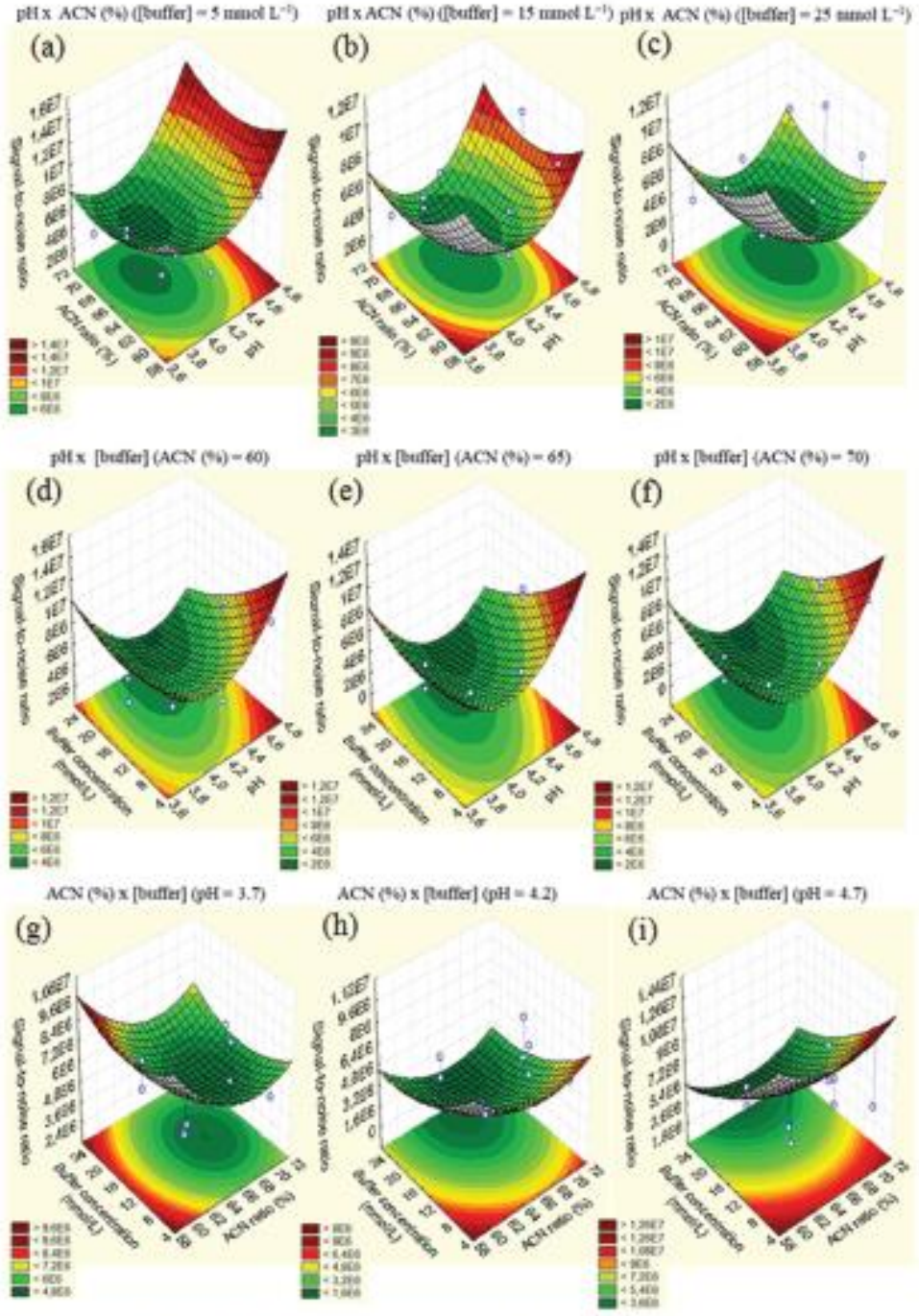

Figure 2. Response surfaces for evaluation of the dependent variable signal-to-noise ratio.

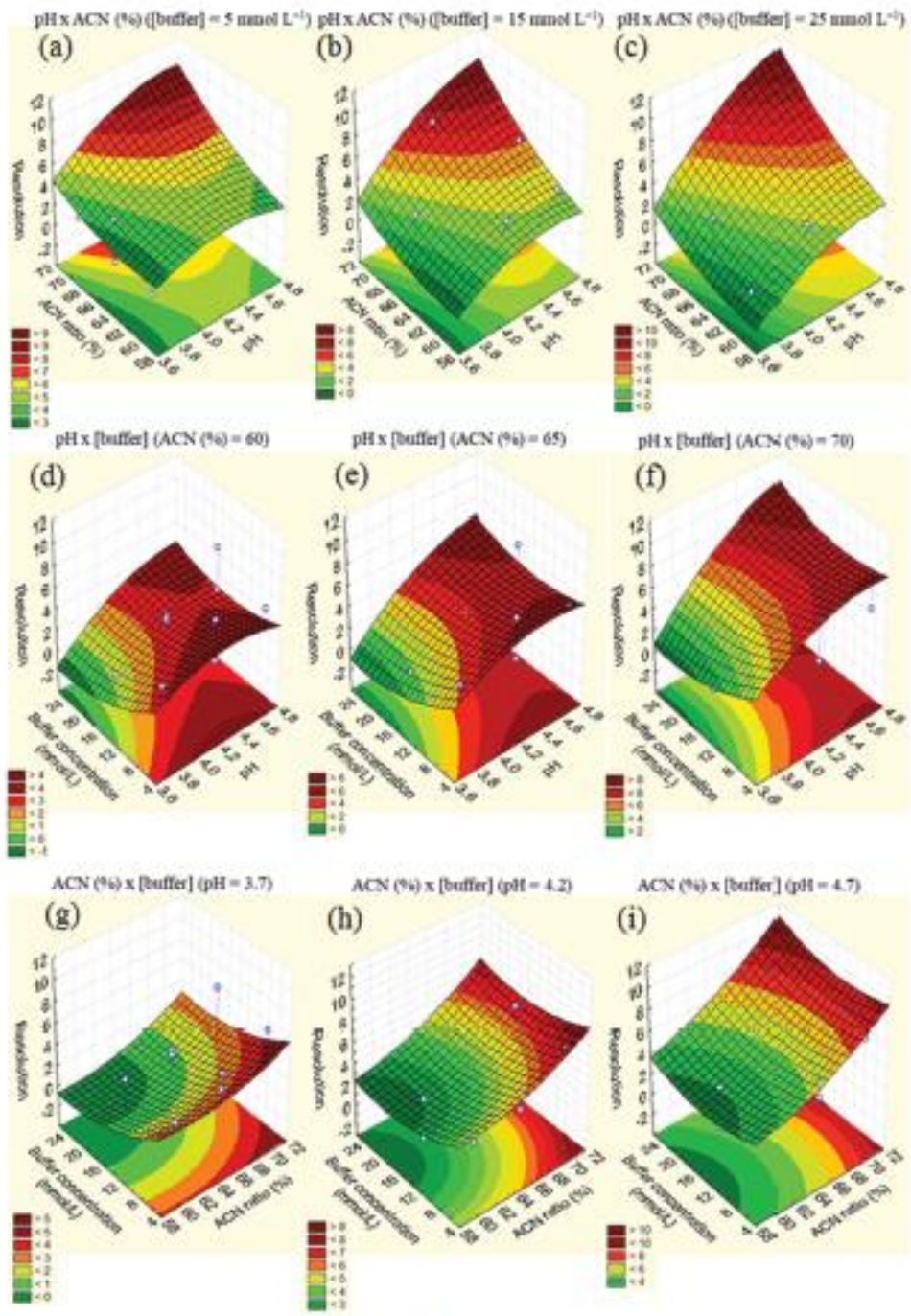

Figure 3. Response surfaces for evaluation of the dependent variable R_s.

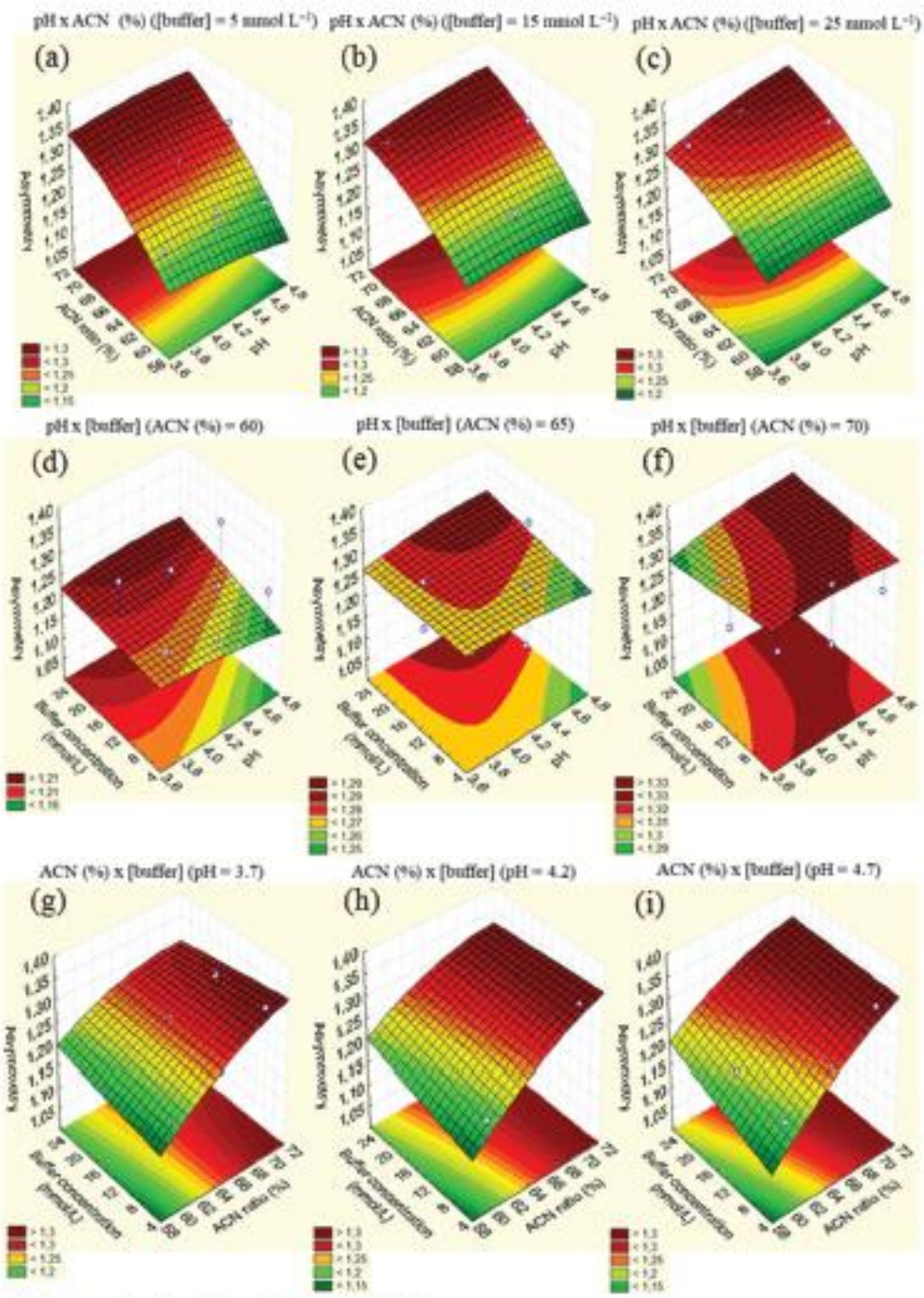

Figure 4. Response surfaces for evaluation of the dependent variable A_s.

adequate, since it is higher than the recommended value ($R_s \geq 2$) to obtain a satisfactory separation between the drug and the possible interferences.[49-51] The A_s obtained after optimization of the chromatographic parameters was 1.11. This value corresponds to the best response obtained for this parameter, considering all the experiments performed. In addition, it complies with the limits established by the FDA.[54]

The Van Deemter curve obtained to optimize the mobile phase flow-rate is shown in Figure 5. The maximum efficiency observed (H around 18 µm), using the optimized chromatographic conditions, was observed in U_0 close to 0.16 mm s^{-1}, corresponding to a flow of 0.1 mL min^{-1}. This flow-rate is not feasible to be used in the routine analyses, since it results in a very long t_R for Gd-DTPA-BMA (t_R = 44.15 min). Thus, the optimization of the mobile phase flow-rate was performed evaluating the parameters t_R, N, peak height and R_s (Table S4, SI section). Based on the results obtained, the flow-rate of 0.6 mL min^{-1} was selected for use in the developed method. When compared to the flow-rate of 1.0 mL min^{-1}, it resulted in a higher Gd-DTPA-BMA t_R (t_R = 7.1 min). However, this flow rate allowed increasing 29% efficiency (directly related to N) and 12% of detectability and R_s of the proposed method.

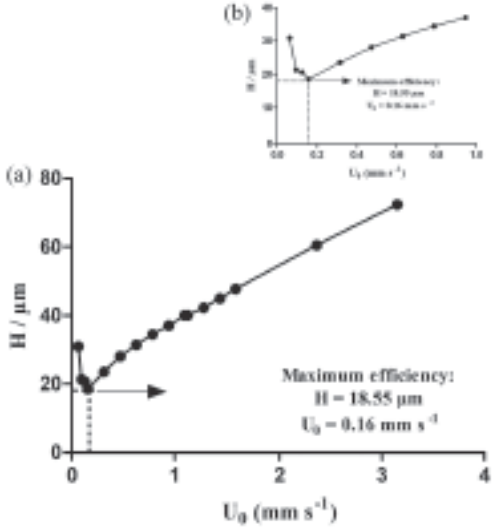

Figure 5. Van Deemter curve using the optimized chromatographic conditions of the developed method.

Method validation

Chromatograms of the formulations, without Gd-DTPA-BMA (TTSL/LTSL), isopropyl alcohol, fetal bovine serum, and mobile phase (Figure 6), showed no interfering peaks at the retention time of Gd-DTPA-BMA (t_R = 7.1 min), demonstrating the selectivity of the method. The resolution obtained between Gd-DTPA-BMA and TTSL/LTSL was adequate (R_s = 3.6). In addition, the purity of the Gd-DTPA-BMA peak, calculated by DAD, was equal to 100% in all determinations. Although the aim of this study is to determine Gd-DTPA-BMA in liposomes, the selectivity in a biological sample (fetal bovine serum) was evaluated to demonstrate that, if necessary, the developed method can be applied in more complex matrices.

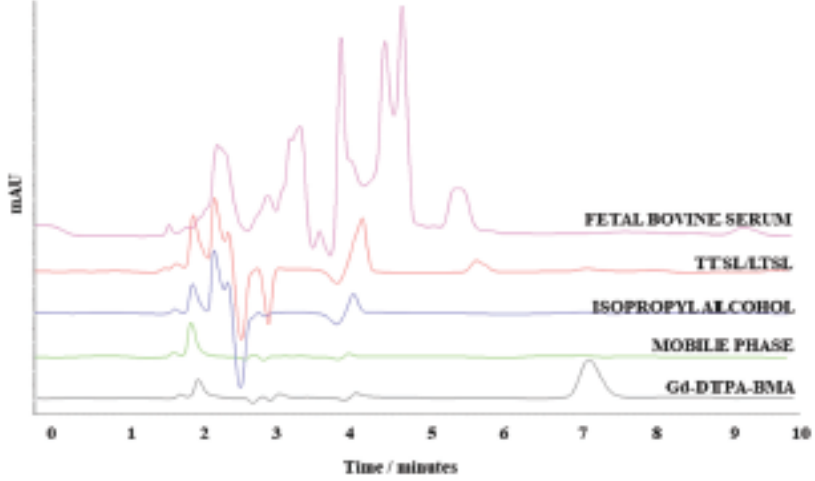

Figure 6. Representative chromatograms from the selectivity study: fetal bovine serum, TTSL/LTSL, isopropyl alcohol, mobile phase, and Gd-DTPA-BMA (40 mmol mL^{-1}).

The method showed to be linear in the range between 40 and 120 nmol L^{-1}. The equation of the calibration curve obtained was $y = 803100x + 964900$. The r and r^2 obtained were satisfactory (> 0.999).[30] There was no significant difference between the slopes of the three calibration curves obtained ($p < 0.05$).

The determination of LOD and LOQ of Gd-DTPA-BMA was performed initially by means of the evaluation of the signal-to-noise ratio in order to include LOQ as the lowest concentration level of the linear range of the analytical curve. After linearity evaluation, the theoretical values of LOD and LOQ, calculated based on the parameters of linear regression, were 4.56 and 6.78 nmol mL^{-1}, respectively.

From our knowledge, no studies dealing with Gd-DTPA-BMA determination by HILIC in liposomes have been reported in the literature until the present date. Moreover, no studies of determination of Gd-DTPA-BMA by HILIC with DAD detection were found. In contrast, some studies of determination of Gd-DTPA-BMA by HILIC using MS detection have already been described.[20,25-28] Despite the indisputable detectability provided by MS, the high cost of analysis and instrumentation justifies the development of simpler and less costly method. In a previous study by our research group,[2] an analytical method for the determination of Gd-DTPA-BMA by RP-LC/DAD was developed and validated. It showed to be linear in the range between 100 and 500 nmol mL^{-1}. At the present HILIC method, lower concentrations can be included in the analytical curve (40 to 120 nmol mL^{-1}). In addition, comparing the LOD and LOQ obtained in the two studies, one can conclude that the HILIC method showed detectability five-fold higher using the same type of detector (DAD).

The developed method demonstrated adequate precision (Table 4). The obtained RSD values for intra-day and inter-day precisions were satisfactory and in agreement with the specification established by RE 899,[30] which recommends RSD ≤ 5%.

The accuracy of the developed method was demonstrated (Table 4). The result for mean recovery was 98.61% for TTSL/LTSL formulations. In addition, the value of RSD between measurements did not exceed 5%.

The results of robustness were presented in Table 5. According to the obtained data, the method showed to be robust for all the evaluated parameters, since the effects of each variable were lower than the respective largest effect calculated.

Determination of Gd-DTPA-BMA entrapment and drug encapsulation percentage

The developed method was used to evaluate the Gd-DTPA-BMA content in TTSL-Gd and LTSL-Gd formulations. Three batches of each formulation were prepared for this analysis. The chromatograms were obtained by using the mobile phase as sample diluent. The values obtained were 26.41 ± 4.04 μmol mL^{-1} (10.56 ± 1.62%) and 22.95 ± 3.07 μmol mL^{-1} (9.18 ± 1.23%) for TTSL-Gd and LTSL-Gd, respectively. The amount of Gd-DTPA-BMA entrapment found, in terms of μmol mL^{-1}, was similar to the concentration determined for pH-sensitive and stealth pH-sensitive liposomes developed in a previously study from our research group.[3] The encapsulation percentages found are in agreement with values obtained in thermosensitive formulations containing Gd-DTPA-BMA, developed for use in magnetic resonance.[7] The drug entrapment is an essential physicochemical parameter in the development of a new drug delivery system. The results of this analysis confirms the applicability of the HILIC method to the development and characterization of liposomal formulations containing Gd-DTPA-BMA.

Table 4. Intra-day precision, inter-day precision, and values of Gd-DTPA-BMA recovery obtained with HILIC method

Linear range / %	Gd-DTPA-BMA mean concentration ± SD / (nmol mL^{-1})			RSD / %			Accuracy result		
	Intra-day[a]		Inter-day[b]	Intra-day[a]		Inter-day[b]	Gd-DTPA-BMA amount added / (nmol mL^{-1})	Gd-DTPA-BMA mean concentration[a] ± SD / (nmol mL^{-1})	Mean recovery[a] ± SD / %
	Day 1	Day 2		Day 1	Day 2				
50	39.59 ± 0.41	38.82 ± 0.52	39.20 ± 0.59	1.05	1.33	1.51	40	38.93 ± 0.37	97.32 ± 0.93
100	79.80 ± 0.86	79.13 ± 0.23	79.47 ± 0.67	1.08	0.29	0.85	80	79.41 ± 0.31	99.26 ± 0.38
150	119.50 ± 0.60	119.49 ± 0.94	119.50 ± 0.71	0.50	0.79	0.59	120	119.10 ± 1.97	99.25 ± 1.65
Mean[c]									98.61 ± 1.37
RSD[c] / %									1.38

[a]Mean of three determinations; [b]mean of six determinations; [c]mean of nine determinations. Gd-DTPA-BMA: gadodiamide; SD: standard deviation; RSD: relative standard deviation.

Table 5. Evaluation of the effect of the variables, in terms of content, R_s and A_s, in the determination of Gd-DTPA-BMA using the developed method

Variable	Content[a] / %	R_s[a]	A_s[a]
ACN ratio in the mobile phase (A = 60%; a = 63%)	101.37 – 100.87 = 0.50	3.21 – 4.57 = –1.36	1.32 – 1.28 = 0.04
The aqueous phase pH of the mobile phase (B = 4.5; b = 4.7)	100.61 – 101.64 = –1.03	4.06 – 3.72 = 0.34	1.26 – 1.34 = –0.08
Buffer concentration (C = 5 mmol L^{-1}; c = 5.5 mmol L^{-1})	101.46 – 100.78 = 0.68	3.56 – 4.22 = –0.66	1.29 – 1.30 = –0.01
Column temperature (D = 30 °C; d = 33 °C)	101.35 – 100.90 = 0.45	3.80 – 3.98 = –0.18	1.29 – 1.31 = –0.02
Flow (E = 0.6 mL. min^{-1}; e = 0.7 mL. min^{-1})	101.16 – 101.09 = 0.07	4.37 – 3.41 = 0.96	1.28 – 1.31 = –0.03
ACN brand (F = Tedia; f = J.T.Baker)	101.54 – 100.70 = 0.84	3.83 – 3.95 = –0.12	1.25 – 1.35 = –0.10
Buffer brand (G = Vetec; g = Spectrum)	101.26 – 100.98 = 0.28	4.05 – 3.73 = 0.32	1.26 – 1.34 = –0.08
Largest effect[b]	1.24	36.06	8.97

[a]Mean values obtained at nominal conditions subtracted from the mean values obtained under the varied conditions; [b]RSD (relative standard deviation) between the values obtained in the 8 experiments multiplied by root of 2. R_s: resolution; A_s: asymmetry.

Conclusions

In the present study, an analytical method for the determination of Gd-DTPA-BMA in liposomes by HILIC was developed, using chemometric tools, validated and applied for determination of Gd-DTPA-BMA entrapment and drug encapsulation percentage in liposomes. The developed method showed to be simple, fast and selective. In addition, it presented adequate detectability, proving to be suitable to determine Gd-DTPA-BMA in the development of liposomal formulations. Although this method has been used to determine a single analyte, it presented selectivity to be used in more complex samples, as demonstrated for fetal bovine serum sample. In this context, the use of Box-Behnken factorial design and response surface methodology was effective for method development. This approach allowed evaluating the interaction between the parameters and obtaining results that probable would not be observed in a univariate analysis. Although some methods for determining Gd-DTPA-BMA in different matrices by HILIC have been described, none has been applied for analysis of liposomes. In addition, from our knowledge, until the present date, no quantification study of Gd-DTPA-BMA by a rational chemometric-assisted HILIC has been found in the literature.

Supplementary Information

Supplementary information is available free of charge at http://jbcs.sbq.org.br as PDF file.

Acknowledgments

The authors would like to thank CNPq (Conselho Nacional de Desenvolvimento Científico e Tecnológico), FAPEMIG (Fundação de Amparo à Pesquisa do Estado de Minas Gerais) and CAPES (Coordenação de Aperfeiçoamento de Pessoal de Nível Superior) for their financial support.

References

1. Telgmann, L.; Sperling, M.; Karst, U.; *Anal. Chim. Acta* **2013**, *764*, 1.
2. Maia, A. L. C.; Silva, T. D.; Oliveira, C. N. P.; Silveira, J. N.; Ramaldes, G. A.; *Anal. Methods* **2015**, *7*, 8315.
3. Maia, A. L. C.; Fernandes, C.; Oliveira, C. N. P.; Teixeira, C. S.; Oliveira, M. S.; Soares, D. C. F.; Ramaldes, G. A.; *Curr. Drug Delivery* **2017**, *14*, 566.
4. EMA/625317/2017: *EMA's Final Opinion Confirms Restrictions on Use of Linear Gadolinium Agents in Body Scans*, European Medicines Agency (EMA): London, UK, 2017.
5. Ghaghada, K.; Hawley, C.; Kawaji, K.; Annapragada, A.; Mukundan Jr., S.; *Acad. Radiol.* **2008**, *15*, 1259.
6. Grahn, A. Y.; Bankiewicz, K. S.; Dugich-djordjevic, M.; Bringas, J. R.; Hadaczek, P.; Johnson, G. A.; Eastman, S.; Luz, M.; *J. Neuro-Oncol.* **2009**, *95*, 185.
7. Hossann, M.; Wang, T.; Wiggenhorn, M.; Schmidt, R.; Zengerle, A.; Winter, G.; Eibl, H.; Peller, M.; Reiser, M.; Issels, R. D.; Lindner, L. H.; *J. Controlled Release* **2010**, *147*, 436.
8. Soares, D. C. F.; Oliveira, M. C.; Barros, A. L. B.; Cardoso, V. N.; Ramaldes, G. A.; *Eur. J. Pharm. Sci.* **2011**, *43*, 290.

9. Soares, D. C. F.; Oliveira, M. C.; Santos, R. G.; Andrade, M. S.; Vilela, J. M. C.; Cardoso, V. N.; Ramaldes, G. A.; *Eur. J. Pharm. Sci.* **2011**, *42*, 462.
10. Soares, D. C. F.; Cardoso, V. N.; Barros, A. L. B.; Souza, C. M.; Cassali, G. D.; Oliveira, M. C.; Ramaldes, G. A.; *Eur. J. Pharm. Sci.* **2012**, *45*, 58.
11. Dewi, N.; Yunagie, H.; Zhu, H.; Demachi, K.; Shinohara, A.; Yokoyama, K.; Sekino, M.; Sakurai, Y.; Morishita, Y.; Iyomoto, N.; Nagasaki, T.; Horiguchi, Y.; Nagasaki, Y.; Nakajima, J.; Ono, M.; Kakimi, K.; Takahashi, H.; *Biomed. Pharmacother.* **2013**, *67*, 451.
12. Soares, D. C. F.; Barros, A. L. B.; Santos, R. G. S.; Sousa, E. M. B.; Ramaldes, G. A.; *J. Radioanal. Nucl. Chem.* **2013**, *295*, 63.
13. Issels, R.; Kampmann, E.; Kanaar, R.; Lindner, L. H.; *Int. J. Hyperthermia* **2016**, *32*, 89.
14. Behra-miellet, J.; Briand, C.; Kouach, M.; Gressier, B.; Cazin, M.; Cazin, J. C.; *Biomed. Chromatogr.* **1998**, *12*, 21.
15. Frenzel, T.; Lensfeld, P.; Schirmer, H.; Hütter, J.; Weinmann, H. J.; *Invest. Radiol.* **2008**, *43*, 817.
16. Kahakachchi, C. L.; Moore, D. A.; *J. Anal. At. Spectrom.* **2009**, *24*, 1389.
17. Lindberg, G. M.; Uran, S.; Frilsk, G.; Martinsen, I.; Skotland, T.; *Eur. Radiol.* **2010**, *20*, 1636.
18. United States Pharmacopeia (USP); USP 34-NF 29; The United States Pharmacopeial Convention: Rockville, 2011, p. 2934-2937.
19. Normann, P. T.; Hals, P. A.; *Eur. J. Drug Metab. Pharmacokinet.* **1995**, *20*, 307.
20. Raju, C. S. K.; Cossmer, A.; Scharf, H.; Panne, U.; Lück, D.; *J. Anal. At. Spectrom.* **2010**, *25*, 55.
21. Greco, G.; Letzel, T.; *J. Chromatogr. Sci.* **2013**, *51*, 684.
22. Buszewski, B.; Noga, S.; *Anal. Bioanal. Chem.* **2012**, *402*, 231.
23. Acevska, J.; Stefkov, G.; Petkovska, R.; Kulevanova, S.; Dimitrovska, A.; *Anal. Bioanal. Chem.* **2012**, *403*, 1117.
24. Sahu, P. K.; Patro, C. S.; *J. Liq. Chromatogr. Relat. Technol.* **2014**, *37*, 2444.
25. Künnemeyer, J.; Terborg, L.; Nowak, S.; Scheffer, A.; Telgmann, L.; Tokmak, F.; Günsel, A.; Wiesmüller, G.; Reichelt, S.; Karst, U.; *Anal. Chem.* **2008**, *80*, 8163.
26. Künnemeyer, J.; Terborg, L.; Meermann, B.; Brauckmann, C.; Möller, I.; Scheffer, A.; Karst, U.; *Environ. Sci. Technol.* **2009**, *43*, 2884.
27. Telgmann, L.; Wehe, C. A.; Birka, M.; Künnemeyer, J.; Nowak, S.; Sperling, M.; Karst, U.; *Environ. Sci. Technol.* **2012**, *46*, 11929.
28. Lindner, U.; Lingott, J.; Richter, S.; Jakubowski, N.; Panne, U.; *Anal. Bioanal. Chem.* **2013**, *405*, 1865.
29. Lindner, U.; Lingott, J.; Richter, S.; Jiang, W.; Jakubowski, N.; Panne, U.; *Anal. Bioanal. Chem.* **2015**, *407*, 2415.
30. Ministério da Saúde, Agência Nacional de Vigilância Sanitária; Resolução RE No. 899, de 29 de maio de 2003, *Guia de Validação de Métodos Analíticos e Bioanalíticos*, Diário Oficial da União, Brasília, 2003.
31. International Conference on Harmonisation of Technical Requirements for Registration of Pharmaceuticals for Human Use (ICH); *Guideline Q2(R1) - Validation of Analytical Procedures: Text and Methodology*; ICH: Geneva, 2005.
32. Szoka Jr., F.; Papahadjopoulos, D.; *Proc. Natl. Acad. Sci. U. S. A.* **1978**, *75*, 4194.
33. Li, L.; Hagen, T. L. M. T.; Hossann, M.; Süss, R.; Rhoon, G. C. V.; Eggermont, A. M. M.; Haemmerich, D.; Koning, G. A.; *J. Controlled Release* **2013**, *168*, 142.
34. Bezerra, M. A.; Santelli, R. E.; Oliveira, E. P.; Villar, L. S.; Escaleira, L. A.; *Talanta* **2008**, *76*, 965.
35. *Statistica 7.0*, StatSoft®, Tulsa, USA, 2004.
36. Van Deemter, J. J.; Zuiderweg, F. J.; Klinkenberg, A.; *Chem. Eng. Sci.* **1956**, *5*, 271.
37. *GraphPad Prism 5.0*, GraphPad Software Inc., San Diego, USA, 2007.
38. Ribeiro, F. A. L.; Ferreira, M. M. C.; Morano, S. C.; Silva, L. R.; Schneider, R. P.; *Quím. Nova* **2008**, *31*, 164.
39. Youden, W. J.; Steiner, E. H.; *Statistical Manual of AOAC*; Association of Official Analytical Chemistry (AOAC): Washington, USA, 1975.
40. Cass, Q. B.; Cassiano, N.; *Cromatografia Líquida: Novas Tendências e Aplicações*, 1ª ed.; Elsevier: Rio de Janeiro, 2015.
41. Control No. 169935: *Product Monograph: Omniscan™ (Gadodiamide Injection USP)*, GE Healthcare: Ontario, Canada, 2013.
42. Merbach A.; Helm, L.; Tóth, E.; *The Chemistry of Contrast Agents in Medical Magnetic Resonance Imaging*, 2nd ed.; John Wiley & Sons: United Kingdom, 2013.
43. Chirita, R. I.; West, C.; Finaru, A. L.; Elfakir, C.; *J. Chromatogr. A* **2010**, *1217*, 3091.
44. Hemström, P.; Irgum, K.; *J. Sep. Sci.* **2006**, *29*, 1784.
45. Vora, M. M.; Wukovnig, S.; Finn, R. D.; Emran, A. M.; Boothe, T. E.; Kothari, P. J.; *J. Chromatogr.* **1986**, *369*, 187.
46. Hvattum, E.; Normann, P. T.; Jamieson, G. C.; Lai, J. J.; Skotland, T.; *J. Pharm. Biomed. Anal.* **1995**, *13*, 927.
47. Cao, Y.; Calik, S.; *J. Chromatogr. A* **2011**, *1218*, 5920.
48. Karnatapanis, A. E.; Flamegos, Y. C.; Stalikas, C. D.; *J. Chromatogr. A* **2011**, *1218*, 2871.
49. United States Food and Drug Administration; *Guidance for Industry, Analytical Procedures and Methods Validation*, Rockville, USA, 2000.
50. Ribani, M.; Bottoli, C. B. G.; Collins, C. H.; Jardim, I. C. S. F.; Melo, L. F. C.; *Quím. Nova* **2004**, *27*, 771.
51. Snyder, L. R.; Kirkland, J. J.; Glajch, J. L.; *Practical HPLC Method Development*, 2nd ed.; John Wiley & Sons: New York, 2007.

52. Thermo Scientific; *HILIC Separations Technical Guide. A Practical Guide to HILIC Mechanisms, Method Development and Troubleshooting*, Thermo Scientific, 2014.
53. Teófilo, R. F.; Ferreira, M. M. C.; *Quím. Nova* **2006**, *29*, 338.
54. United States Food and Drug Administration; *Reviewer Guidance Validation of Chromatographic Methods*, Center for Drug Evaluation and Research: Rockville, USA, 1994.

Submitted: January 22, 2018
Published online: June 22, 2018

ANEXO B

Comprovante do depósito de pedido de patente (referente ao assunto do artigo científico apresentado no ANEXO A)


INSTITUTO NACIONAL DA PROPRIEDADE INDUSTRIAL

28/05/2018 870180045208 12:04

3158861707216894

Pedido nacional de Invenção, Modelo de Utilidade, Certificado de Adição de Invenção e entrada na fase nacional do PCT

Número do Processo: BR 10 2018 010797 6

Dados do Pedido

Natureza Patente: 10 - Patente de Invenção (PI)

Título da Invenção ou Modelo de Utilidade (54): "MÉTODO PARA DETECÇÃO E QUANTIFICAÇÃO DE GADODIAMIDA (Gd-DTPA-BMA) EM AMOSTRAS FARMACÊUTICAS E BIOLÓGICAS E USO"

Resumo: A presente invenção descreve um método analítico, por cromatografia líquida de interação hidrofílica (HILIC) utilizando detector de arranjo de diodos (DAD) em uma fase estacionária zwitteriônica, capaz de detectar e quantificar gadodiamida (Gd-DTPA-BMA) em amostras farmacêuticas e biológicas. Este método pode ser utilizado para detectar e quantificar gadodiamida (Gd-DTPA-BMA) em amostras farmacêuticas e biológicas, tais como lipossomas e soro sanguíneo.

MAIA, A. L. C.; SILVA, P. H. R.; FERNANDES, C.; SILVA, A. T. M.; OLIVEIRA, M. S.; BARROS, A. L. B; RAMALDES, G. A.; SOARES, D. C. F. Patente: Privilégio de Inovação. Número de registro: BR10201801079, título: "Método para detecção e quantificação de gadodiamida (Gd-DTPA-BMA) em amostras farmacêuticas e biológicas e uso". Instituição de registro: INPI – Instituto Nacional da Propriedade Industrial. Depósito: 28/05/2018.

ANEXO C

Histórico de disciplinas cursadas (requisito parcial para obtenção do grau de Doutora)

HISTÓRICO DE DISCIPLINAS CURSADAS

Data de início do doutorado: 01/06/2015.

Data de conclusão do doutorado: 31/05/2019.

Número de créditos exigidos: 15.

Número de créditos cursados: 17.

Semestre	Disciplina	Créditos	CH	Nota	Conceito
2015/2	QUI 875 – Propriedade intelectual I: Redação de patentes.	4	60	81	B
2015/2	MOF 881 – Tópicos especiais em Biologia Celular II: Métodos e técnicas em cultura de células.	2	30	86	B
2015/2	APM 859 – Tópicos em Patologia II: Introdução à Citometria de Fluxo.	2	30	100	A
2015/2	FAR 812 – Seminários em Ciências Farmacêuticas II.	1	15	100	A
2015/2	ACT 839 – Nanotecnologia e radiotraçadores.	2	30	92	A
2016/1	FAF 807 – Tópicos em Ciências Farmacêuticas II: Farmácia Nuclear.	2	30	91	A
2016/2	FAF 804 – Estágio Docência (Disciplinas: Farmacotécnica I e Sistemas lipídicos de liberação de fármacos).	1	15	100	A
2016/2	FAF 807 – Tópicos em Ciências Farmacêuticas II: Ensaios Farmacológicos Pré-clínicos.	2	30	95	A
2016/2	FAR 811 – Seminários em Ciências Farmacêuticas I.	1	15	100	A

ANEXO D

Produções científicas realizadas no período do doutorado

1. ARTIGOS PUBLICADOS

1.1 Artigo de revisão, referente à colaboração com o Prof. Daniel Crístian Ferreira Soares:

TEBALDI, M. L.; MAIA, A. L. C.; POLETTO, F.; ANDRADE, F. V.; SOARES, D. C. F. Poly(-3-hydroxybutyrate-*co*-3hydroxyvalerate) (PHBV): Current advances in synthesis methodologies, antitumor applications and biocompatibility. *Journal of Drug Delivery Science and Technology*, v. 51, p. 115-126, 2019.

1. 2 Artigo referente à esta tese de doutorado:

MAIA, A. L. C.; SILVA, P. H. R.; FERNANDES, C.; SILVA, A. T. M.; BARROS, A. L. B.; SOARES, D. C. F.; RAMALDES, G. A. Chemometric-assisted hydrophilic interaction chromatographic method for the determination of gadolinium-based magnetic resonance imaging contrast agent in liposomes. *Journal of the Brazilian Chemical Society*, v. 29, n. 11, p. 2426 – 2440, 2018.

1.3 Artigo referente à colaboração com Aline Teixeira Maciel e Silva no projeto de doutorado: "Avaliação das propriedades furtiva e antitumoral de lipossomas revestidos com carboidratos contendo doxorrubicina":

SILVA, A. T. M.; MAIA, A. L. C.; SILVA, J. O.; BARROS, A. L. B.; SOARES, D. C. F.; MAGALHÃES, M. T. Q.; ALVES, R. J.; RAMALDES, G. A. Synthesis of cholesterol-based neoglycoconjugates and their use in the preparation of liposomes for active liver targeting. *Carbohydrate Research*, v. 465, p. 52-57, 2018.

1.4 Artigos referentes à colaboração com o Prof. Daniel Crístian Ferreira Soares nos projetos: "Nanopartículas de hidroxiapatita como sistema de liberação controlada de fármacos para terapia da osteomielite" e "Nanopartículas de hidroxiapatita contendo vincristina como sistema de liberação prolongada para o tratamento seletivo de metástases ósseas":

MAIA, A. L. C.; FERREIRA, C. A.; BARROS, A. L. C.; SILVA, A. T. M.; RAMALDES, G. A.; JÚNIOR, A. S. C.; OLIVEIRA, D. C. P.; FERNANDES, C.; SOARES, D. C. F. Vincristine-loaded hydroxyapatite nanoparticles as a potential delivery system for bone cancer therapy. *Journal of Drug Targeting*, v. 26, p. 592-603, 2018.

MAIA, A. L. C.; CAVALCANTE, C. H.; SOUZA, M. G. F.; FERREIRA, C. A.; RUBELLO, D.; CHONDROGIANNIS, S.; CARDOSO, V. N.; RAMALDES, G. A.; BARROS, A. L. B.; SOARES, D. C. F. Hydroxyapatite nanoparticles: preparation, characterization, and evaluation of their potential use in bone targeting: an animal study. *Nuclear Medicine Communications*, v. 37, n. 7, p. 775-782, 2016.

1.5 Artigos referentes ao projeto de mestrado: "Lipossomas contendo gadodiamida: aspectos analíticos, farmacotécnicos e avaliação da atividade citotóxica in vitro":

MAIA, A. L. M.; FERNANDES, C.; OLIVEIRA, C. N. P.; TEIXEIRA, C. S.; OLIVEIRA, M. S.; SOARES, D. C. F.; RAMALDES, G. A. Liposomes containing gadodiamide: preparation, physicochemical characterization, and *in vitro* cytotoxic evaluation. *Current Drug Delivery*, v. 13, p. 1-9, 2016.

MAIA, A. L. C.; FERNANDES, C.; SILVA, T. D.; OLIVEIRA, C. N. P.; SILVEIRA, J. N.; RAMALDES, G. A. Development and validation of high performance liquid chromatographic and derivative spectrophotometric methods for determination of gadodiamide in liposomal formulations. *Analytical Methods*, v. 7, p. 8315-8325, 2015.

2. RESUMOS PUBLICADOS

2.1 Resumos referentes à esta tese de doutorado:

MAIA, A. L. C.; SILVA, A. T. M.; GIUBERTI, C. S.; FERNANDES, C.; MALACHIAS, A.; BARROS, A. L. B.; SOARES, D. C. F.; RAMALDES, G. A. Characterization of thermotropic phase transitions in thermosensitive liposomes membranes using DLS, DSC, and SAXS analysis. In: *42ª Reunião Anual da Sociedade Brasileira de Química (SBQ): Eixos Mobilizadores em Química*, 2019, Joinville.

MAIA, A. L. C.; SILVA, A. T. M.; FERNANDES, C.; BARROS, A. L. B.; SOARES, D. C. F.; RAMALDES, G. A. Thermosensitive liposomes containing gadodiamide: preparation, characterization, and preliminar evaluation of their stability and thermosensitivity. In: *IV ABCF Congress*, 2018, São Paulo.

MAIA, A. L. C.; SILVA, A. T. M.; CESAR, A. L. A.; GIUBERTI, C. S.; FERNANDES, C.; BARROS, A. L. B.; SOARES, D. C. F.; RAMALDES, G. A. Lipossomas termossensíveis contendo gadodiamida: influência da composição lipídica na termossensibilidade e na cinética de liberação. In: *III Simpósio Nacional em Ciências Farmacêuticas* – SINCIFAR, 2018, Belo Horizonte.

MAIA, A. L. C.; SILVA, A. T. M.; FERNANDES, C.; BARROS, A. L. B.; SOARES, D. C. F.; RAMALDES, G. A. Development of thermosensitive liposomes containing gadodiamide influence of the preparation method and composition on the physicochemical characteristics. In: *11th CIFARP – 11th International Congress of Pharmaceutical Sciences*, 2017, Ribeirão Preto.

2.3 Resumo referente à colaboração com Isabela Pereira Gomes no projeto de doutorado: "Lipossomas termossensíveis revestidos com ácido hialurônico como estratégia para carreamento de fármacos antitumorais":

GOMES, I. P.; MAIA, A. L. C.; BARROS, A. L. B.; LEITE, E. A. Lipossoma termossensível funcionalizado com ácido hialurônico para veiculaçõa de fármacos antitumoral. In: *III Simpósio Nacional em Ciências Farmacêuticas* – SINCIFAR, 2018, Belo Horizonte.

2.4 Resumo referente à colaboração com Aline Teixeira Maciel e Silva no projeto de doutorado: "Avaliação das propriedades furtiva e antitumoral de lipossomas revestidos com carboidratos contendo doxorrubicina":

SILVA, A. T. M.; MAIA, A. L. C.; BARROS, A. L. B.; SOARES, D. C. F.; ALVES, R. J.; RAMALDES, G. A. Development and characterization of carbohydrate coated liposomes containing doxorubicin. *In: 11th CIFARP – 11th International Congress of Pharmaceutical Sciences*, 2017, Ribeirão Preto.

2.5 Resumo referente ao projeto de mestrado: "Lipossomas contendo gadodiamida: aspectos analíticos, farmacotécnicos e avaliação da atividade citotóxica *in vitro*":

MAIA, A. L. C.; FERNANDES, C.; TEIXEIRA, C. S.; OLIVEIRA, M. S.; SOARES, D. C. F.; RAMALDES, G. A. Avaliação da atividade citotóxica *in vitro* de lipossomas contendo gadodiamida em células de adenocarcinoma mamário murino (4T1). In: *V CONCIFOP – Congresso de Ciências Farmacêuticas de Ouro Preto*, 2016, Ouro Preto.

3. PREMIAÇÃO RECEBIDA REFERENTE À ESTA TESE DE DOUTORADO

3.1 The best presentation of the poster session Pharmaceutical and Cosmetic Technology at the IV ABCF Congress, Associação Brasileira de Ciências Farmacêuticas:

MAIA, A. L. C.; SILVA, A. T. M.; FERNANDES, C.; BARROS, A. L. B.; SOARES, D. C. F.; RAMALDES, G. A. Development of thermosensitive liposomes containing gadodiamide influence of the preparation method and composition on the physicochemical characteristics. In: *11th CIFARP – 11th International Congress of Pharmaceutical Sciences*, 2017, Ribeirão Preto.

4. DEPÓSITO DE PEDIDO DE PATENTE REFERENTE À ESTA TESE DE DOUTORADO

MAIA, A. L. C.; SILVA, P. H. R.; FERNANDES, C.; SILVA, A. T. M.; OLIVEIRA, M. S.; BARROS, A. L. B; RAMALDES, G. A.; SOARES, D. C. F. Patente: Privilégio de Inovação. Número de registro: BR10201801079, título: "Método para detecção e quantificação de gadodiamida (Gd-DTPA-BMA) em amostras farmacêuticas e biológicas e uso". Instituição de registro: INPI – Instituto Nacional da Propriedade Industrial. Depósito: 28/05/2018.